

SMART SENSOR SYSTEMS

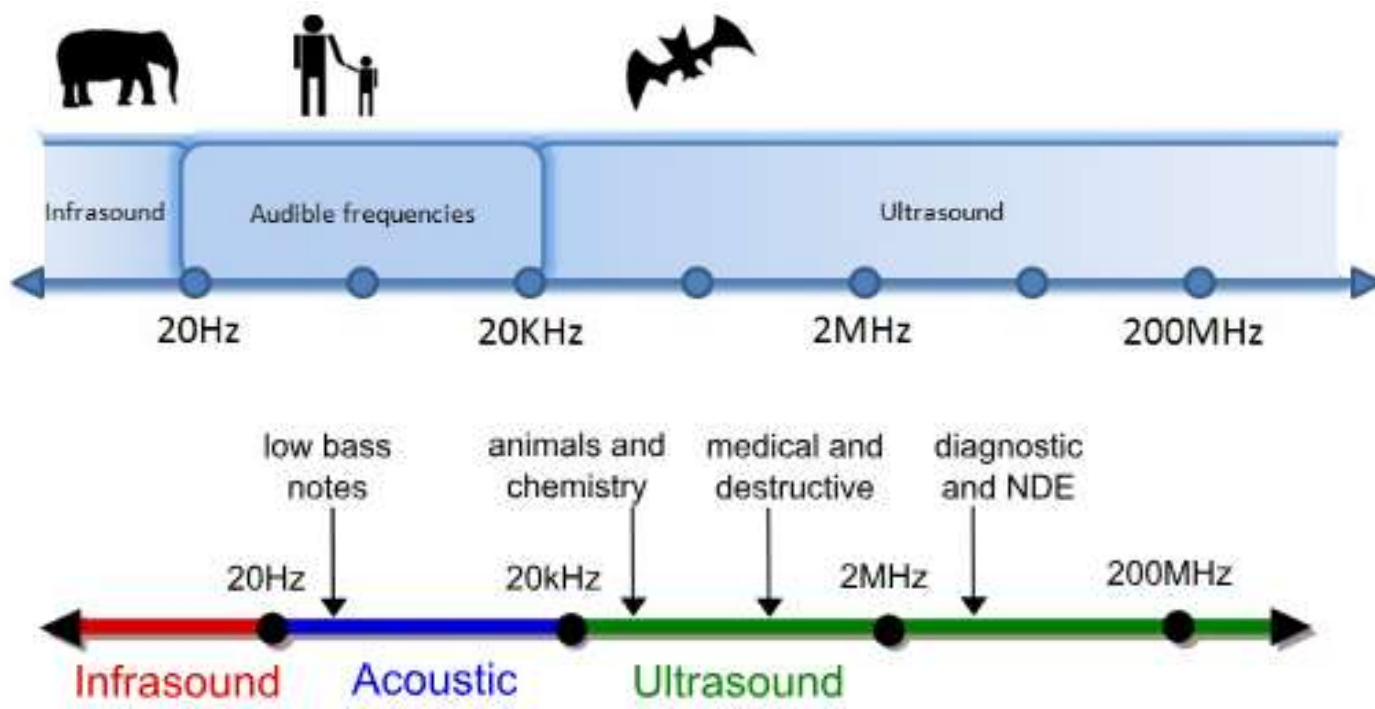
UNIT 2 &3



UNIT-II

Acoustic waves

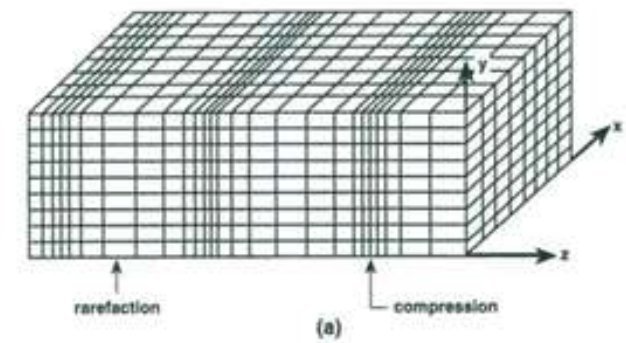
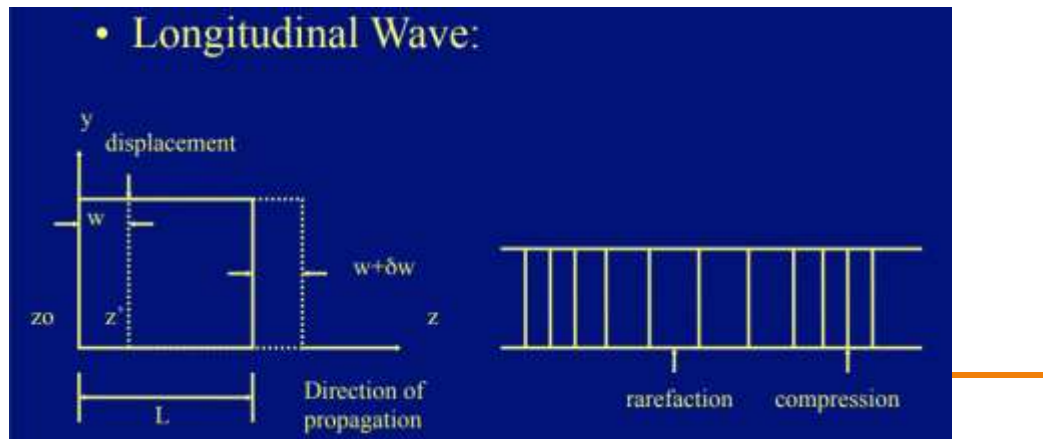


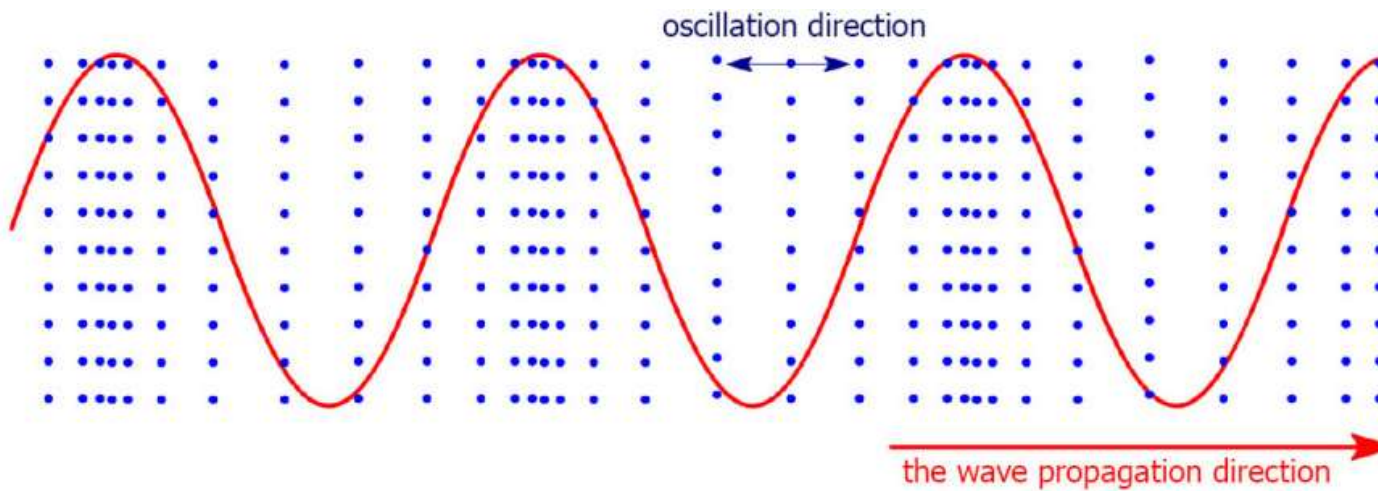


What are acoustic waves?

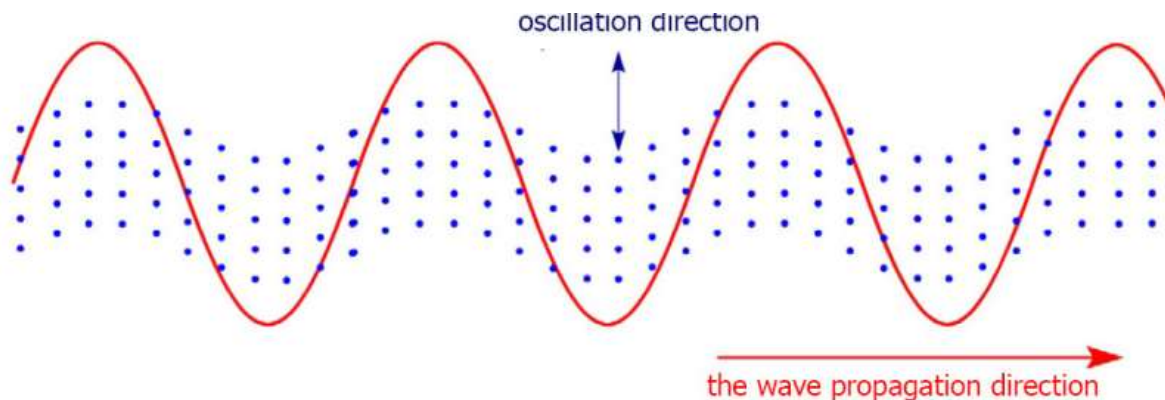
- The acoustic waves are mechanical waves that need a medium to carry their energy from any position to another.
- The acoustic waves, which are mechanical waves, are incapable to travel over a vacuum.

The **longitudinal wave**, in which the motion of a particle in the acoustic medium is only in the direction of propagation. Thus when a force is applied to the acoustic medium, the medium extends or contracts in the z direction, as shown in Fig

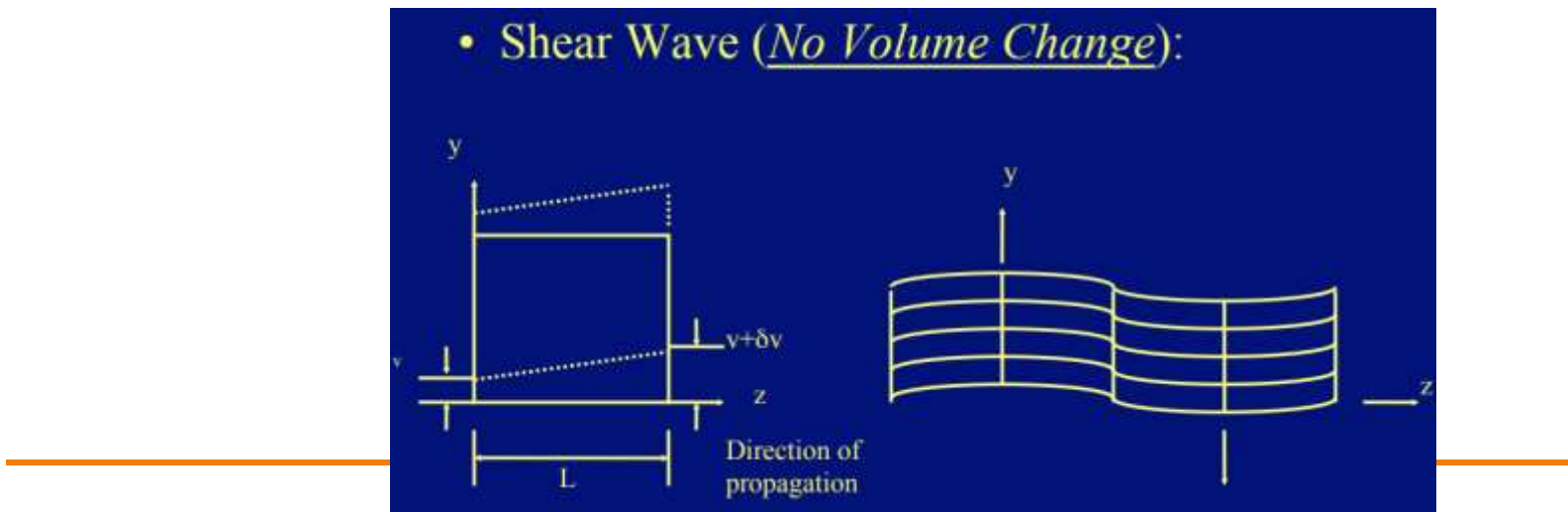




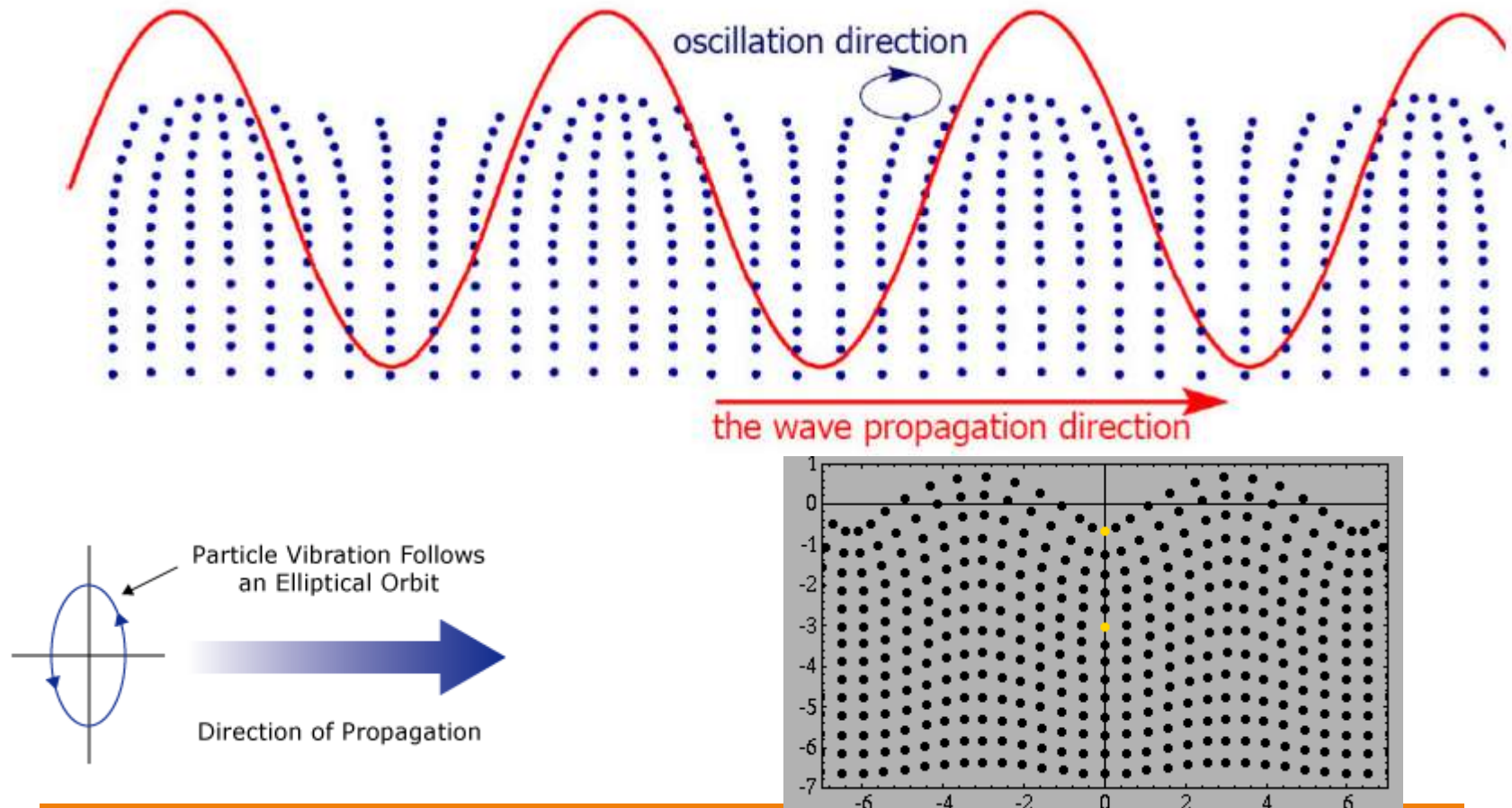
Transverse waves – are acoustic waves, in which the particles of the medium vibrate perpendicular to the direction of wave propagation. Under the influence of waves the material undergoes shear deformation.



- Shear Wave (No Volume Change):



Surface waves (Rayleigh waves) – are the acoustic waves that propagate along the boundary between two media, in layer with a typical thickness of 1.5 to 2 wavelength $(1.5\text{-}2) \cdot \lambda$. Fluctuations medium particles of the wave combine the longitudinal and transverse vibrations, the particles move along locked elliptical trajectories



There are various kinds of acoustic waves.

Bulk acoustic waves are acoustic waves propagated through the bulk substrate material.

Surface acoustic waves

propagate along the surface of a substrate.

There are some types of the surface acoustic waves. In the case of the Rayleigh waves particles in the surface layer move both up and down and back and forth tracing out elliptical paths.

Typical velocities are 6000 m/s for longitudinal waves and 3000 m/s for transverse waves.

Piezoelectric materials



On the surface of the piezoelectric material, electric charges are produced due to applying any mechanical stress, such as the one applied from the sound waves. In the direct piezoelectric effect, the convinced charges are proportional to the mechanical stress.

This piezoelectricity effect has a wide application in detecting the acoustic sound and electronic frequency/high voltage generation.

The negative and positive electrical charges are divided in the piezoelectric crystal leading to electrically neutral overall crystal.

This symmetry is disturbed with applying a stress to the piezoelectric materials, and the asymmetry of the charge produces a voltage.

The piezoelectric material can be categorized according its cutting procedure, namely, shear, longitudinal, and transverse, which are defined as follows

Shear effect: due to this effect, the generated charges are independent of the element's shape/size and proportional to the applied forces

Longitudinal effect: due to this effect, the displaced amount of charge is independent of the piezoelectric element's shape/size and proportional to the applied forces.

Transverse effect: due to this effect, the applied force along the y-axis transfers charges along the x-direction, which is perpendicular to the force line.

Piezoelectric Materials

Quartz remains still one of the most important piezoelectric materials and is in great demand.

A large part of this demand is increasingly being met by mass production of artificial quartz based on the technique of hydrothermal growth.

During World War II., about 75 million quartz plates were produced for the armed forces of the United States. As the supply of good quality raw material started to decline, interest in artificial growth was renewed.

The size of synthetic crystals increased tenfold thanks to the concentrated effort and modern technology. As a result, we now have a virtually unlimited supply.

Synthetic quartz has been commercially available since 1958. Today, the manufacture of synthetic quartz has become an important industry.

Rochelle salt was often used in various transducers because it has a great piezoelectric effect. In spite of being a piezoelectric crystal with the highest electromechanical coupling coefficient, Rochelle salt is of limited use because it is soluble in water, and some parameters do not have a suitable temperature characteristic

Since 1935 attempts were made to produce piezoelectric crystals, which could replace quartz. Piezoelectric crystals such as ammonium and potassium salts ($\text{NH}_4\text{H}_2\text{PO}_4$ – ADP, KH_2PO_4 – KDP), ethylene diamine tartrate (EDT), dipotassium tartrate (DKT) and lithium sulphate monohydrate (LH) were developed.

Many of these materials are no longer in use as a result of development and production of artificial quartz, ferroelectric crystals or piezoelectric ceramics. The discovery of the strong piezoelectric properties of ferroelectric ceramics is a major milestone in applications of piezoelectricity.

With the exception to quartz few single crystals are used in piezoelectric devices. Popular choices are LiNbO_3 , LiTaO_3 . In recent times considerable attention is given to the synthesis of berlinitite (aluminium phosphate) and langasite. This material could combine some useful characteristics of quartz with a high coupling factor. The single crystals are anisotropic, exhibiting different material properties depending on the cut of the materials and the direction of bulk or surface wave propagation.

In the last 20 years intensive research was done on the synthesis of new piezoelectric crystal compositions.

The main objectives consisted in the search for new single crystals with improved piezoelectric properties like high sensitivity, high electromechanical coupling and high stability at elevated temperatures.

More than 40 single crystal compounds used for sensor application like force sensors, strain sensors and high temperature pressure sensors were synthesized.

Pyroelectric and piezoelectric materials, which generate an electric field with the input of heat and stress, respectively, are called “smart” materials.

These offdiagonal couplings have corresponding converse effects, the electrocaloric and converse piezoelectric effects, and both “sensing” and “actuating” functions can be realized in the same materials. “Intelligent” materials must possess a function, which is adaptive to changes in environmental conditions.

An elastic medium behaves as a distributed mass-spring system in which displacement of a single element results in the propagation of a disturbance through out the medium. A particle at a free surface is different from one interior to the solid, in that it is constrained by adjacent particles from only one side. Thus, disturbances at a surface can behave somewhat differently from those in the interior of a solid.

Like the one-dimensional vibrating string, particle displacement in the solid is a function both of time and position.

The waves that can propagate in a solid depend upon both the properties of the solid and its boundaries

Acoustic sensing



There are several methods to measure the sound waves, namely, the

- (i) frequency;**
- (ii) wavelength, where the distance that the disturbance travels via the medium represents a complete wave cycle;**
- (iii) amplitude which is related to the sound volume, loudness, and intensity;**
- (iv) phase; and (v) speed of sound that depends on the medium state/type, which is affected by the elasticity and the inertia.**

Acoustic (sound) sensors can detect and transmit vibrations and sound waves from **infrasound** (very low frequencies) up to **ultrasound** (very high frequencies).

Acoustic wave sensors detect acoustic or mechanical waves produced by the human body.

During the propagation of the acoustic wave through the body, the propagation path characteristics change, which affect the amplitude/velocity of the acoustic wave.

Measuring the phase/frequency characteristics of sensed signals reflects the occurred changes in the velocity, which is correlated to the consistent physical measured quantity

Acoustic wave sensors

Acoustic wave sensors are so named because they utilize a mechanical, or acoustic, wave as the sensing mechanism.

As the acoustic wave propagates through or on the surface of the material, any changes to the characteristics of the propagation path affect the velocity and/or amplitude of the wave.

Changes in velocity can be monitored by measuring the frequency or phase characteristics of the sensor and can then be correlated to the corresponding physical quantity that is being measured.

Virtually all acoustic wave devices and sensors use a piezoelectric material to generate the acoustic wave.

PIEZOELECTRIC SUBSTRATE MATERIALS FOR ACOUSTIC WAVE SENSORS

There are several piezoelectric substrate materials that may be used for acoustic wave sensors and devices. The most common are quartz (SiO_2) and lithium tantalate (LiTaO_3), and to a lesser degree, lithium niobate (LiNbO_3). Each material has specific advantages and disadvantages, which include cost, Temperature dependence, attenuation, and propagation velocity.

Other materials that have commercial potential include gallium arsenide (GaAs), silicon carbide (SiC), langasite (LGS), zinc oxide (ZnO), aluminum nitride (AlN), lead zirconium titanate (PZT), and polyvinylidene fluoride (PVDF).

THE DIRECT AND THE CONVERSE PIEZOELECTRIC EFFECT

The direct piezoelectric effect may be defined as the change of electric polarization proportional to the strain. A material is said to be piezoelectric if the application of an external mechanical stress gives rise to dielectric displacement in this material. This displacement manifests itself as internal electric polarization.

It should be noted that the piezoelectric effect strongly depends on the symmetry of the crystal. A crystal having sufficiently low symmetry produces electric polarization under the influence of external mechanical force.

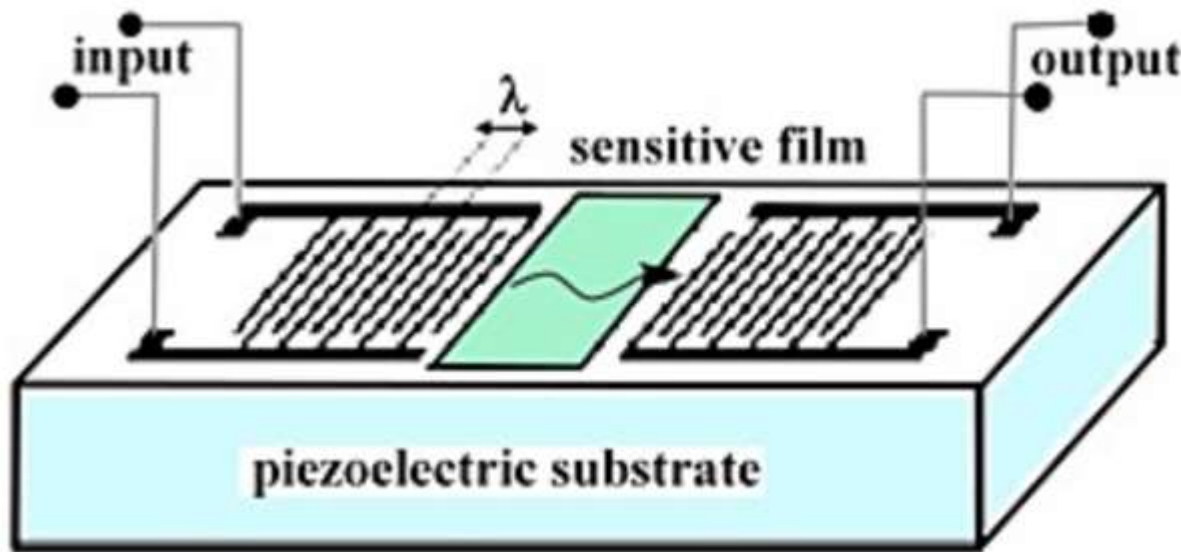
Closely related is the converse effect, whereby a piezoelectric crystal becomes strained if an external electric field is applied. Both effects are the manifestation of the same fundamental property of the non-centric crystal.

saw sensors



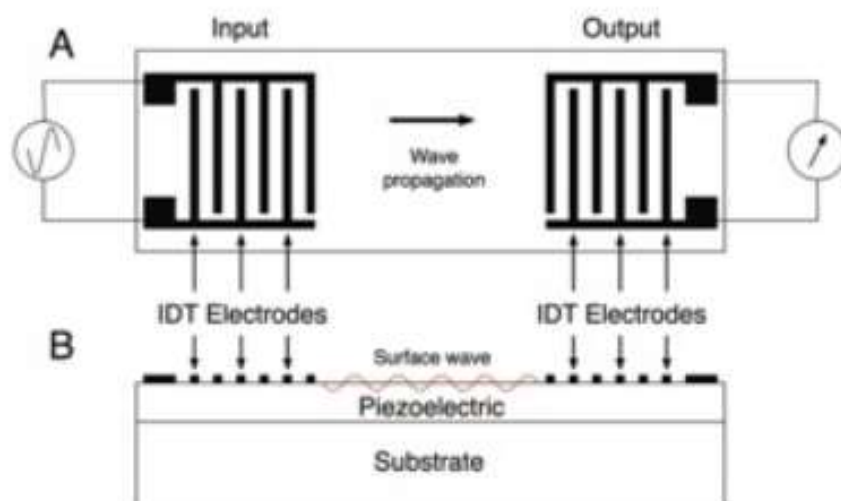
Surface Acoustic Wave Sensors

The largest consumer for SAW devices is the telecommunications industry, where SAWs are used as band pass filters in the radio frequency (RF) range in mobile phones and base stations. Some of the emerging applications for acoustic wave devices include sensors for the automotive (e.g., torque and pressure sensors), medical (e.g., chemical sensors) and industrial markets (e.g., humidity, temperature and mass sensors). SAWs are also used for advanced touch screens..



Surface Acoustic Wave devices (SAW) are acoustic devices commonly used for high frequency filtering applications such as in mobile telephony. Acoustic waves are generated by applying an alternating voltage across electrodes on the piezoelectric. As the piezoelectric starts to oscillate it generates an acoustic wave, **the resonant frequency being a function of the spacing between the electrodes and the acoustic wave velocity of the material**. This wave is received at a second set of electrodes and converted back to **an a.c. voltage**.

The resonant frequency of such devices can be increased by either reducing the electrode spacing in the IDT or using a material of higher sound wave velocity. Diamond has the highest acoustic wave velocity of any material and thus offers the highest possible resonant frequencies of any SAW device.



Schematic of a Surface Acoustic Wave (SAW) device, plan view (A) and side view (B). The Inter - Digitated - Transducer (IDT) Electrodes are used to apply an alternating potential across the piezoelectric at the input. This generates a surface acoustic wave which is converted back to an electric potential at the output.

Diamond is not a piezoelectric and thus has to be combined with a piezoelectric material such as AlN in order to fabricate a discrete device. The integration of AlN onto diamond films requires very smooth surfaces, typically below 2 nm over several micron.

SAW parameters

The most important parameter for SAW device design is the center frequency, which is determined by the period of the IDT fingers and the acoustic velocity.

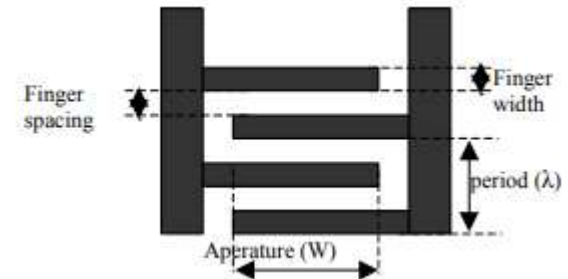
The governing equation that determines the operation frequency is:

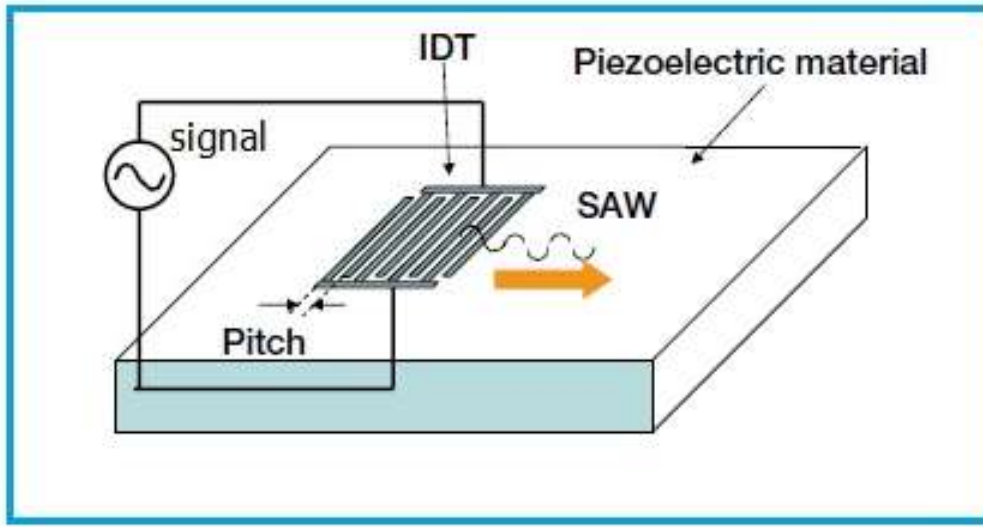
$$f_0 = v_{SAW}/f$$

Where f is the wavelength, determined by the periodicity of the IDT and v_{SAW} is the acoustic wave velocity . For the technology being used in this research:

$$f = p = \text{finger width} \times 4$$

with the finger is determined by the design rule of the technology which sets the minimum metal to metal distance. v_{SAW} is surface acoustic wave velocity.





Electrical signals are transformed into surface acoustic waves with the help of piezoelectric materials. When electric field is applied, piezoelectric material changes shape i.e. gets deformed.

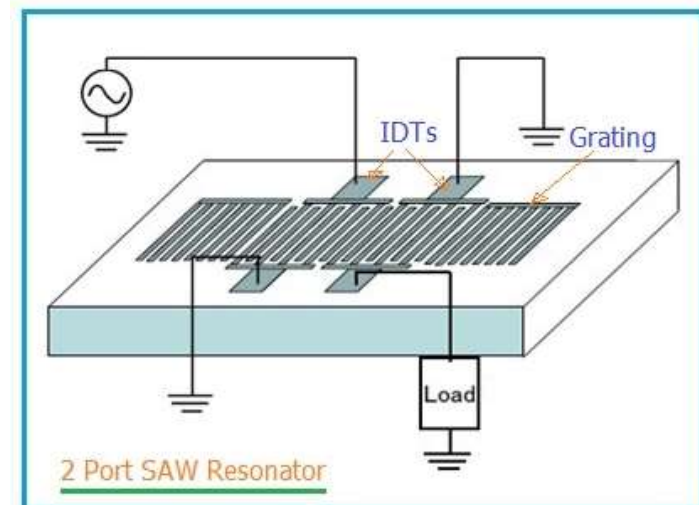
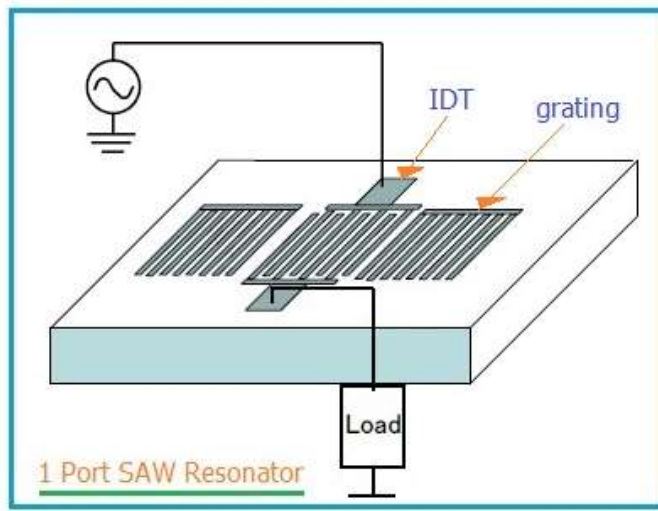
Hence by forming comb shaped electrodes known as IDT (Inter Digital Transducers) and with signal application, SAW waves are generated. This is shown in the figure-1. The velocity of acoustic wave usually depends on substrate type or wave type (rayleigh wave,) used.

The variation in pitch of IDT electrodes will change frequency of generated waves.

What is Resonator?

The device which naturally oscillates (or resonates) at some frequency with higher magnitude is known as resonator. The frequency at which maximum amplitude is obtained is known as resonant frequency or resonance frequency. The oscillations can be either EM (electro-magnetic) or acoustic in nature.

The resonator is used to generate wave at specific frequency or to select particular frequencies from signal. The resonator which uses structure as shown in the figures below are known as SAW resonator.



2 port SAW resonator. It uses two IDTs, one for input and the other for output between the gratings. The 2-port SAW resonator is used as filter due to its propagation characteristics between IDTs.

Acoustic Sensing **Remote Sensing with Sound**

Acoustics is a key component of ocean observation at all scales. This is a result of the rapid attenuation of optical and electromagnetic waves in water that renders useless in the oceans most of the primary remote sensing tools we use in the atmosphere and in space.

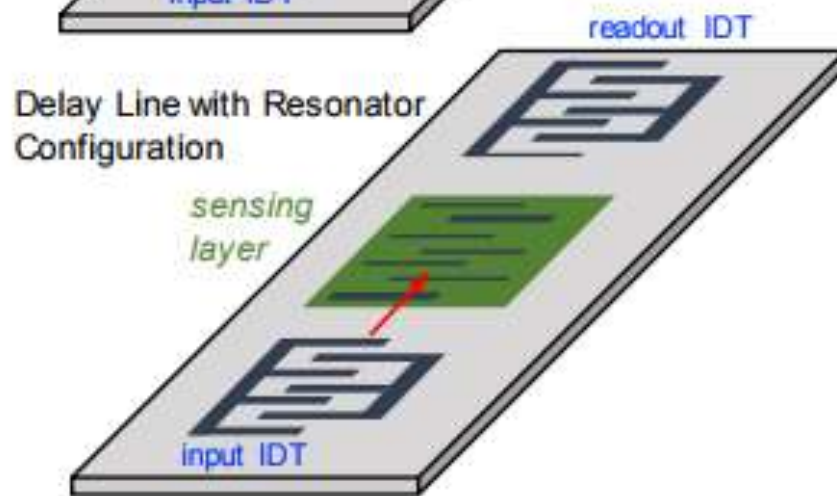
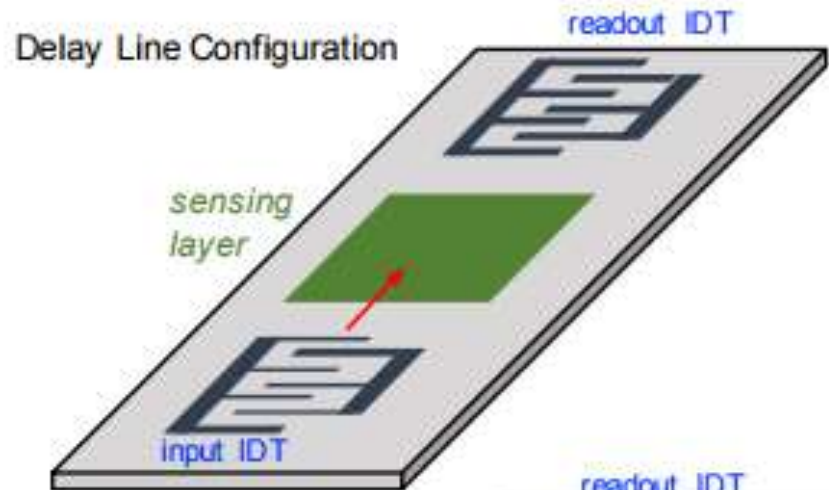
Acoustic waves, on the other hand, can travel great distances underwater. They provide the primary mechanism for remote sensing in the ocean by mankind and many marine creatures.

Approximately 4-5 billion SAW devices are produced each year

SAW-Based Chemical Sensing Fundamentals

The principle behind SAW-based sensing devices is that chemical targets that adsorb on a functionalized surface on the SAW substrate fundamentally change the frequency of the SAW, and measurement of the frequency shift (Δf) can be correlated to the concentration of the target species.

The main advantage associated with SAW sensors is their high sensitivity and capability for the trace detection of a wide variety of chemical materials including bio/chemicals, organic and inorganic vapors, and explosives.

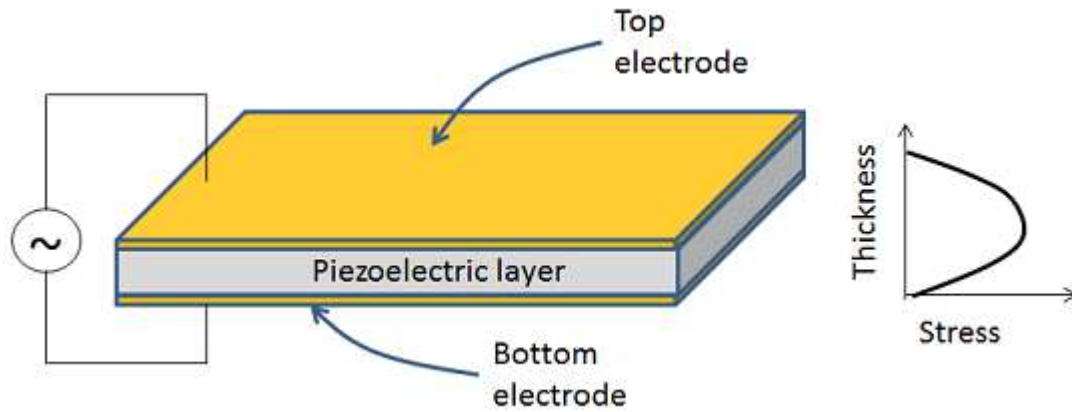


The distance between the input IDT and readout IDT is the delay line, and the sensing layer is deposited in this region of the substrate.

On the bottom is a similar configuration but with additional IDT electrodes beneath the sensing layer. This resonator IDT acts as a reflector to set up a resonant cavity and increase sensitivity.

What is a BAW Resonator?

A BAW resonator is an electromechanical device in which a standing acoustic wave is generated by an electrical signal in the bulk of a piezoelectric material. In the simplest configuration, a device will consist of a piezoelectric material (typically quartz, AlN, or ZnO) sandwiched between two metallic electrodes. The natural frequency of the material and the thickness are used as design parameters to obtain a desired operating frequency.



In a bulk acoustic wave sensor a resonant or standing wave is excited by an AC voltage applied to a piezoelectric crystal. This wave must be shear and therefore have displacement components that are purely transverse to the propagation direction. The allowed wavelengths associated with this wave are directly related to the crystal thickness, t , as follows

$$\lambda_n = 2t/n$$

where $n = 1, 3, 5, \dots$

The displacements associated with $n = 1$ and 3 resonant shear waves are shown in Figure. The $n = 1$ configuration is commonly called the fundamental mode, and the $n = 3, 5, \dots$, configurations are referred to as higher-order harmonics. Note that even though acoustic waves with displacement components in the direction of propagation may be excited, they will not be resonant in this structure. This is due to the fact that energy will be leaked out at the crystal surfaces in the form of longitudinal acoustic waves.

Before describing the details of using a piezoelectric crystal as an acoustic wave sensing platform, methods of exciting the resonant acoustic wave will be discussed. This wave may be excited with a thickness field excitation (TFE) or a lateral field excitation (LFE). In the case of the TFE, metal electrodes are deposited on the top and bottom faces of the piezoelectric

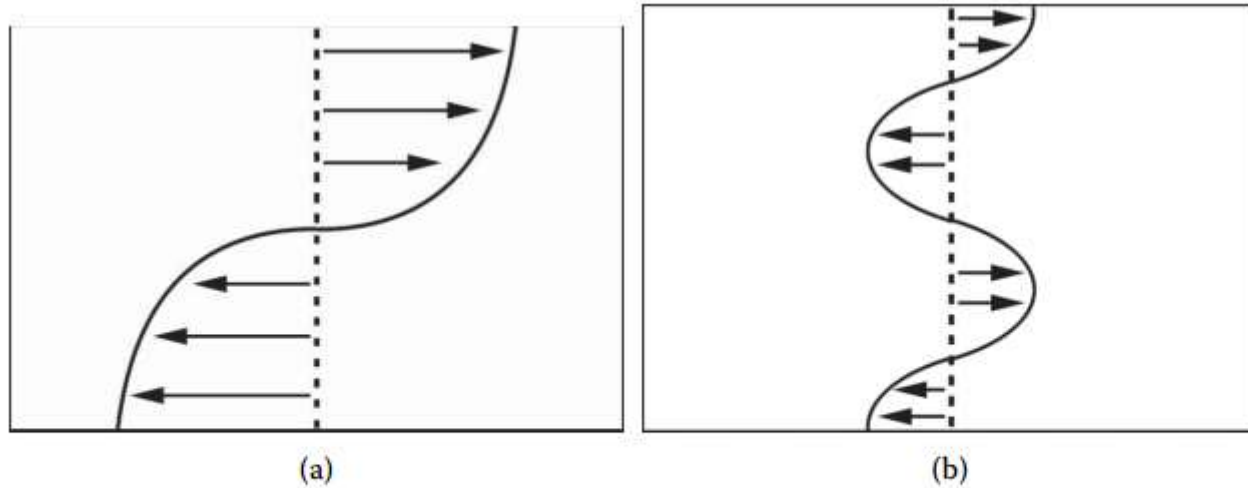
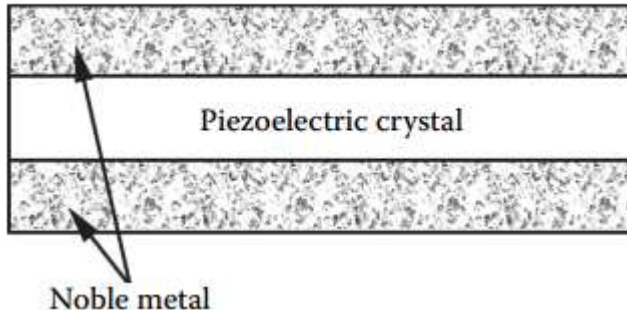


FIGURE 3.24

Displacement associated with the fundamental ($n = 1$) (a) and first-order harmonic ($n = 3$) (b) resonant shear mode in a piezoelectric crystal.

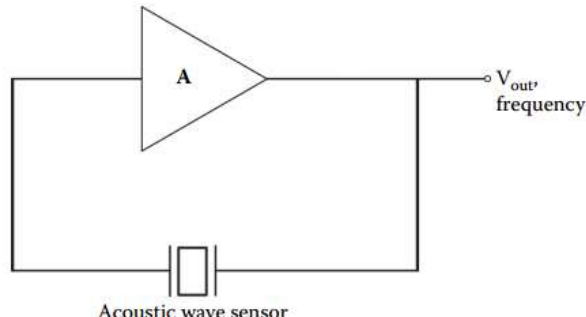
crystal. These electrodes are vacuum deposited noble metals, usually gold. The exact configuration associated with the electrodes could be a gold film on each crystal surface or a more complicated structure, each of which is shown Figure 3.25.



Bulk Acoustic Wave Sensor Response Measurement

The response of resonant bulk acoustic wave sensors to perturbations in the environment is commonly measured in two ways. The acoustic wave sensor can be utilized as the feedback element in a crystal-controlled oscillator, where the frequency and voltage of the output can be measured or the impedance of the acoustic wave sensor can be measured using an impedance analyzer or network analyzer. The advantage of the oscillator configuration is that the measurement system is compact and well suited to remote or portable sensing systems. However, it is possible to measure only two parameters of the oscillator, voltage and frequency. Thus, it is not possible to determine the origin of the response if the sensor is responding to more than two analytes in the environment, or responding to more than two property changes of a single analyte, i.e., viscosity, permittivity, and conductivity changes in a liquid. The measurement of the impedance of the sensor will enable one to determine more exactly the nature of the response. Unfortunately, commercially available impedance analyzers are bulky and not well suited to be remote or portable sensors.

Crystal-controlled oscillator.



Among the piezoelectric substrate materials that can be used for acoustic wave sensors and devices, the most common are quartz (SiO_2), lithium tantalate (LiTaO_3), and, to a lesser degree, lithium niobate (LiNbO_3). An interesting property of quartz is that it is possible to select the temperature dependence of the material by the cut angle and the wave propagation direction.

The advantage of using acoustic waves (vs electromagnetic waves) is the slow speed of propagation (5 orders of magnitude slower). For the same frequency, therefore, the wavelength of the elastic wave is 100,000 times shorter than the corresponding electromagnetic shortwave.

Magnetic sensors: effects and materials



Magnetic sensors account for a significant portion of the sensing market.

Manufactures such as **Honeywell, Phillips, Optek, Cherry, and Infineon** primarily make commercial and automotive sensors while Fujitsu, IBM, Maxtor and Seagate control the information sector additionally, Asahi Chemicals has a significant position in fan speed sensing.

There are **two types of magnetic sensors**.

The first type of magnetic sensor commonly used is the Hall-effect sensor.

The second type of magnetic sensor is the magnetoresistor

On the basis of the materials and structures, MR effects can be classified as

1. *Ordinary magnetoresistance* (OMR) effect in nonmagnetic metals;
2. *Anisotropic magnetoresistance* (AMR) effect in ferromagnetic alloys;
3. *Giant magnetoresistance* (GMR) effect in multiple alternating ferromagnetic-alloy and metallic layer structures;
4. *Tunneling magnetoresistance* (TMR) effect in multiple alternating ferromagnetic-alloy and thin-insulating layer structures;
5. *Ballistic magnetoresistance* (BMR) effect in multiple alternating ferromagnetic-alloy-layer and nonferromagnetic-point structures; and
6. *Colossal magnetoresistance* (CMR) effect in $\text{La}_{1-x}\text{M}_x\text{MnO}_{3+8}$ ($\text{M} = \text{Ca}$ or Sr) perovskite structures.

These commercial devices, manufactured by the above companies, have diverse applications such as **proximity sensors, gear-tooth sensors, and read head sensors**

A search of the United States Patent Data Base shows over **three thousand patents using hall-elements**. Additionally there are over **four hundred patents using magnetoresistors**.

There is an art and a science to building commercial sensors.
Often it takes a diverse group of scientists and engineers to
characterize and model these sensors prior to committing a
design to production.

When a magnetic field is applied to the plate so that it is at right angles to the current flow, as shown in Figure 1-1, a small voltage appears across the plate, which can be measured by the probes. If you reverse the direction (polarity) of the magnetic field, the polarity of this induced voltage will also reverse. This phenomenon is called the Hall effect, named after Edwin Hall.

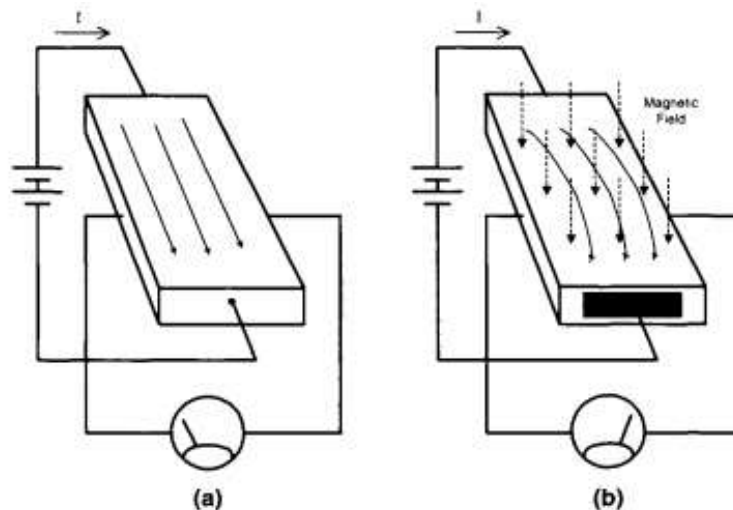


Figure 1-1: The Hall effect in a conductive sheet.

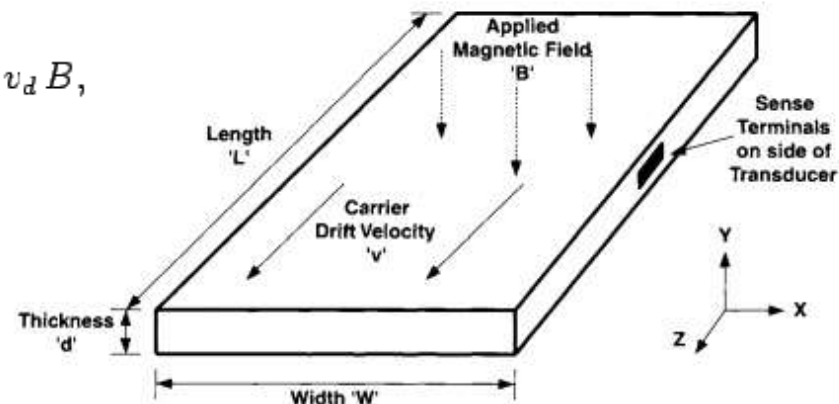
Although the magnetic field forces the charge carriers to one side of the Hall transducer, this process is self-limiting, because the excess concentration of charges to one side and consequent depletion on the other gives rise to an electric field across the transducer. This field causes the carriers to try to redistribute themselves more evenly.

It also gives rise to a voltage that can be measured across the plate. An equilibrium develops where the magnetic force pushing the charge carriers aside is balanced out by the electric force trying to push them back toward the middle.

$$\therefore E = V_H/w.$$

$$qE = \frac{qV_H}{w} = qv_d B,$$

E_H is the Hall electric field across the transducer



which means that the Hall field is solely a function of the velocity of the charge carriers and the strength of the magnetic field. For a transducer with a given width w between sense electrodes, the Hall electric field can be integrated over w , assuming it is uniform, giving us the Hall voltage.

$$V_H = v_d w B.$$

$$I = q n w d v_d,$$

$$V_H = \frac{IB}{qn d}.$$

The Hall voltage is therefore a linear function of:

- a) the charge carrier velocity in the body of the transducer,
- b) the applied magnetic field in the "sensitive" axis,
- c) the spatial separation of the sense contacts, at right angles to carrier motion.

Hall Effect in Metals

Even for the case of a magnetic field as strong as 10,000 gauss, the voltage resulting from the Hall effect is extremely small. For this reason, it is not usually practical to make Hall-effect transducers with most metals.

$$V_H = \frac{IB}{q_0 N d}$$

It can be seen that one means of improvement might be to find materials that do not have as many carriers per unit volume as metals do. A material with a lower carrier density will exhibit the Hall effect more strongly for a given current and depth. Fortunately, semiconductor materials such as silicon, germanium, and gallium-arsenide provide the low carrier densities needed to realize practical transducer elements. In the case of semiconductors, carrier density is usually referred to as carrier concentration.

Material	Carrier Concentration (cm^{-3})
Copper (est.)	8.4×10^{22}
Silicon	1.4×10^{10}
Germanium	2.1×10^{12}
Gallium-Arsenide	1.1×10^7

Consider the case of a transducer consisting of a piece of copper foil, similar to that shown back in Figure 1-1. Assume the current to be 1 ampere and the thickness to be 25 μm (0.001"). For a magnetic field of 1 tesla (10,000 gauss) the resulting Hall voltage will be:

$$V_H = \frac{1\text{A} \cdot 1\text{T}}{1.6 \times 10^{-19}\text{C} \cdot 8.42 \times 10^{28}\text{m}^{-3} \cdot 25 \times 10^{-6}\text{m}} = 3.0 \times 10^{-6}\text{V} \quad (\text{Equation 1-11})$$

Note the conversion of all quantities to SI (meter-kilogram-second) units for consistency in the calculation.

Even for the case of a magnetic field as strong as 10,000 gauss, the voltage resulting from the Hall effect is extremely small. For this reason, it is not usually practical to make Hall-effect transducers with most metals.

Consider a Hall transducer constructed from N-type silicon that has been doped to a level of $3 \times 10^{15}\text{ cm}^{-3}$. The thickness is 25 μm and the current is 1 mA. By substituting the relevant numbers into Equation 1-10, we can calculate the voltage output for a 1-tesla field:

$$V_H = \frac{0.001\text{A} \cdot 1\text{T}}{1.6 \times 10^{-19}\text{C} \cdot 3 \times 10^{21}\text{ m}^{-3} \cdot 25 \times 10^{-6}\text{m}} = 0.083\text{V} \quad (\text{Equation 1-12})$$

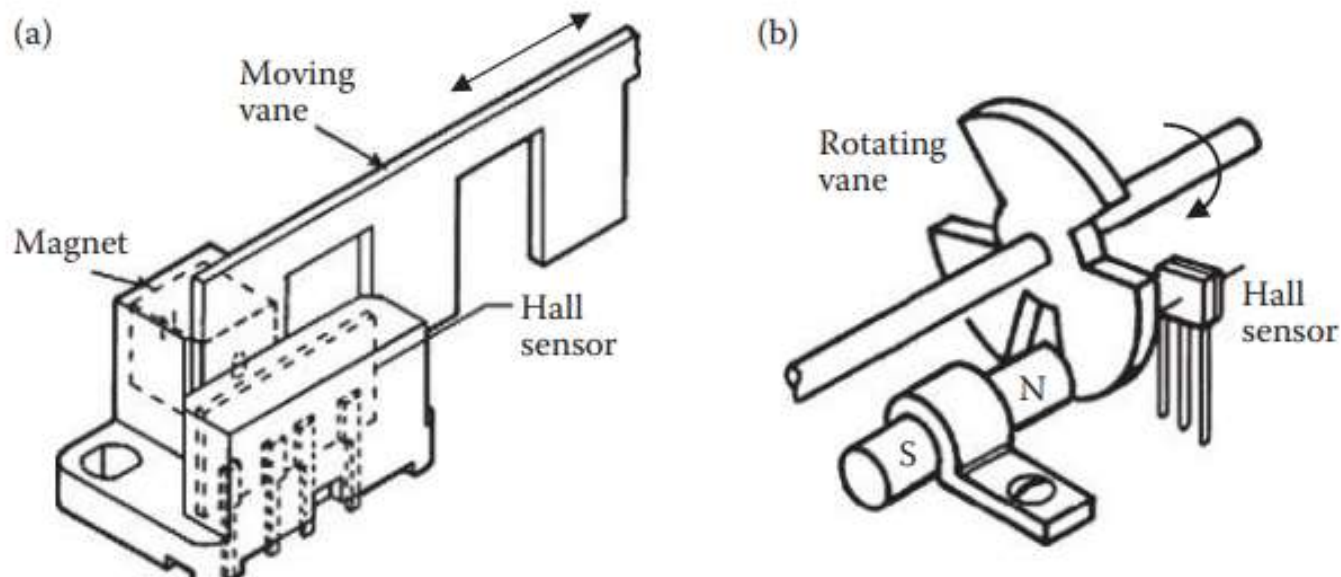
The resultant voltage in this case is 83 mV, which is more than 20,000 times the signal of the copper transducer described previously. Equally significant is that the necessary bias current is 1/1000 that used to bias the copper transducer. Millivolt-level output signals and milliamp-level bias currents make for practical sensors.

Applications of Hall Sensors

Hall sensors are widely used in automobile, security, brushless DC motors, damper control, various instrumentation, or any applications that involve electric current or magnetic field measurements.

High-quality Hall sensors can be constructed inexpensively with the standard IC processes used in the microelectronics industry, and integrate ancillary signal processing circuitry on the same silicon die.

It consists of a magnet and a Hall sensor—both are mounted rigidly in a fixture made of a nonmagnetic material. A ferrous vane can move in and out through the gap, which alters the magnetic flux lines in the gap. The Hall sensor then detects the presence, absence, or position of the vane,



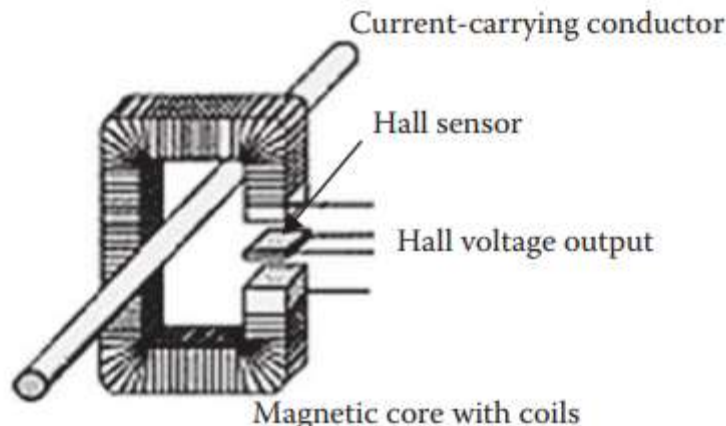
**A Hall angular speed
sensor**

**Allegro Microsystems,
LLC,, Massachusetts,
USA**

**A Hall position sensor,
Honeywell Inc.**

Hall Current Sensor

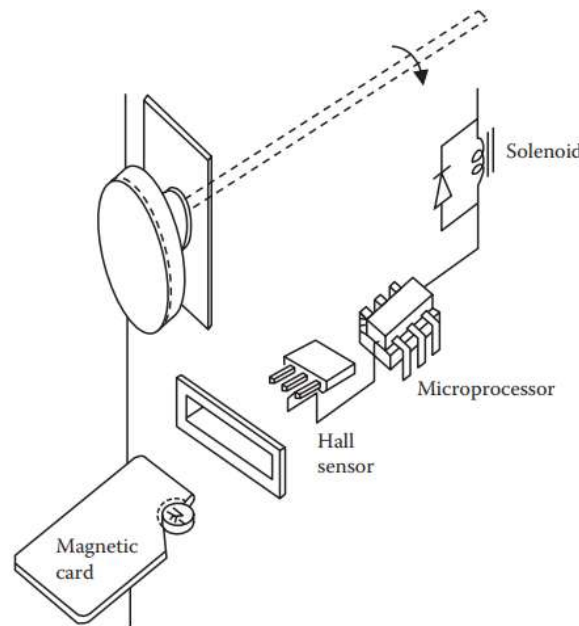
Hall sensors measure current via the intensity of the magnetic field generated by current flow. A larger current produces a stronger magnetic field. A Hall sensor's output voltage is therefore directly proportional to the current. Hall sensors can measure both AC and DC currents, and pulsed waveforms.



A C-core of soft magnetic material is placed around a conductor to concentrate the field. The Hall sensor, placed in the small air gap, delivers a voltage that is proportional to the current in the conductor. Hall current sensors are usually surface-mount types that can be mounted on a PCB to measure the current in the traces. Hall current sensors have advantages. of maintaining galvanic isolation between the sensor and the measuring circuits, and measuring the current without interrupting the circuit.

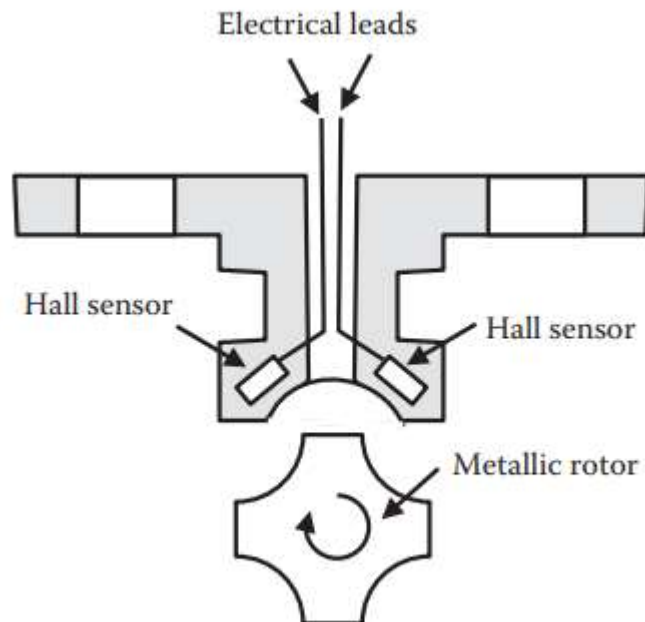
Door Security System

Figure shows a door interlock security system. It consists of a Hall sensor, a magnetic card, an actuator, and a circuit. When the keycard slides by, the Hall sensor detects the magnetic embedded in the card, and then sends an output signal to the microprocessor where the analog signal is converted into digital pulse to pull in the relay to open the door.



Flow Rate Meter

Hall sensors can also be used to measure flow rate . Two Hall sensors measure the rotational velocity of the metal rotor that relates to the flow rate of a liquid transmitted through a pipe. The rotor is modified to have four recessed areas that have magnetic properties on their surfaces. The two Hall sensors pickup the magnetic field changes due to the rotor's rotation, and the signals are converted into the flow rate.

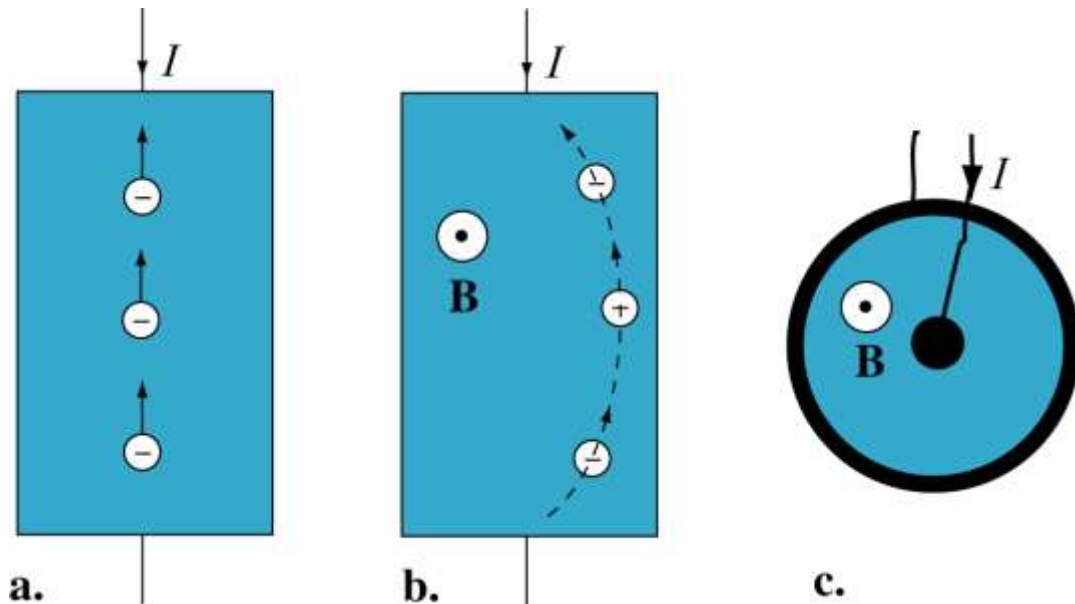


Flow-rate meter using two Hall sensors. (Based on US Patent)

Magnetoresistive sensors

- Two basic principles:
 - Similar to Hall elements
 - The same basic structure is used but
 - No Hall voltage electrodes.
 - The electrons are affected by the magnetic field as in the hall element
 - Because of the magnetic force on them, they will flow in an arc.
-

The magnetoresistive sensor



Magnetoresistive sensors

- The larger the magnetic field, the larger the arc radius
 - Forces electrons to take a longer path
 - The resistance to their flow increases (exactly the same as if the effective length of the plate were larger).
 - A relationship between magnetic field and current is established.
 - The resistance of the device becomes a measure of field.
-

Magnetoresistive sensors

- The relation between field and current is proportional to B for most configurations
- It is dependent on carrier mobility in the material used (usually a semiconductor).
- The exact relationship is rather complicated and depends on the geometry of the device.

Magnetoresistive sensors

- Magnetoresistors are also used where hall elements cannot be used.
- One important application is in magnetoresistive read heads where the magnetic field corresponding to recorded data is sensed.
- Much more sensitive than hall elements

The magnitude of the effect, MR (unit less), depends on the material of the conductor as

$$M_R = \frac{\rho_B - \rho_0}{\rho_0} \times 100\%$$

where ρ_B (in $\Omega \cdot m$) is the resistivity of the conductor under an applied magnetic field B, and ρ_0 (in $\Omega \cdot m$) is the resistivity of the conductor without an applied magnetic field B.

The value of the effect MR is in the order of few percentage points.

On the basis of the materials and structures, MR effects can be classified as

1. *Ordinary magnetoresistance* (OMR) effect in nonmagnetic metals;
2. *Anisotropic magnetoresistance* (AMR) effect in ferromagnetic alloys;
3. *Giant magnetoresistance* (GMR) effect in multiple alternating ferromagnetic-alloy and metallic layer structures;
4. *Tunneling magnetoresistance* (TMR) effect in multiple alternating ferromagnetic-alloy and thin-insulating layer structures;
5. *Ballistic magnetoresistance* (BMR) effect in multiple alternating ferromagnetic-alloy-layer and nonferromagnetic-point structures; and
6. *Colossal magnetoresistance* (CMR) effect in $\text{La}_{1-x}\text{M}_x\text{MnO}_{3+8}$ ($\text{M} = \text{Ca}$ or Sr) perovskite structures.

Ordinary Magnetoresistance (OMR) Effect

OMR effect is present in normal (nonmagnetic) metals. It arises from the effect of Lorentz force acting on an electron in a magnetic field, causing a circular or helical motion of the electron. The resistivity ρ (in $\Omega \cdot m$) to determine the MR value for the OMR effect is

$$\rho = \frac{B}{nqc\omega_c\tau_r}$$

where B is the applied magnetic field strength (in T); n is the electron density of the metal (in m^{-3}); q is the electron charge ($1.602 \times 10^{-19} C$); c is the speed of light ($3 \times 10^8 m \cdot s^{-1}$); ω_c is the cyclotron frequency (in $rad \cdot s^{-1}$); and τ_r is the electron relaxation time (the mean time between collisions, in s). ω_c can be found by

$$\omega_c = \frac{qB}{m^*c} \quad (5.10)$$

where m^* is the *effective mass* of an electron (in kg). Thus, the resistivity becomes

$$\rho = \frac{m^*}{nq^2\tau_r} \quad (5.11)$$

In Equation 5.9, $\omega_c\tau_r$ is the dominant factor for the OMR effect. In metals, such as Cu, Ag, and Au, the dependence of $\omega_c\tau_r$ value on magnetic field can be approximately described by $\omega_c\tau_r \approx 0.005B$. Thus, their OMR value is smaller than 1% under 1 T. To have a substantial M_R , $\omega_c\tau_r$ should be at least of order 1. Research has found that for some metals (e.g., Bi) the $\omega_c\tau_r$ value can be increased up to 100 times [7].

Anisotropic Magnetoresistance (AMR) Effect

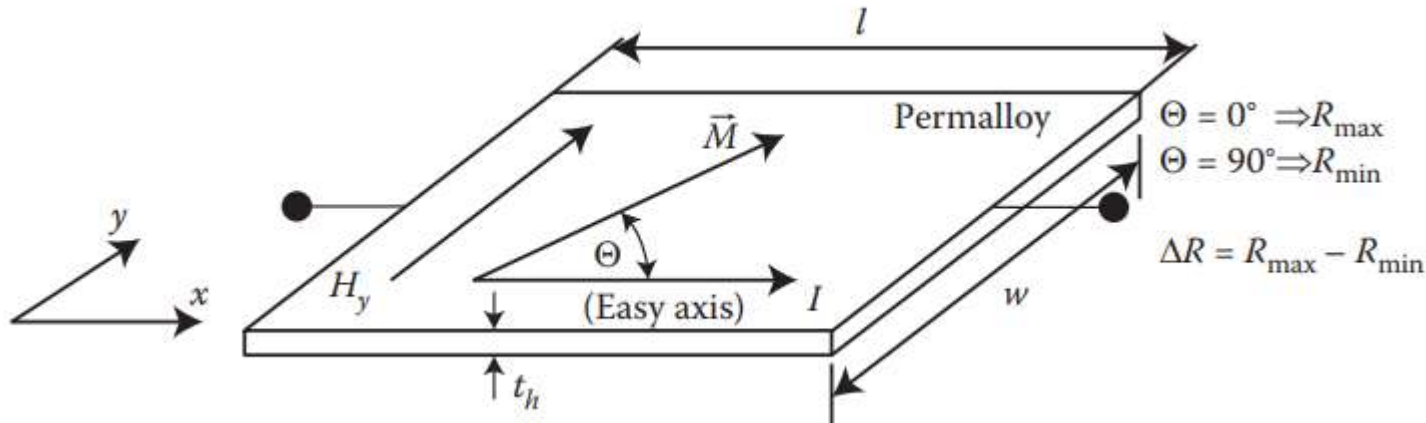
AMR, discovered in 1857 by William Thomson, is a typical effect in ferromagnetic (FM) materials. The term anisotropic is from the dependence of the resistivity on the orientation of the magnetic field relative to the current direction Θ .

Mathematically it is expressed by:

$$\rho(\Theta) = \rho_0 + \Delta\rho \cos^2 \Theta$$

where ρ_0 is the resistivity of the material without an applied magnetic field, and $\Delta\rho (= \rho(0^\circ) - \rho(90^\circ))$ is the resistivity difference between the parallel ($\Theta = 0^\circ$) and perpendicular ($\Theta = 90^\circ$) relationship between the current direction and the applied magnetic field direction. Thus, the resistance is at maximum when the current and the magnetic field directions are parallel and is at minimum when their directions are perpendicular. The AMR effect reflects the change of electron scattering in the atomic orbitals due to a magnetic field.

The dependence of the sensor resistance R on the angle Θ is described by



The MR effect in permalloy

$$R(\Theta) = \underbrace{\rho_{\perp} \frac{l}{wt_h}}_{R_0} + \underbrace{(\rho_{||} - \rho_{\perp}) \frac{l}{wt_h}}_{\Delta R} \cos^2 \Theta = R_0 + \underbrace{(R_{\max} - R_{\min})}_{\Delta R} \cos^2 \Theta$$

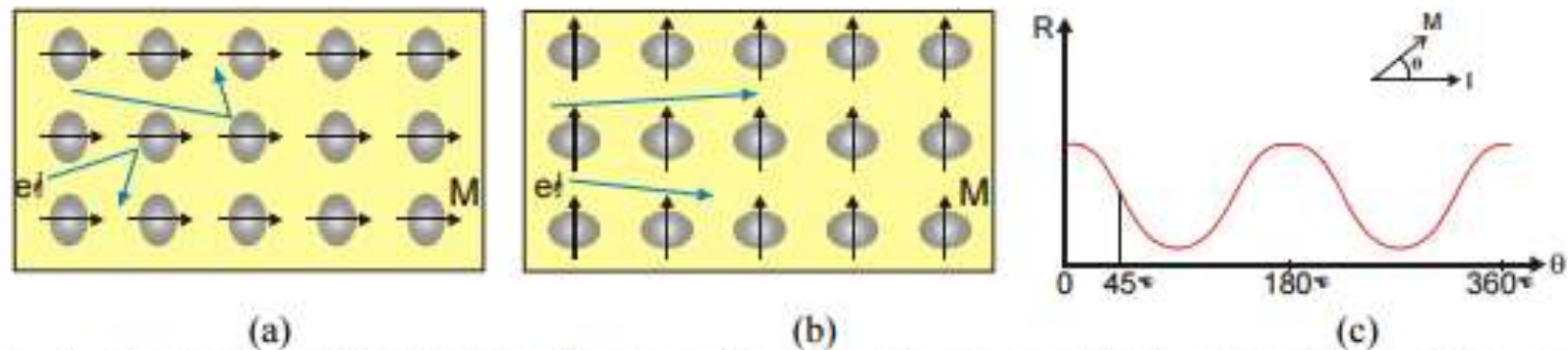
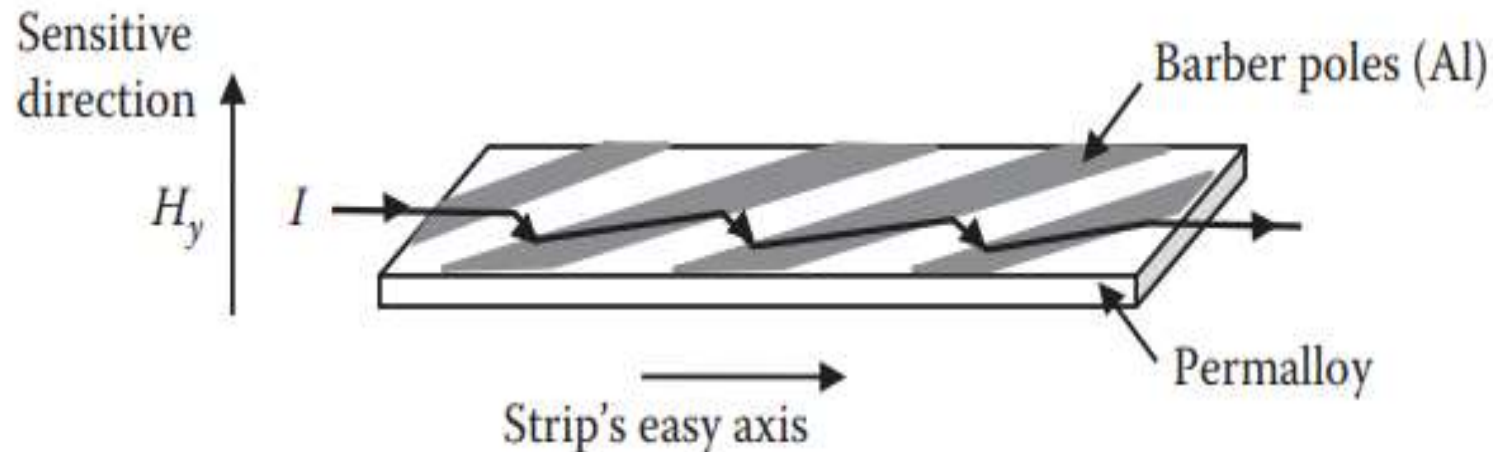


Fig. 1. Illustration of AMR effect showing distortion of electron orbitals and resulting difference in scattering when the magnetization is (a) parallel to the current or (b) perpendicular to the current direction. (c) Variation of resistance as a function of angle between the current and magnetization. The optimum operating point is at 45° .



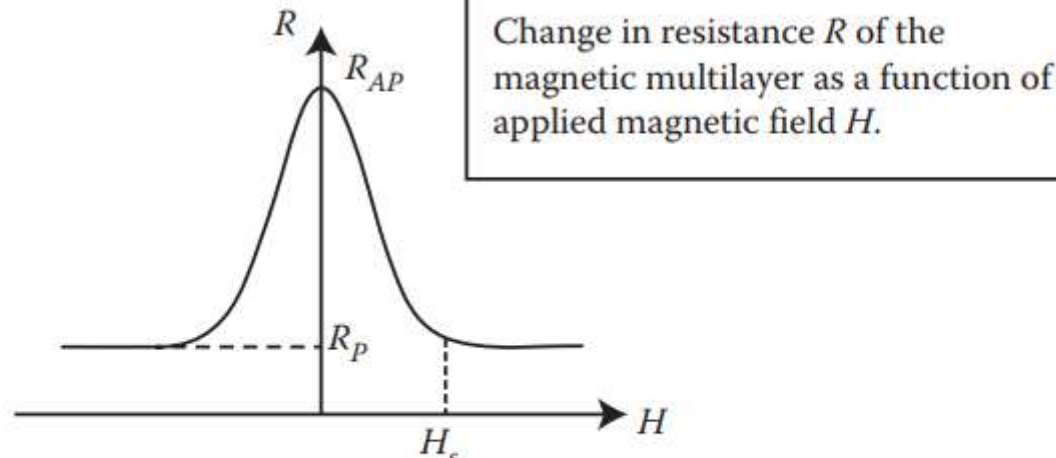
Giant Magnetoresistance (GMR) Effect

Baibich et al. and Binasch et al. are the first who reported “Giant” magnetoresistance measured on Fe/Cr/Fe thin multilayers.

They demonstrated that the electric current was strongly influenced by the relative orientation of the magnetizations of the magnetic layers. The cause of this giant change in resistance is attributed to the scattering of the electrons at the layers’ interfaces. Thus, any structure with metal–FM interfaces is a candidate to display the GMR effect. Since then, a huge effort has been carried out on improving structures to maximize the effect.

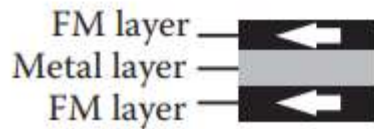
Today above 200% of MR value can be achieved at room temperature, which is much higher than the MR value of either OMR or AMR effect.

(a)



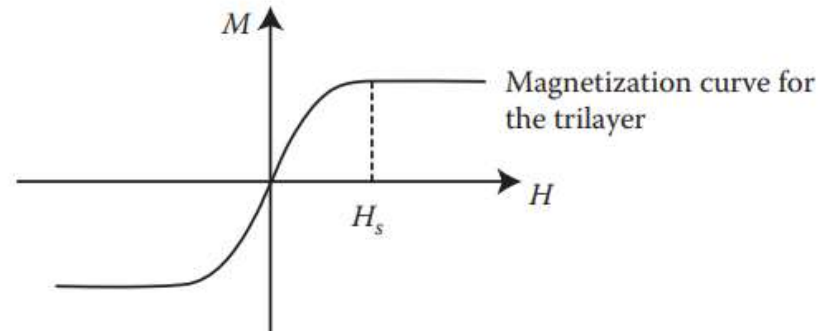
Change in resistance R of the magnetic multilayer as a function of applied magnetic field H .

(b)



Three magnetization configurations:
parallel, antiparallel, and parallel

$$M_R \text{ (for GMR)} = \frac{R_{AP} - R_P}{R_P} \times 100\%$$



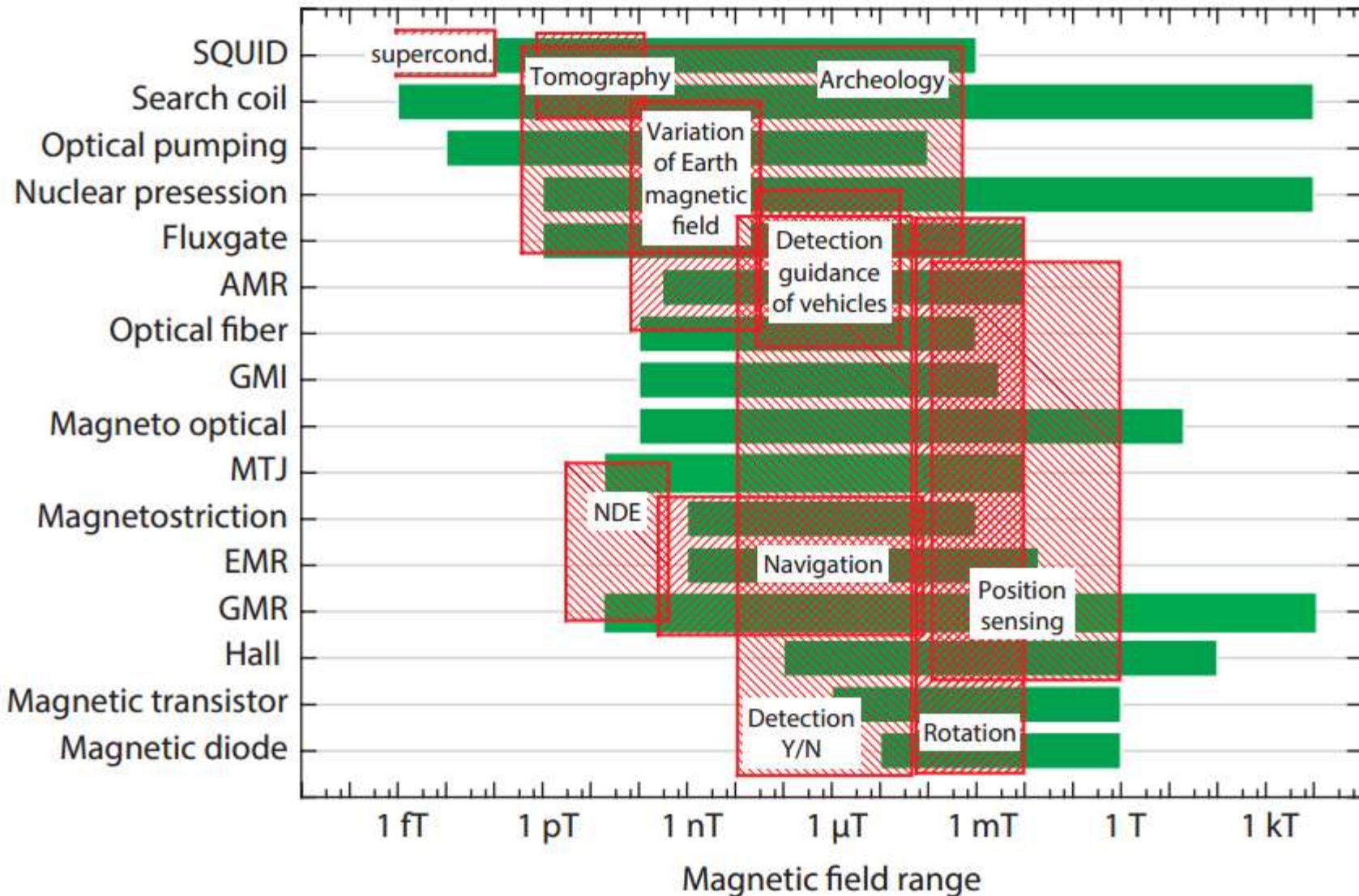
The change in electrical resistance can be made to over 200% of MR, depending on the number and thickness of layers, materials, and manufacturing processes.

Comparison of MR Effects

MR Effect	$\Delta R/R$ (%)	B (T)	Mechanism	Comments
OMR	<1	1 T (metal)	Lorentz force	There is no saturation at large magnetic field.
AMR	1–5	0.5 mT–1 T (depend on bulk or wire permalloy)	Electron spin–orbit interaction (leads to scattering of conducting electrons).	R is directly related to the orientation of magnetization M relative to current I .
GMR	10–200	1–10 T	Spin-dependent electron transport. In FM-metal-FM alternating layer structure.	Interface quality is crucial. They are broadly applied in sensors and read-heads of magnetic hard disks.

The discovery of giant magnetoresistance (GMR) by Albert Fert and Peter Grünberg in 1988 raised MR sensors' maximum MR value from 2–5% to 10% or more , a feat honored by the 2007 Nobel Prize in Physics.

Range of applications of different magnetic field sensors



Integrated Hall sensors



The first Hall effect magnetic sensors became commercially available in the mid-1950s, a few years after the discovery of high-mobility compound semiconductors. Since then, the development of Hall effect devices has taken advantage of using high-quality materials and sophisticated, highly productive fabrication methods available in the microelectronics industry.

Today, Hall effect magnetic sensors form the basis of a mature and important industrial activity. They are mostly used as key elements in contactless sensors for linear position, angular position, velocity, rotation, electrical current, end so on Most of currently produced Hall magnetic sensors are discrete elements; but the sales of discrete Hall elements stagnates, whereas the sales of integrated Hall sensors grows at more than 10 % per year. Integrated Hall magnetic sensors are ‘smart’: they incorporate electronic circuits for biasing, offset reduction, compensation of temperature effects, signal amplification, and more. The integration helps improve sensor sys-tem performance at moderate costs, which allows a continuous penetration of Hall magnetic sensors into new application areasA great majority of integrated circuits (IC) have been made of silicon. Silicon IC technology is very mature, easily accessible and low cost. This makes this technology very attractive for the realization of Hall plates, in spite of moderate mobility of electrons in silicon. We shall now describe a few conventional structures of Hall devices fabricated with the aid of silicon integrated circuit technology. The conventional Hall plates are parallel with the chip surface; so considering a chip as an ocean in which floats a Hall plate, we say that such a Hall plate is ‘horizontal’. ~~Horizontal Hall plates are sensitive to the magnetic field perpendicular to the chip plane~~

MOS Hall effect devices

The idea of implementing a Hall device in the form of an MOS device looks especially attractive for sensor applications: such a device is readily integrable with MOS bias and signal-processing circuits.

Unfortunately, an MOS Hall effect device also has a few serious drawbacks: the carrier mobility in the channel amounts to only half its value in the bulk.

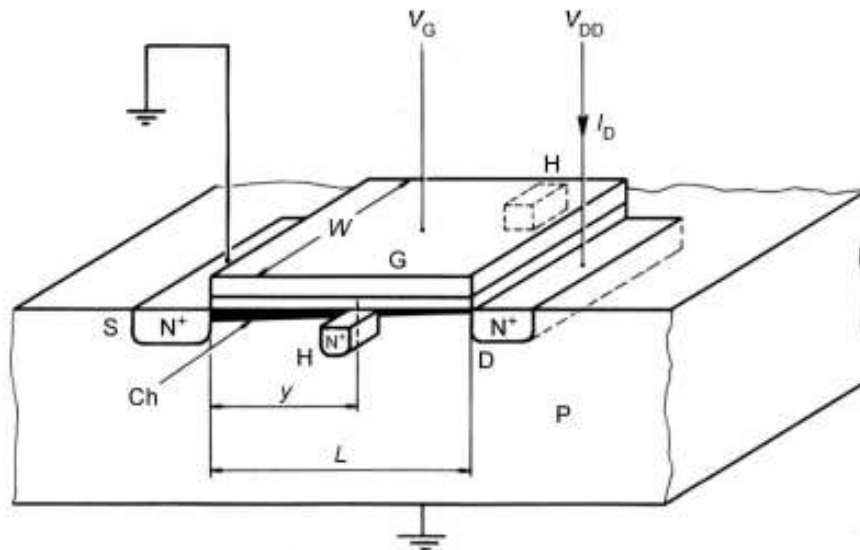


Figure 7.1. MOS Hall plate: the channel (Ch) of a MOSFET is exploited as an extremely thin conductive plate. Two Hall voltage probes H are added to the usual MOSFET structure. (Adapted from [1]. © 1986 IEEE.)

thin Hall plate, the source (S) and drain (D) as the biasing contacts, and the two additional heavily doped regions (H) are provided for sensing the Hall voltage (compare with figure 5.7). The two sense regions are fabricated simultaneously with the source and drain regions. The channel length is L, its width is W, and the sense probes are positioned at a distance y from the source.

Let us now consider the operation of an MOS Hall device in the Hall voltage mode. An MOS Hall plate working in the linear region is equivalent to a conventional Hall plate. The only difference is that, in a conventional Hall plate, the charge carriers in the plate are provided by the material itself; and in an MOS Hall plate, the charge carriers are due to the surface field effect.

$$V_H \simeq \mu_{ch} \frac{W}{L} G_H V_D B_{\perp}$$

At a higher drain voltage, the channel charge in the MOS Hall plate decreases with an increase in the distance from the source 'y'. The lower the channel charge, the higher the Hall electric field. Therefore, if we could neglect the short-circuiting effect by the supply electrodes, the Hall voltage would steadily increase by moving the sense contacts towards the drain.

At very low drain voltages, when

$$V_D \ll V_G - V_T \quad (7.1)$$

the area density of carriers in the channel is approximately constant over the channel. This charge density is given by

$$Q_{ch} \simeq C_{ox}(V_G - V_T) \quad (7.2)$$

where C_{ox} denotes the gate oxide capacitance per unit area. Then the drain current is given by

$$I \simeq \frac{W}{L} \mu_{ch} C_{ox} (V_G - V_T) V_D \quad (7.3)$$

where μ_{ch} denotes the drift mobility of carriers in the channel. This is the linear region of operation of a MOSFET.

At higher drain voltages, the carrier charge density in the channel continuously decreases with increasing distance from the source. The drain current is generally given by

$$I \simeq \frac{W}{L} \mu_{ch} C_{ox} [(V_G - V_T) V_D - \frac{1}{2} V_D^2] \quad \text{for } V_D \leq V_G - V_T. \quad (7.4)$$

When the drain voltage reaches the value

$$V_{Dsat} \simeq V_G - V_T \quad (7.5)$$

the carrier density at the drain end of the channel reduces virtually to zero. This is the pinch-off point. Beyond the pinch-off point, the drain current stays essentially constant. The saturated drain current is given by I_{Dsat} (V_{Dsat}) according to (7.4) and (7.5).

Magnetotransistors (BJT)

A magnetotransistor is a bipolar junction transistor (BJT) whose structure and operating conditions are optimized with respect to the magnetic sensitivity of its collector current.

The magnetic sensitivity of a magnetotransistor is usually defined

$$S_I = \left| \frac{1}{I_c} \frac{\Delta I_c}{B} \right|. \quad (7.15)$$

Here, I_c denotes the collector current, and ΔI_c is the change in the collector current due to a magnetic induction B :

$$\Delta I_c = I_c(B) - I_c(0). \quad (7.16)$$

The sensitivities of magnetotransistors reported hitherto cover a surprisingly wide range: from 10^{-2} to over 10 T^{-1} . This large spread of sensitivities indicates that the operation of various magnetotransistors is based on different effects. Indeed, the Hall effect may interfere with the action of a bipolar transistor in many ways and give rise to different end effects. The following three major end effects may be distinguished:

- The current deflection effect. This is essentially the same effect that we studied in large-contact Hall plates.
- The injection modulation. The Hall voltage generated in the base region of a magnetotransistor modulates the emitter-base voltage, and thus also the carrier injection.
- The magnetodiode effect. The emitter-base diode of a transistor may function as a magnetodiode. This leads to a magnetic sensitivity of collector current. In principle, these three effects coexist and cooperate in any magnetotransistor.

The magnetodiode effect comes about as a result of the cooperation of the Hall effect and a few other effects pertinent to a p–n junction diode. The basic effects are: the conductivity modulation due to a high injection level ; the current deflection ; and the magnetoconcentration effect

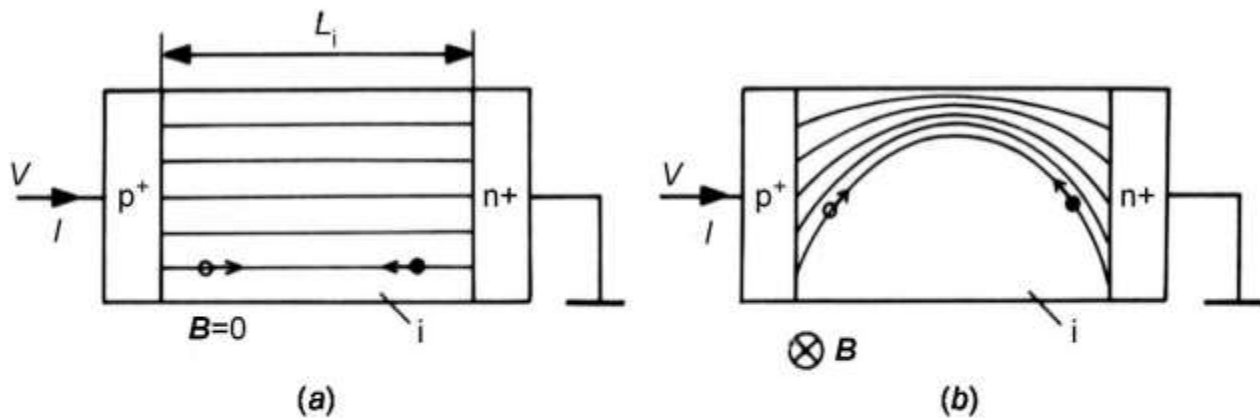


Figure 7.10. Current density lines in a magnetodiode with volume recombination. (a) No magnetic field; (b) a magnetic field perpendicular to the drawing plane is present. Then both electrons (●) and holes (○) are deflected towards the same boundary of the slab, and the current lines get longer.

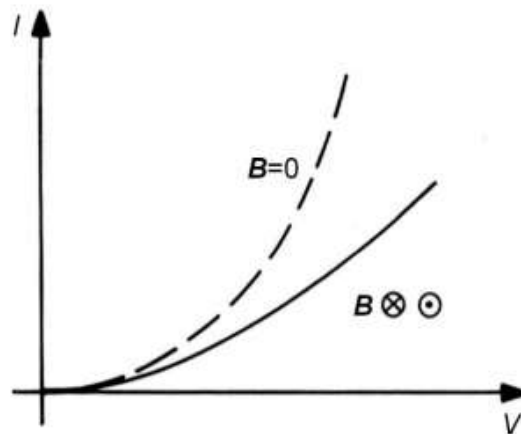


Figure 7.11. Current–voltage characteristics of a magnetodiode with volume recombination. At a constant bias voltage, a magnetic field causes a decrease in diode current, irrespective of the sign of the magnetic field.

The current in the magnetodiode decreases in the presence of a magnetic field. The lower the current, the lower the injection level and the higher the resistance of the i-region. Then the larger portion of the diode voltage drops across the i-region, the voltage across the injecting junctions decreases, and the diode current decreases. Thus at a high injection level, a magnetic field triggers a cumulative process of current reduction, which greatly boosts the magnetic sensitivity of the magnetodiode.

Magnetodiodes have been made of various semiconductors, including germanium, silicon and GaAs. Early devices were discrete

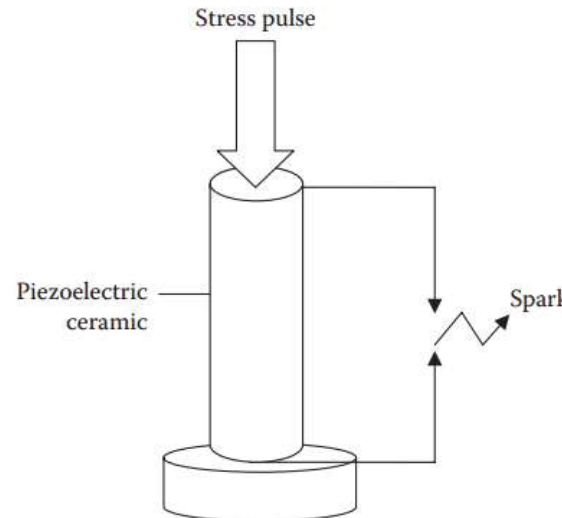
REQUIREMENTS OF PIEZOELECTRIC MATERIALS FOR SENSORS

- high piezoelectric sensitivity,**
- high mechanical strength,**
- high rigidity (high modulus of elasticity),**
- high electric insulation resistance (also at high temperatures),**
- minimal hygroscopicity,**
- linear relationship between mechanical stress and electric polarization,**
- absence of hysteresis,**
- high stability of all properties,**
- low temperature dependence of all properties within a wide temperature range,**
- low anisotropy of mechanical properties, such as thermal expansion coefficients**
- and elastic constants,**
- good machinability,**
- low production cost.**

Gas Lighter

A gas lighter is a common piezoelectric household device which makes use of the direct piezoelectric effect to generate electric sparks.

In a gas lighter, a high voltage pulse is required to be generated across a narrow electrode gap. A piezoelectric gas lighter consists of a PZT cylinder which is subjected to a stress pulse using a spring mechanism. When a button is pressed, a stress pulse is applied on the piezoelectric cylinder. The stress causes a high voltage to be generated which is made to appear across a small air gap between two closely spaced electrodes. The arrangement is shown in Figure 4.1. The voltage developed is high enough to cause breakdown of the air gap between the two electrodes, resulting in a spark.



Piezoresistivity

Piezoresistivity derives its name from the Greek word *piezin*, meaning “to press.” It is an effect exhibited by various materials that exhibit a change in resistivity due to an applied pressure. The effect was first discovered by Lord Kelvin in 1856, who noted that the resistance of copper and iron wires increased when in tension. He also observed that iron wires showed a larger change in resistance than those made of copper. The first application of the piezoresistive effect did not appear until the 1930s, some 75 years after Lord Kelvin’s discovery. Rather than using metal wires, these so-called strain gauges are generally made from a thin metal foil mounted on a backing film, which can be glued onto a surface. A typical metal foil strain gauge is depicted in Figure 5.1.

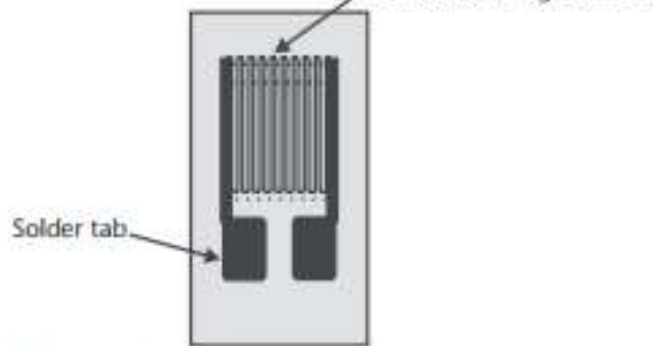


Illustration of a metal foil strain gauge.

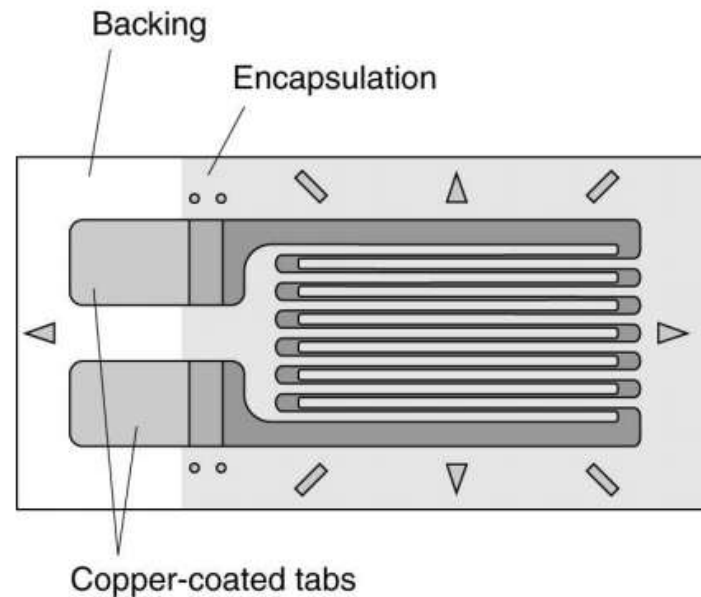
The strain gage is the most frequently used resistive sensor. A typical strain gage is shown in figure The gage consists of a very fine, etched wire of length L that winds back and forth over a flat, insulating sensing area. For the strain gage shown, there are 12 wire segments, yielding a total wire length of 12 cm.

A local gage factor, G_l , can be defined as the ratio of the relative resistance change to the relative length change,

$$G_l = \frac{dR/R}{dL/L}.$$

An engineering gage factor, G_e , can be defined as

$$G_e = \frac{\Delta R/R}{\Delta L/L}.$$

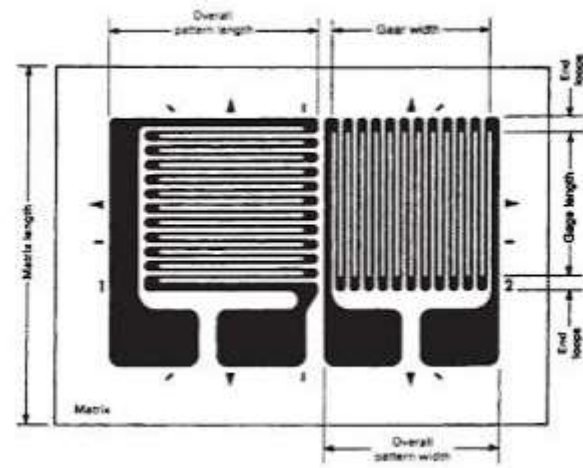


Different forms of metal foil strain gauges

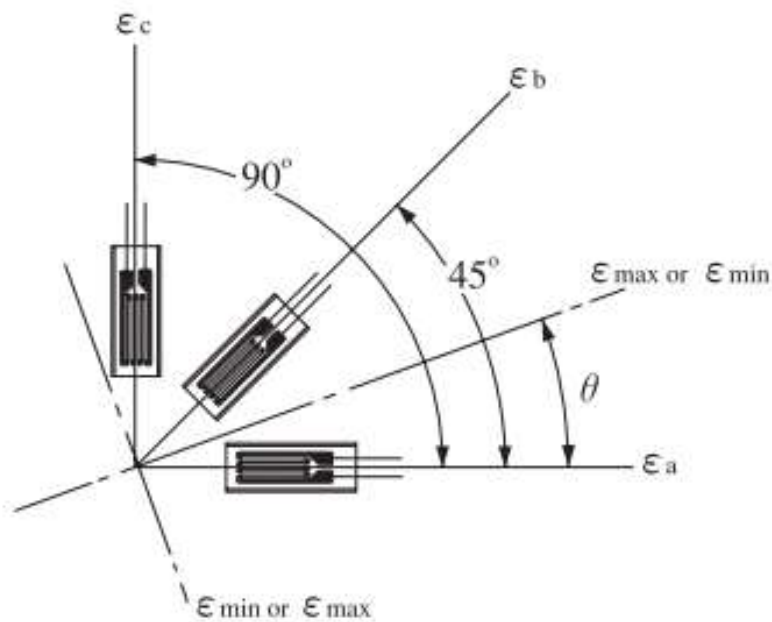
A two-element 90° rosette-type foil gage.

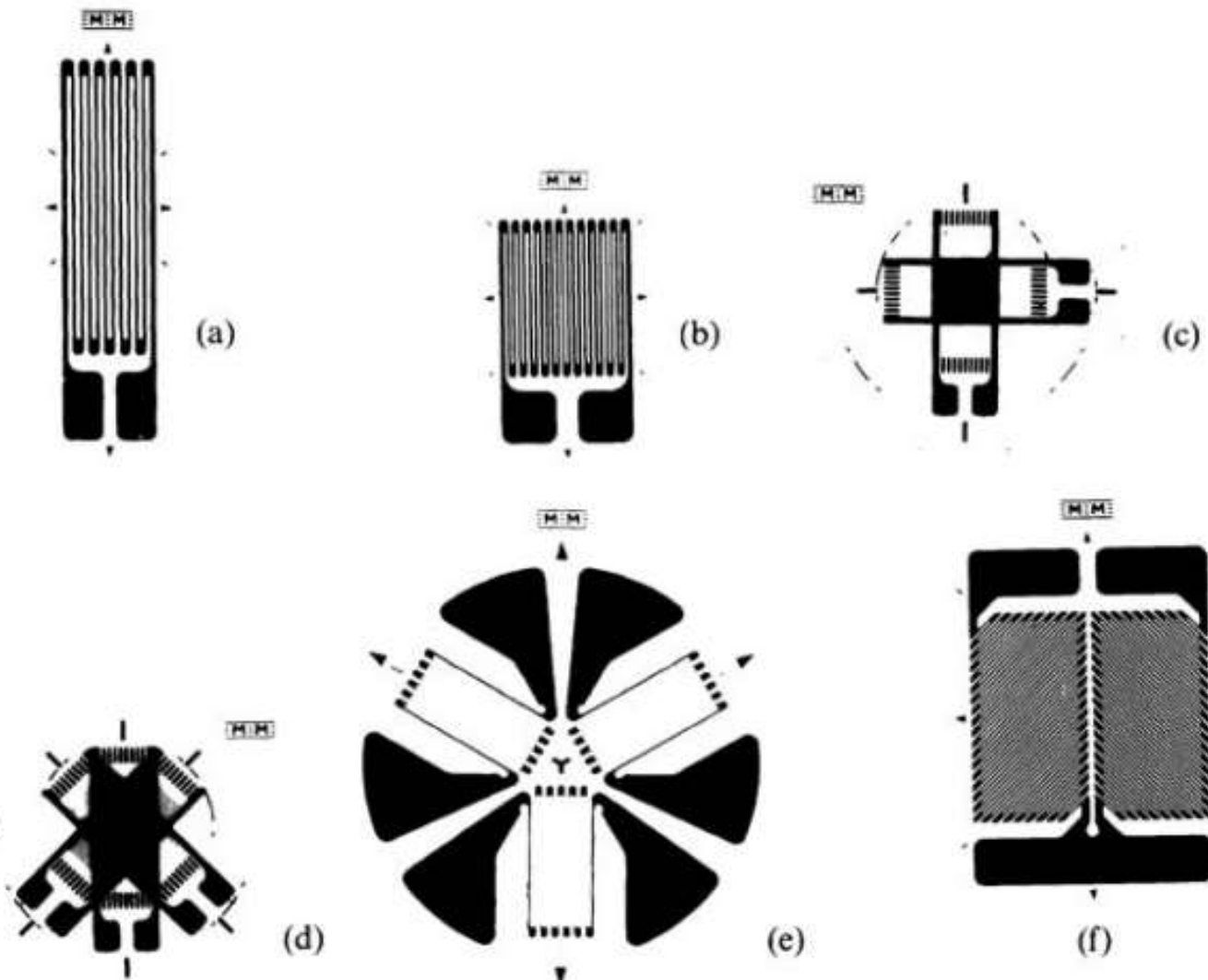
When a force or pressure is applied to the sensing element of metal foil strain gauge the physical dimensions of it will change.

Since, the strain gauge element is pasted on its surface, the dimensions of the strain gauge changes due to which the resistance of the gauge changes.



If we want to measure the strain in two or more directions at the same point, strain gage rosette, which is manufactured by stacking multiple strain gages in different directions, is used. Fig shows a three-element strain gage rosette stacked at 45^0 .





Foil strain gages, (a, b) Single-element gages, (c) Stacked two-element rectangular rosette, (d) Stacked three-element rectangular rosette, (e) Three-element delta rosette, (f) Two-element rectangular rosette torque gage

The sensitivity of a strain gauge is generally termed the gauge factor. This is a dimensionless quantity and is given by

$$GF = \frac{\text{relative change in resistance}}{\text{applied strain}} = \frac{\Delta R / R}{\Delta L / L} = \frac{\Delta R / R}{\epsilon} \quad (5.1)$$

where R is the initial resistance of the strain gauge and ΔR is the change in resistance. The term $\Delta L/L$ is, by definition, the applied strain and is denoted as ϵ (dimensionless). For all elastic materials, there is a relationship between the stress $\sigma(\text{N/m}^2)$ and the strain ϵ ; that is, they obey Hooke's law and thus deform linearly with applied force. The constant of proportionality is the elastic modulus or Young's modulus of the material and is given by

$$\text{Young's modulus, } E = \frac{\text{Stress}}{\text{Strain}} = \frac{\sigma}{\epsilon} (\text{N/m}^2) \quad (5.2)$$

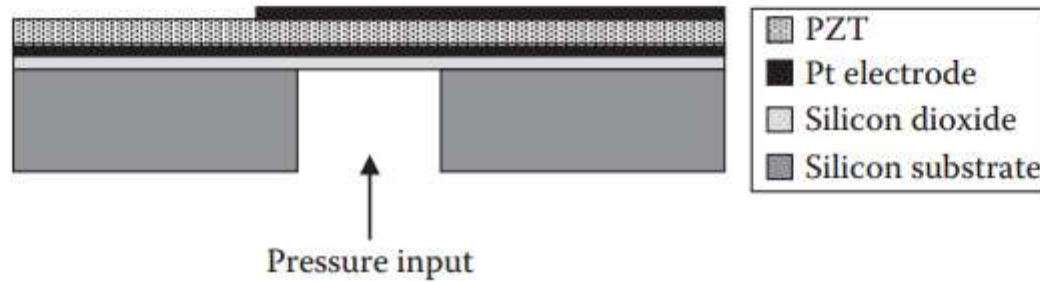
The Young's modulus of silicon is 190 GPa (1 Pa = 1 N/m²), which is close to that of typical stainless steel (around 200 GPa). For a given material, the higher the value of Young's modulus, the less it deforms for a given applied stress (i.e., it is stiffer).

Thick-film resistors, often used in hybrid circuits, have also been shown to be piezoresistive. Their gauge factor is around 10, and therefore, they offer a sensitivity between that of a semiconductor and foil strain gauge. The TCR is around 100 parts per million (ppm) per degree Celsius and matching between adjacent resistors is often less than 10 ppm/°C, making them well suited for use as active elements in Wheatstone bridge circuits, which reduce the overall temperature sensitivity.

An associated effect that has been observed in semiconductors is the so-called piezojunction effect, whereby a shift in the I-V characteristic of a *p-n* junction is observed as a result of an applied stress. Although this is an interesting physical effect, it has found little use in commercial micromachined devices.

Basic design of piezoresistive silicon pressure sensors

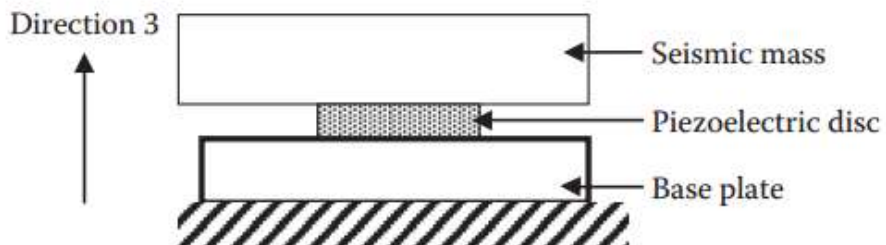
A quartz crystal piezoelectric pressure sensor. Courtesy: Intertechnology Inc.—Testing and Measurement Solutions, Ontario, Canada.



MEMS.PZT.pressure.sensor.

Accelerometer

Accelerometers are used for measurement of vibrations in many applications which include impact acceleration levels experienced by vehicles during crash, shock experienced by space vehicles and cargo during stage separation, testing of shock resistance of packaged products, vibrations in mining activities, seismic vibrations during earthquakes, etc.



When the system is subjected to acceleration, the seismic mass exerts a force F on the piezoelectric disc given by

$$F = Ma \quad (4.3)$$

where a is the acceleration experienced by the disc. The mechanical stress in direction 3 on the piezoelectric disc is given by

$$X_3 = \frac{F}{A} = \frac{Ma}{A} \quad (4.4)$$

where A is the area of the disc. The mechanical stress causes an electric field E to be generated across the thickness of the disc given by (Equation 2.4)

$$E_3 = g_{33} X_3 \quad (4.5)$$

The open circuit voltage across the piezoelectric disc of thickness t will be

$$V = E_3 t = g_{33} X_3 t \quad (4.6)$$

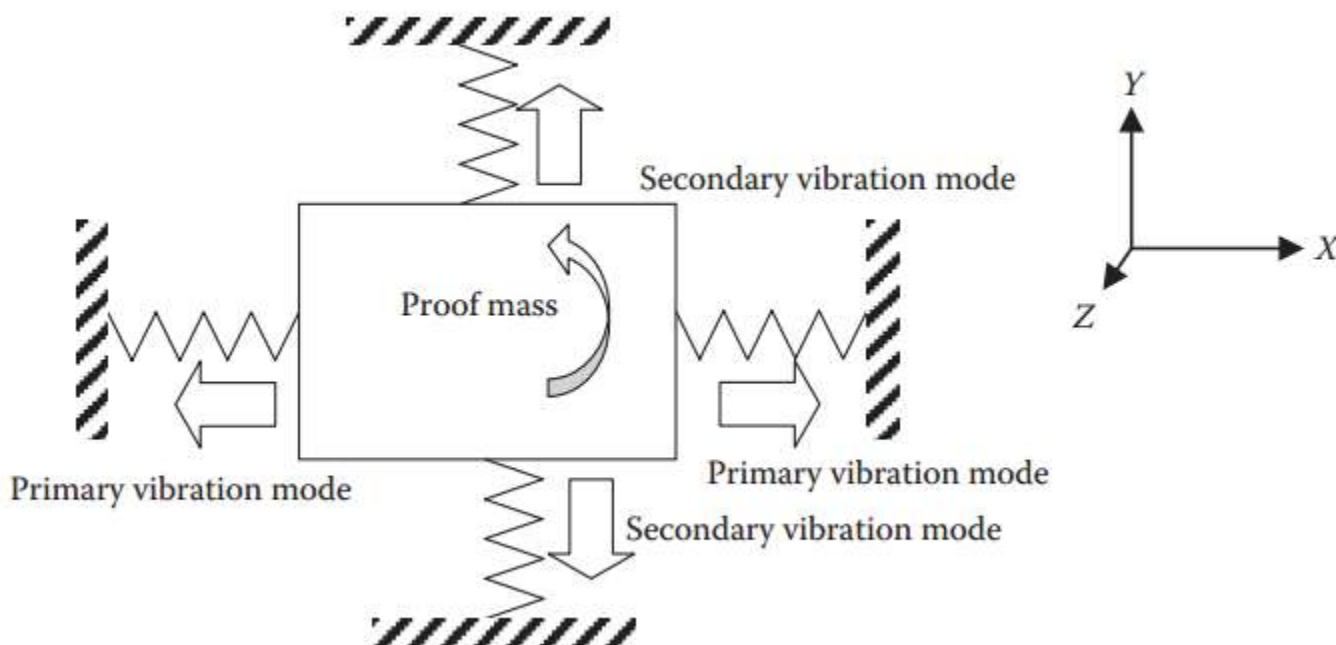
Substituting for X_3 from Equation 4.4,

$$V = g_{33} \frac{t}{A} Ma \quad (4.7)$$

The output voltage is proportional to the acceleration. The proportionality constant is determined by the seismic mass M , the piezoelectric coefficient g_{33} , and the dimensions of the piezoelectric disc.

Piezoelectric Gyroscope

Gyroscopes are devices used for measuring the angular rate of rotating objects. They have several engineering applications: in automobiles they are used for stability control, navigation assistance, and rollover detection; in marine engineering, they are used for stabilization and navigation of ships and in military applications for missile stabilization and guidance. There are



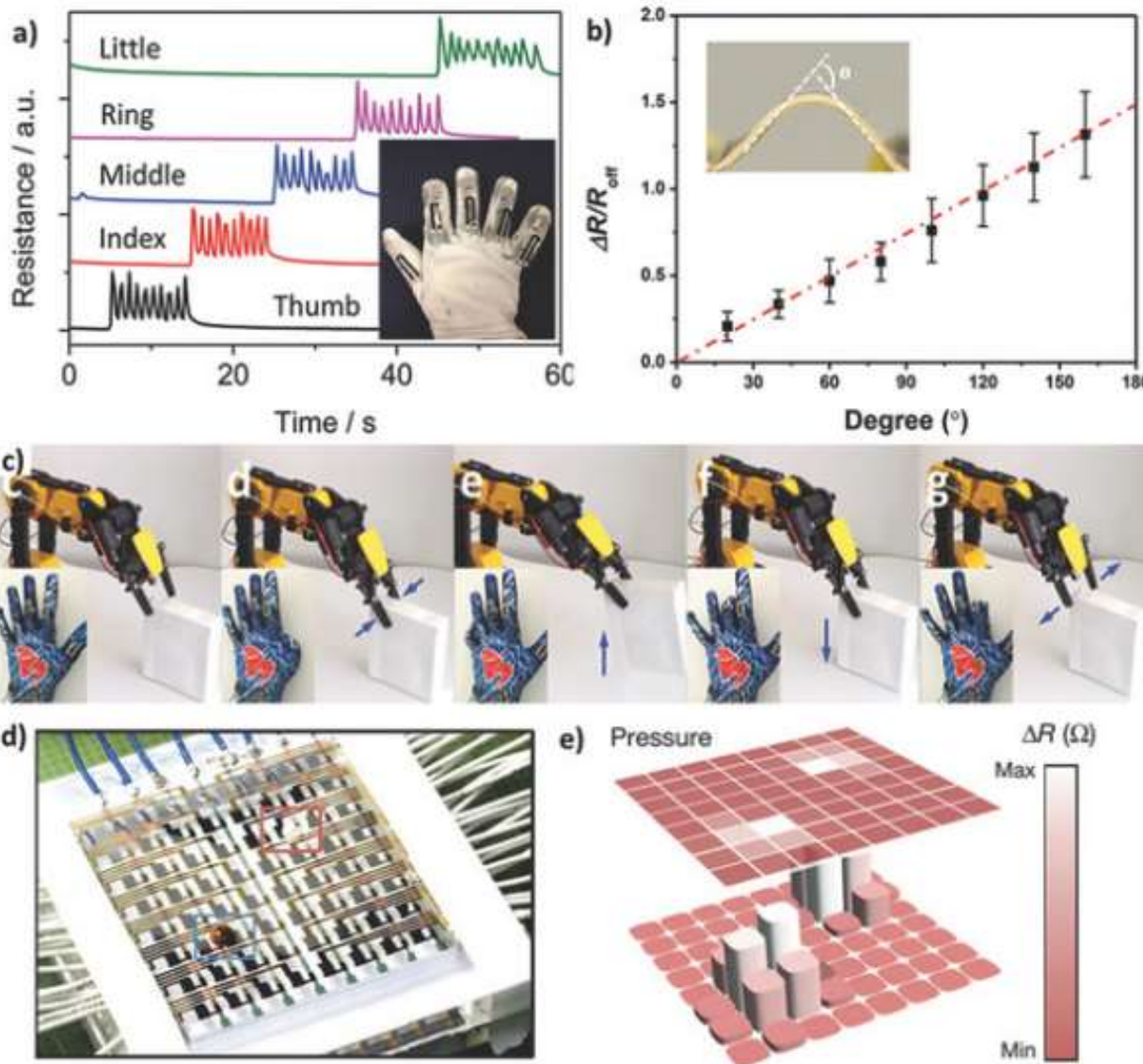
The primary mode of vibration is along the X-direction. The rotation of the object is anticlockwise with the axis of rotation in the Z-direction. The secondary mode of vibration acquired due to the Coriolis effect is in the Y-direction as shown. In a piezoelectric gyroscope, the primary mode is induced using a piezoelectric actuator, and the secondary mode is detected using a piezoelectric sensor.

The principle used in all types of gyroscopes is the Coriolis effect, which arises in a rotating frame of reference. The Coriolis effect may be stated as follows: "When a moving object is subjected to rotation about an axis perpendicular to the direction of motion, the object experiences an acceleration in a direction mutually perpendicular to the original direction of motion and the axis of rotation." The equation that describes the Coriolis effect is

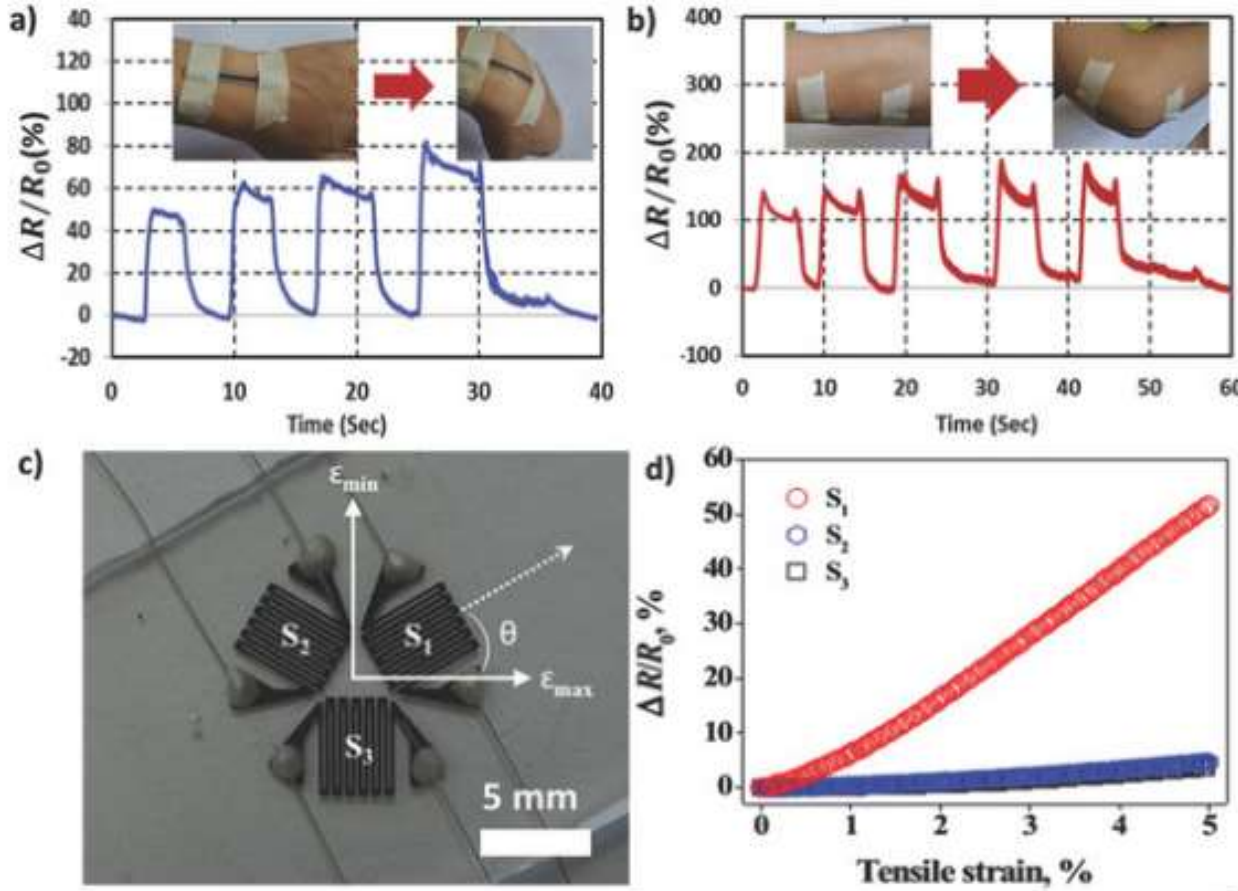
$$\vec{a} = -2\vec{\Omega} \times \vec{v} \quad (4.8)$$

where \vec{v} is the initial velocity of the object, $\vec{\Omega}$ is the angular velocity of rotation, and \vec{a} is the acceleration acquired.

Robotic applications of flexible strain sensors

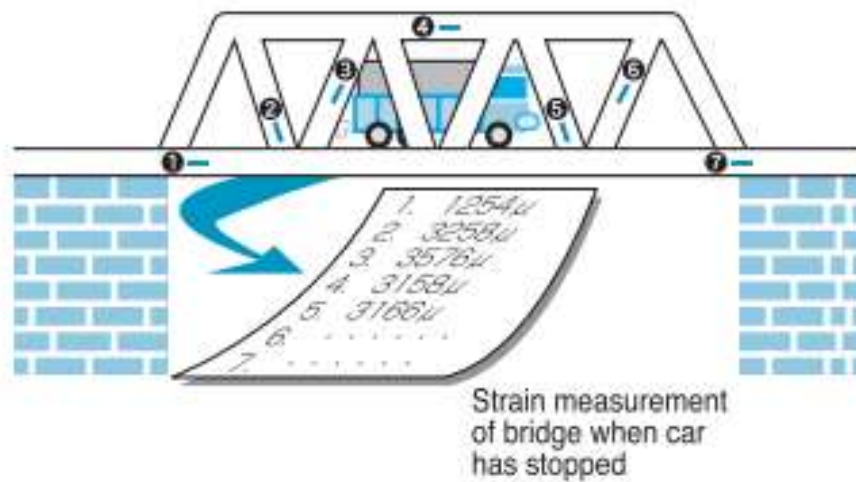


Wearable and skin-mountable strain sensors for sport performance monitoring



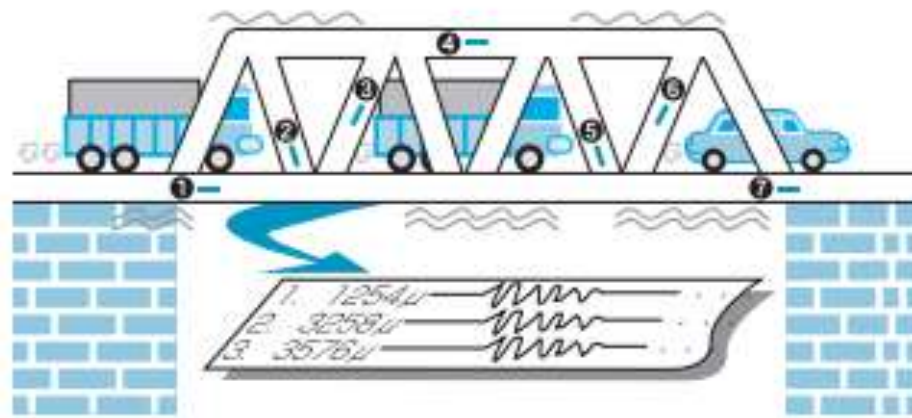
Static Strain Measurement

Measurement of strain initiated on a bridge by a stopped vehicle



Dynamic Strain Measurement

Measurement of strain initiated on a bridge by running vehicles

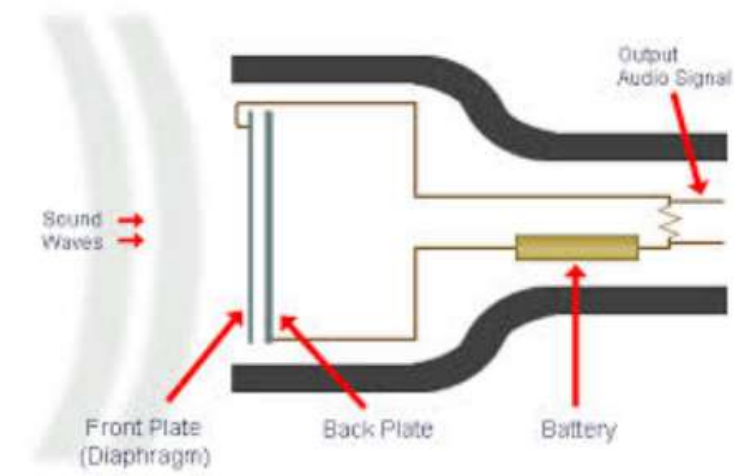


Condenser Microphones

If a parallel-plate capacitor is given an electric charge, q , voltage across its plates is governed by the equation below. On the other hand, according to equation the capacitance depends on distance d between the plates. Thus solving these two equations for voltage we arrive at

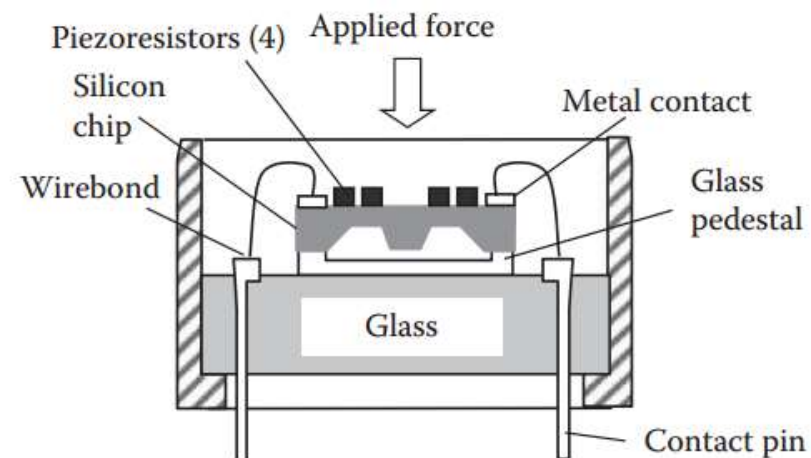
$$V = q \frac{d}{A\epsilon_0},$$

The above equation is the basis for operation of the condenser microphones, which is the other way to say “capacitive” microphones. Thus, a capacitive microphone linearly converts a distance between the plates into electrical voltage, which can be further amplified. The device essentially requires a source of an electric charge q whose magnitude directly determines the microphone sensitivity. The charge can be provided either from an external power supply having a voltage in the range from 20 to 200 V, or from an internal source capable of producing such a charge. This is accomplished by a built-in electret layer, which is a polarized dielectric crystal.



Piezoresistive Pressure Sensor

Piezoresistive pressure sensors are critical devices in a variety of control and automobile applications. Figure shows an internal combustion engine sensor designed by Kulite Semiconductor Products Inc., Leonia, New Jersey. It uses four piezoresistors to measure the stress in a silicon diaphragm caused by the force or pressure of the media. These four piezoresistors are connected electrically to form a Wheatstone bridge. At the corners of the diaphragm, five 0.024-mm-diameter gold bond wires (ultrasonically ball bonded to the sensor) allow electrical connections to the bridge. The sensor has a resonant frequency above 150 kHz, which also meets the stringent combustion requirements . This sensor can withstand the engine's harsh environment—extreme operating temperature of ~~500°C~~ and high vibration.



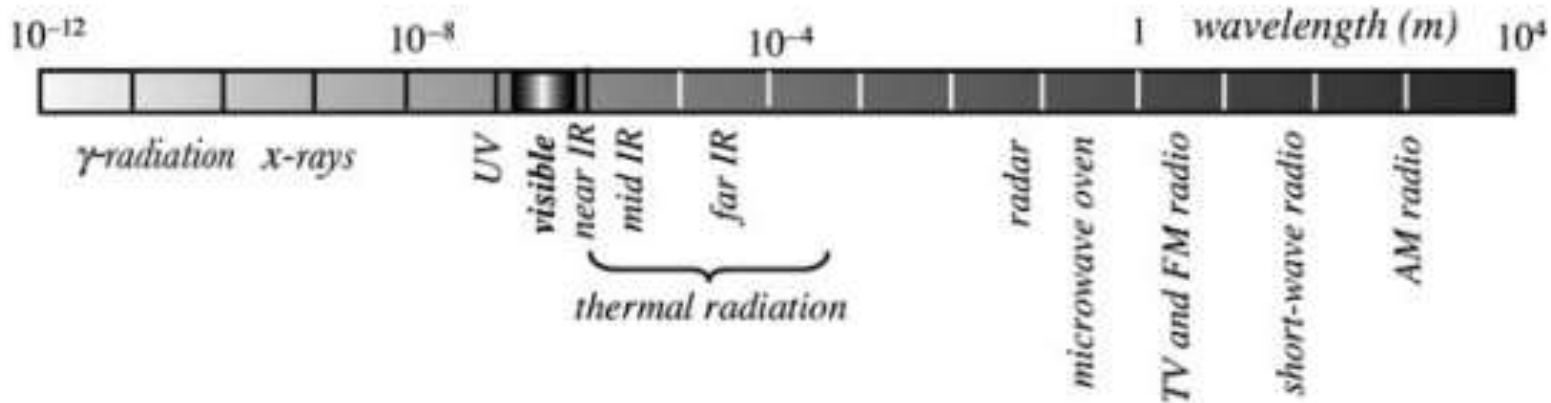
A piezoresistive internal combustion engine sensor.

UNIT -3

Radiation basics



Electromagnetic radiation spectrum spreading From g rays to radio waves.



The electromagnetic waves can be reflected, filtered focused

On its left-hand side, there is a region of the g-radiation. Then, there are the X-rays that depending on the wavelengths are divided into hard, soft, and ultrasoft rays.

However, a spontaneous radiation from the matter not necessarily should be electromagnetic: There is the so-called nuclear radiation, which is emission of particles from the atomic nuclei.

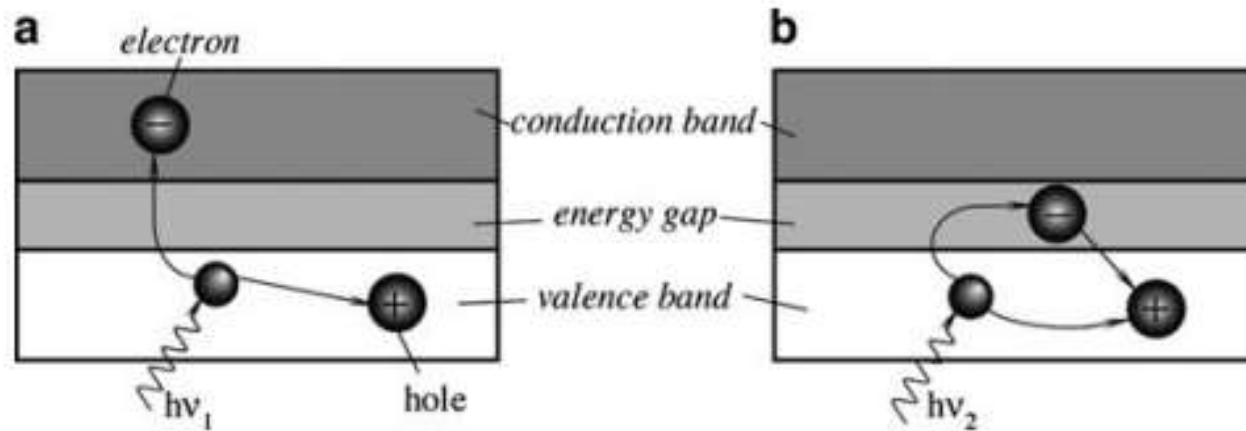
A spontaneous decay can be of two types: The charged particles (alpha and beta particles, and protons) and uncharged particles that are the neutrons. Some particles are complex like the alpha particles, which are the nuclei of helium atoms consisting of two neutrons, while other particles are generally simpler, like the beta particles that are either electrons or positrons. Ionizing radiations are given that name because as they pass through various media that absorb their energy, additional ions, photons, or free radicals are created.

Detectors of electromagnetic radiation in the spectral range from ultraviolet to far infrared are called light detectors.

Therefore, all light detectors are divided into two major groups that are called quantum and thermal.

The quantum detectors operate from the ultraviolet to mid-infrared spectral ranges, while thermal detectors are most useful in the mid- and far-infrared spectral ranges where their efficiency at room temperatures exceeds that of the quantum detectors.

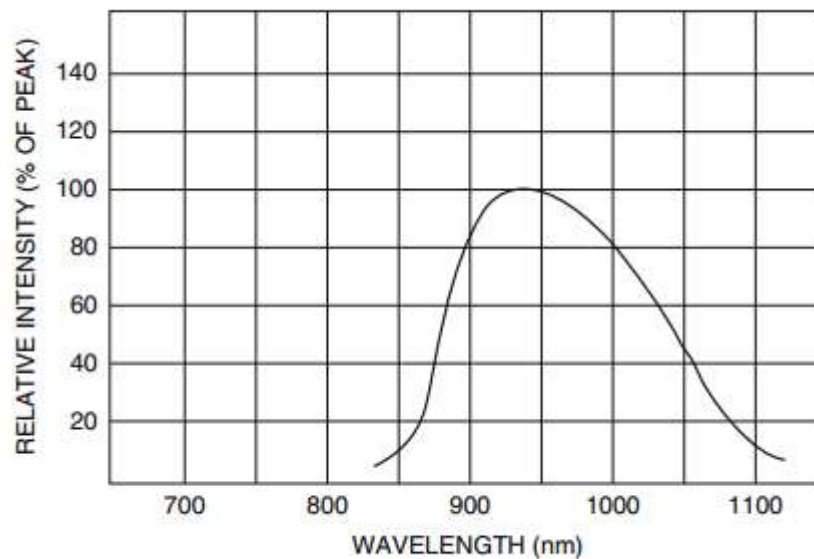
Solid-state quantum detectors (**photovoltaic and photoconductive devices**) relay on the interaction of individual photons with a crystalline lattice of semiconductor materials. Their operations are based on the photoeffect that was discovered by Albert Einstein, which won him the Nobel Prize.



14.1 Photoeffect in a semiconductor for high (a) and low (b) energy photons

A typical spectral response of a semiconductive material is shown in Fig. The light response of a bulk material can be altered by adding various impurities in the material. They can be used to reshape and shift a spectral response of the material.

All devices that directly convert photons of electromagnetic radiation into charge carriers are called quantum detectors, which are generally produced in the form of photodiodes, phototransistors, and photoresistors.



! Spectral response of an infrared photodiode

Photodetector principle

Photodetectors are of many types but they can be divided into two main classes

1. Thermal - thermal detectors detect light by a rise in temperature when the light is absorbed. They work mostly in the far IR region.
2. Photon - photon detectors work by creating electron-hole pairs on absorption of the incident radiation. The carrier concentration is proportional to the intensity of the incident radiation.

If λ is the wavelength of the incident radiation, then it can be ‘detected’ if

$$\lambda \leq \frac{hc}{\Delta E}$$

where ΔE is the energy of the *relevant transition* within the active region

Photodetectors are usually wavelength specific i.e. the material and device are chosen to work over a specific wavelength region

Photodetectors are usually wavelength specific i.e. the material and device are chosen to work over a specific wavelength region. Solar cells, on the other hand, are designed to work with the solar spectrum, which extends from the IR region to the visible and then UV.

An important factor in choosing the photodetector is the absorption coefficient of the semiconductor material. Optical absorption coefficients for different semiconductor materials are shown in figure 1. The absorption coefficient decides the *penetration depth* of the radiation into the device. This is given by Beer-Lambert law, and the penetration depth is the inverse of the absorption coefficient. If α is very large then most of the absorption will be close to the surface. On the other hand, if α is very small, then most of the light will pass through without absorption. The absorption coefficient, and through it the penetration depth, determines the working wavelength range of the photodetector, especially the lower limit. The upper wavelength limit

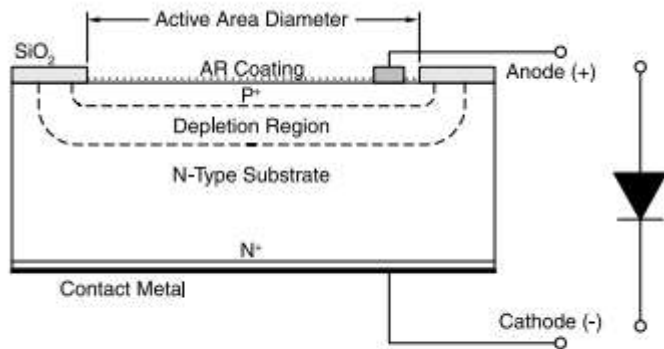


Figure 1. Planar diffused silicon photodiode

Photodetector I-V Curves

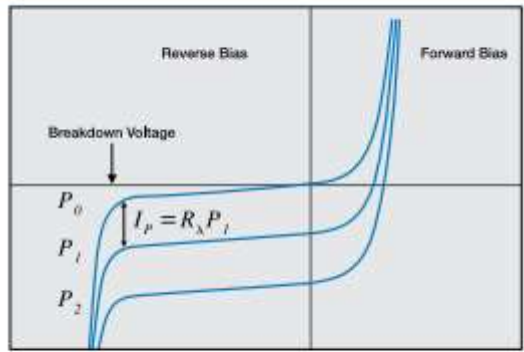


Figure 7. Characteristic I-V Curves of an OSI Optoelectronics photodiode for Photoconductive and Photovoltaic modes of operation. P_0-P_2 represent different light levels.

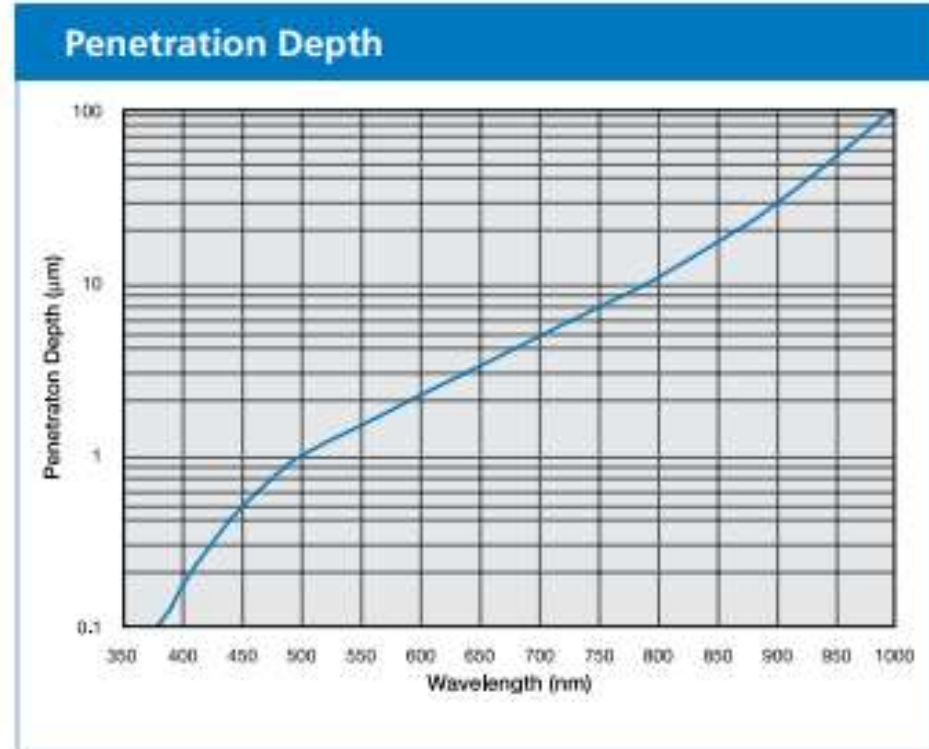
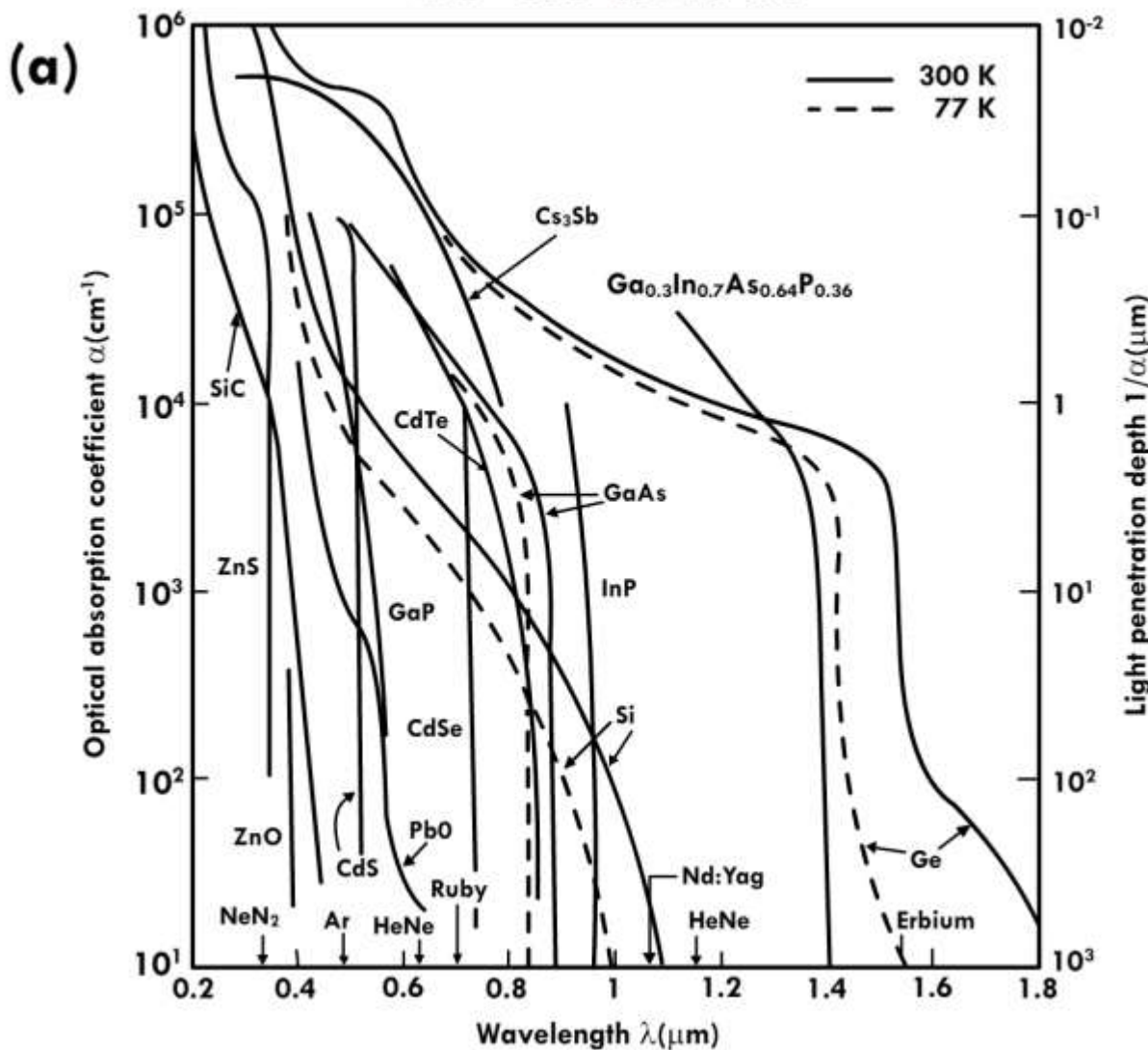


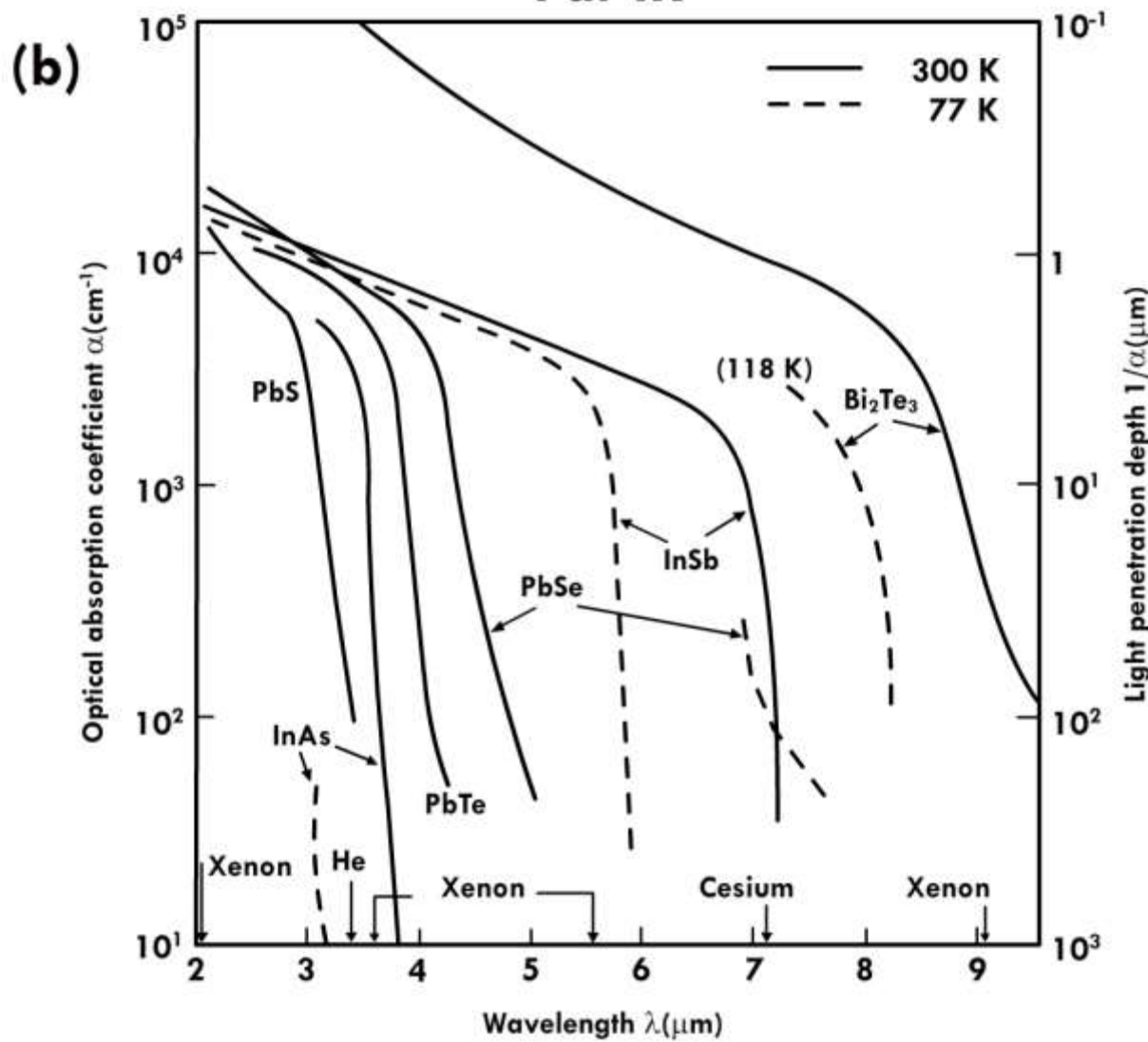
Figure 2. Penetration depth ($1/e$) of light into silicon substrate for various wavelengths.

Optical absorption coefficients for different semiconductors as a function of wavelength

UV-Vis-near IR



Far IR



Another factor in photodetectors is the response time, especially when the radiation arrives in the form of pulses. The device speed is determined by the carrier generation rate. Also, the carrier generation and detection should be faster than the arrival rate of the next pulse. Carrier detection is related to the lifetime and also the distance the carriers have to travel before reaching the electrodes. One way to reduce the transit time is to reduce the size of the device, esp. in the active region. For a *pn* junction based photodetector, the active region is the depletion region, and this can be made smaller by increasing the doping concentration. But a smaller depletion region will also lead to a lower sensitivity, since the amount of light absorbed will be smaller.

The basic metric of the photodetector is the *quantum efficiency* (η). This is defined as the *number of carriers generated per photon*.

$$\eta = \frac{I_{ph}}{e\phi} = \frac{I_{ph}}{e} \left(\frac{h\nu}{P_{ot}} \right) \quad (2)$$

where I_{ph} is the photocurrent generated from the photon flux, ϕ , and this is related to the optical power P_{ot} .

Photosensors made of semiconductor materials gained much attention in recent years because they can be specially tailored for the needs of any optical application and they can be produced at low cost in big numbers within a rather short time of a few months. The size, the geometry in general, the spectral response and other parameters can be chosen almost freely. There are various structures available like PIN diodes, drift diodes, avalanche photodiodes, CCDs, phototransistors, etc. and the sensors can be made from all sorts of semiconductor materials like Si, Ge, GaAs, InGaAs.

HgCdTe(MCT) infrared sensors





HgCdTe infrared sensors

At present, HgCdTe is the most widely used variable gap semiconductor for infrared (IR) photodetectors. Over the last forty years it has successfully fought off major challenges from extrinsic silicon and lead-tin telluride devices, but despite that it has more competitors today than ever before.

Progress in IR detector technology is connected with semiconductor IR detectors, which are included in the class of photon detectors. In this class of detectors the radiation is absorbed within the material by interaction with electrons either bound to lattice atoms or to impurity atoms or with free electrons. The observed electrical output signal results from the changed electronic energy distribution. The photon detectors show a selective wavelength dependence of response per unit incident radiation power. They exhibit both perfect signal-to-noise performance and a very fast response.

But to achieve this, the photon detectors require cryogenic cooling. Photon detectors having long-wavelength limits above about 3 pm are generally cooled.

This is necessary to prevent the thermal generation of charge carriers. The thermal transitions compete with the optical ones, making non-cooled devices very noisy.

Cooling requirements are the main obstacle to the more widespread use of IR systems based on semiconductor photodetectors, making them bulky, heavy, expensive and inconvenient to use.

Current cooled IR detector systems use material such as HgCdTe, InSb, PtSi, and doped Si.

HgCdTe has inspired the development of three “generations” of detector devices.

The first generation, linear arrays of photoconductive detectors, has been produced in large quantities and is in widespread use today.

The second generation, two-dimensional arrays of photovoltaic detectors, is now in high-rate production – thousands of arrays annually.

Third generation devices, defined here to encompass the more exotic device structures embodied in two-colour detectors, avalanche photodiodes, and hyperspectral arrays, are now fielded in demonstration programs.

HgCdTe infrared sensors

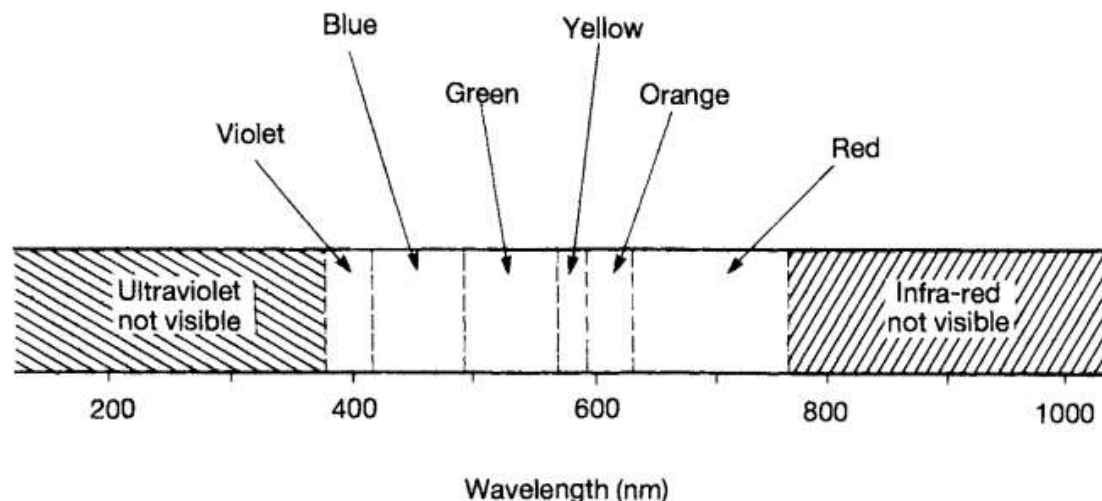


Fig. 1.2 The spectrum, with a rough indication of the colours seen.

$\text{Hg}_{1-x}\text{Cd}_x\text{Te}$ is the most widely used material for high performance infrared detectors at present. By changing the composition x , the detector spectral response can be made to cover the range from $1 \mu\text{m}$ to beyond $17 \mu\text{m}$. The advantages of this system arise from a number of features, notably: close lattice matching, high optical absorption coefficient, low trap density, high electron mobility and readily available doping techniques. These advantages mean that background limited performance can be achieved at relatively high operating temperatures. HgCdTe continues to be developed as the material of choice for high performance long wavelength ($8\text{--}12 \mu\text{m}$) arrays and has an established market at the medium ($3\text{--}5 \mu\text{m}$) and short wavelength ($1\text{--}3 \mu\text{m}$) ranges.

In MEDIUM WAVE arrays the current–voltage ($I - V$) characteristics are usually close to ideal but at longer wavelength a number of leakage currents can impact on the $I - V$ characteristics and degrade the performance of the detector. Figure illustrates a typical $I - V$ characteristic for a LONG WAVE diode, along with two types of MCT photodiode, a planar diode and a via-hole diode.

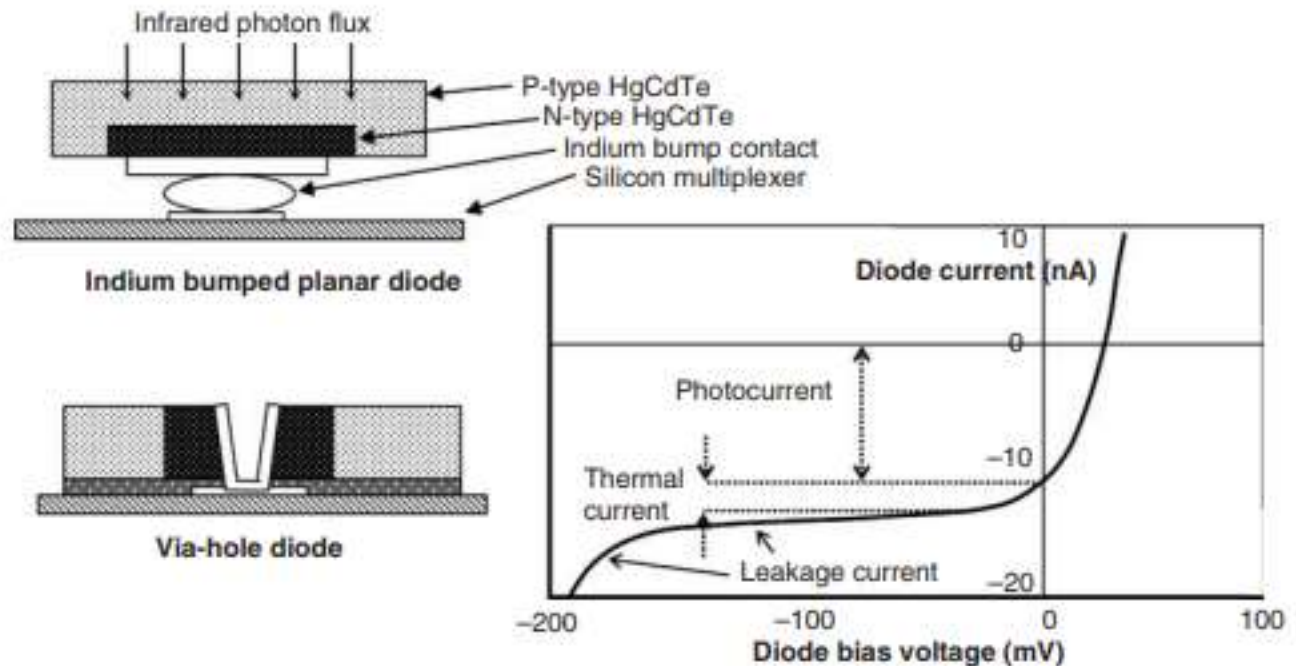
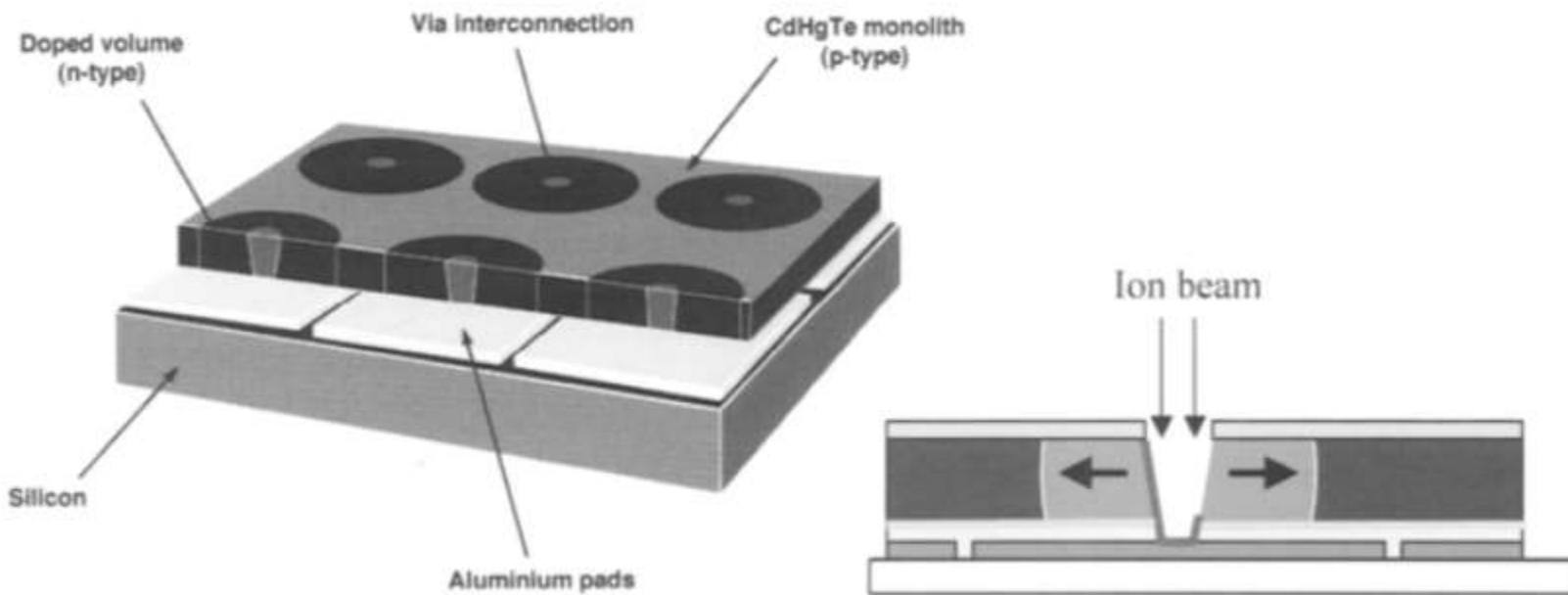


Figure 19.2 Types of HgCdTe diode and a typical current–voltage characteristic for a LW diode showing main non-ideal features.



Photocurrent and quantum efficiency

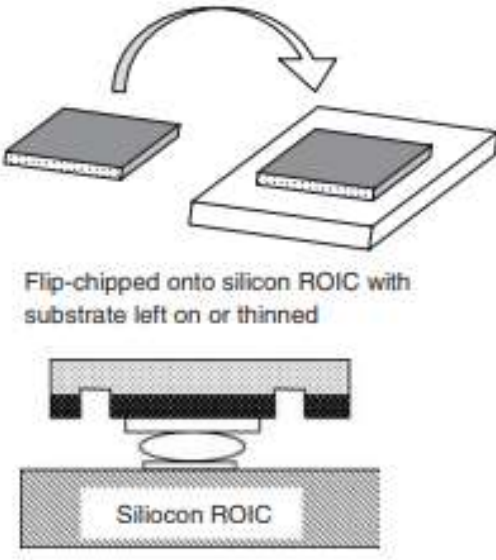
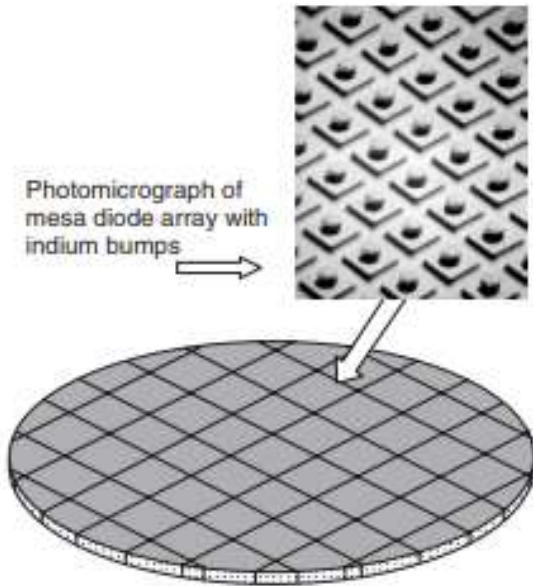
MCT has a strong optical absorption coefficient and only thin layers are needed to produce high quantum efficiency. Typically in MW detectors the absorber need only be 4–5 μm thick and about twice this in LW detectors. Ideally, the absorption should occur well within a diffusion length of the p–n junction to avoid signal loss due to recombination.

A long carrier lifetime is nearly always observed in n-type material with low carrier concentration. Device engineers tend to favor using n-type absorbers for the best quantum efficiency and try to minimize the volume of the p-region for lower thermal leakage currents.

MANUFACTURING TECHNOLOGY FOR MCT ARRAYS

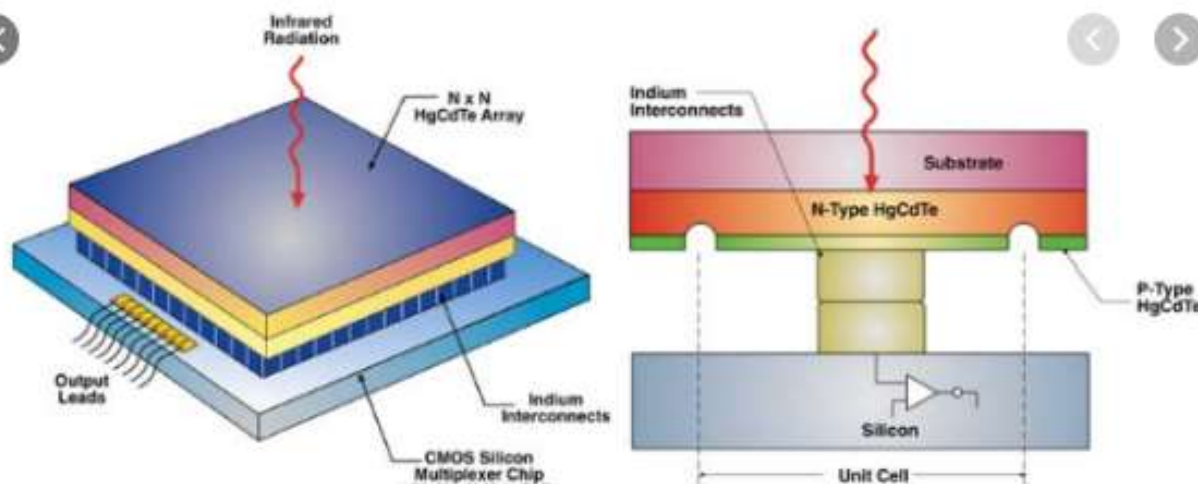
Considerable progress has been made in the past two decades on the epitaxial growth of MCT. Manufacturers select a technique that suits their device technology and the type of detectors they require. It is the aim of most manufacturers to produce high-quality layers in large areas at low cost, but this ideal has been elusive. At the present time the best structural quality material is grown using liquid phase epitaxy (LPE) onto lattice-matched crystals of CdZnTe, and this has been used successfully in homojunction technologies. CdZnTe is expensive, however, and both LPE and VPE now use a variety of alternative substrates. Many groups favor VPE because the composition and doping profile can be easily controlled to produce complex devices, such as two-color detectors.

Two VPE methods are commonly used: metal organic vapor phase epitaxy (MOVPE) and molecular beam epitaxy (MBE).



HgCdTe layer grown on large area substrate (Si, GaAs or sapphire) using VPE growth method. Processed into arrays with indium bumps and sawn up into array blocks.

The main commercial drive though is to cost reduce the manufacture of large-area arrays and avoid expensive CdZnTe substrates. Silicon, gallium arsenide and sapphire are the commonest substrates used because they are available commercially in large area wafers at relatively low cost



Wafer-scale processing using VPE MCT material, mesa diodes, and indium bump interconnect technology

Visible-light color sensors



Visible-light color sensors

In the food & beverages industry, color is a very important measurand which can be used either for quality estimation, or for automatic selection of products in different categories.

Reflectivity measurements can be easily employed for solid foods, whereas for liquid samples, it is much more appropriate to measure the sample in transmission.

dependence of blood color on the concentration of deoxygenated and oxygenated hemoglobin can also be applied to estimate quantitatively the freshness of fresh meat. Thus, by analyzing the reflectance spectrum of beef meat and its variation in time during storage, it was deduced that the typical spectrum changes in time due to exposure to oxygen, which causes the oxymyoglobin to be oxidized into methemyoglobin, resulting in a quality degradation-induced color change that can be automatically sensed so that packaged meat that exceeded its shelf-life could be promptly removed and replaced with fresh one.

Similar color-based quality analysis has also been successfully performed on other foods (for diagnosis of storage conservation or for estimation of their alimentary properties), e.g., milk, orange or strawberry juice, or peach nectar.

Another example is the reported realization of an accurate real-time color classification microsystem that integrated the photosensors, together with pre-processing circuitry and a subsequent neural network processor, onto a single IC. The usage of neural networks offers distinct advantages, such as extreme ease of usage by the user of the final product, flexibility by **self-adaptation to new circumstances, and reduced cost and extreme suitability of monolithic integration with standard CMOS fabrication processes.**

This one-chip smart sensing microsystem had low cost, was robust, was mass-producible using standard commercial CMOS processes, and exhibited a significantly higher performance. The chip was successfully applied practically in freshness tests for several fruits (apples, tangerines, and lemons)

Phenolic compounds are responsible for the characteristic color, flavor, and aroma in wines and also act as antioxidants, with alleged beneficial effects on human health (reduced incidence of coronary heart disease and certain forms of cancer).

Color sensing has been employed not only for fresh produce but also to characterize the cooking of foods. This is important in order to avoid under- or over-cooking, and also to ensure objectivity of assessment since human evaluation is highly subjective, may also depend on other variables, and does not guarantee accurate reproducibility.

One reported realization for this purpose comprised an optical fiber sensor in conjunction with a small portable Ocean Optics spectrometer in order to monitor the color of the food while it was being cooked by examining the light reflected from both the sample's surface and core.

Many modern manufacturing processes require the detection of different colors and hues of visible light, i.e., wavelengths in the range 400–700 nm.

Color detection can be used to sort objects, verify position of objects, recognize color sequence, control color in dyeing and coating applications, and detect changes in color of liquid during titration.

Hence, color sensors are becoming an integral part in many industries, e.g., cosmetics, textile, food, publishing, optoelectronics, and image processing, including digital cameras.

Photodiodes

Photodiodes are semiconducting optical sensors, which if broadly defined may even include solar batteries. However, here we consider only the information aspect of these devices rather than the power conversion.

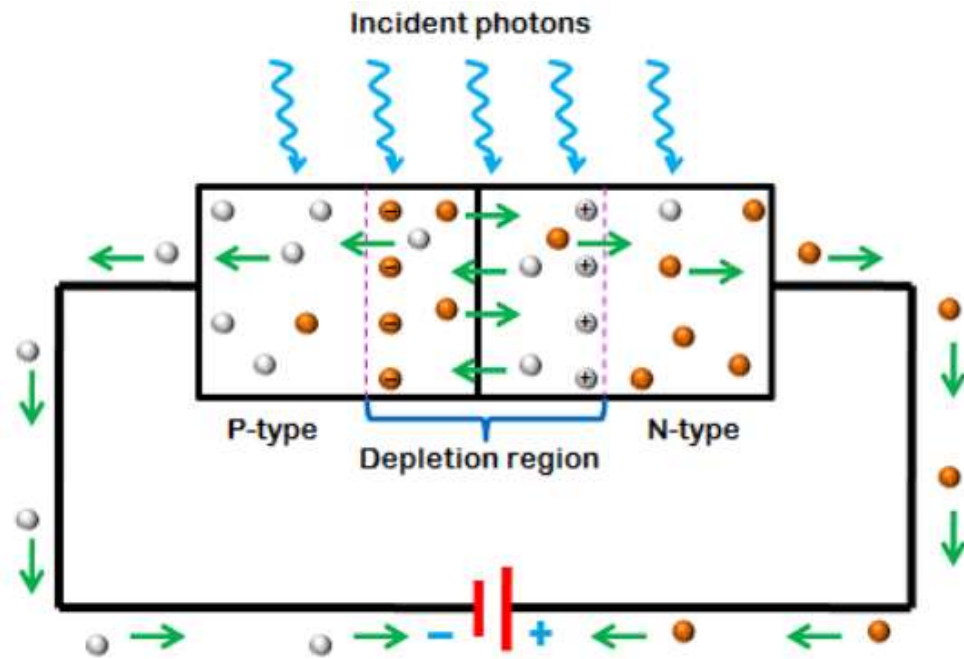
In a simple way, the operation of a photodiode can be described as follows.

If a pn-junction is forward biased (positive side of a battery is connected to the p side) and is exposed to light of proper frequency, the current increase will be very small with respect to a dark current. In other words, the bias current is much greater than the current generated by light, and the diode is just a diode, not really useful for sensing light.

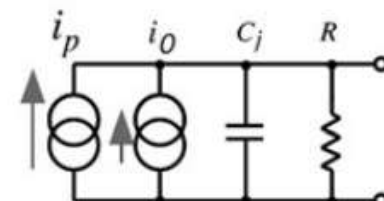
If the junction is reverse biased , when light strikes the semiconductor, the current will increase quite noticeably. Impinging photons create electron– hole pairs on both sides of the junction. When electrons enter the conduction band, they start flowing toward the positive side of the battery. Correspondingly, the

created holes flow to the negative terminal, meaning that photocurrent i_p flows in the network. Under dark conditions, dark current i_0 is independent of applied voltage and mainly is the result of thermal generation of charge carriers. Thus, a reverse-biased photodiode electrical equivalent circuit contains two current sources and a RCnetwork

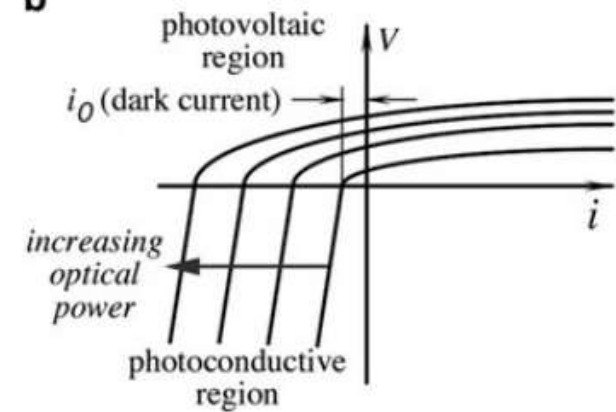
Photodiodes



a



b



4 An equivalent circuit of a photodiode (a) and its volt-ampere characteristic (b)

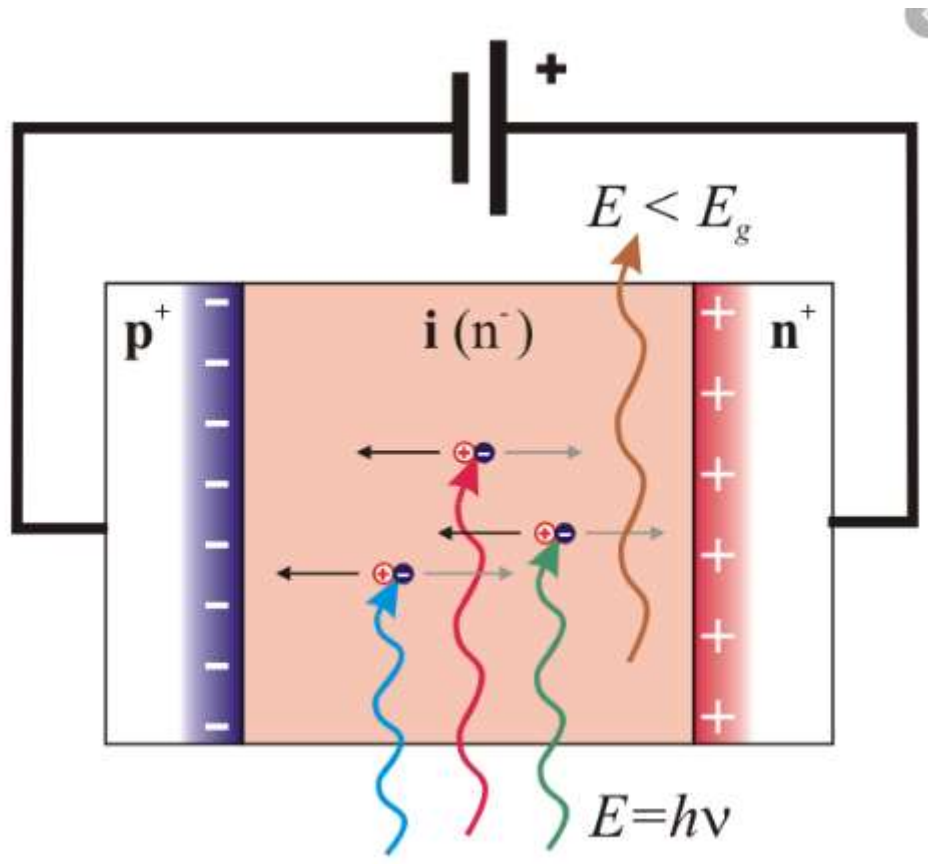
The current-to-voltage response of the photodiode is given by

$$i = i_0 \left(e^{eV/k_b T} - 1 \right) - i_s,$$

$$i = i_0 \left(e^{eV/k_b T} - 1 \right) - \frac{\eta e P}{h\nu},$$

$$i = \frac{\eta e P}{h\nu},$$

If the probability that a photon of energy $h\nu$ will produce an electron in a detection is η then the average rate of the production of electrons for an incident beam of optical power P is given by



PN photodiode:

- A PN photodiode does not require a reverse bias and as a result is more suitable for low light applications as a result of the improved noise performance.

PIN photodiode:

- Reverse bias required by the PIN photodiode introduces a noise current which reduces signal to noise ratio
- The reverse bias offers better performance for high dynamic range applications
- The reverse bias required offers better performance for high bandwidth applications as the capacitance between the P and N regions as well as charge storage is small.

Avalanche photodiode advantages

- High level of sensitivity as a result of avalanche gain

Avalanche photodiode disadvantages:

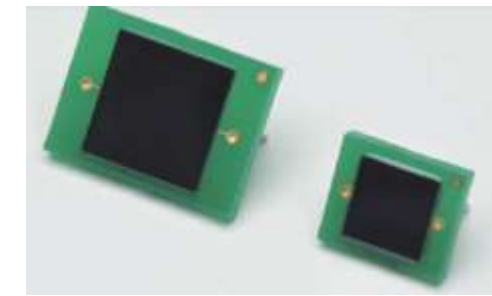
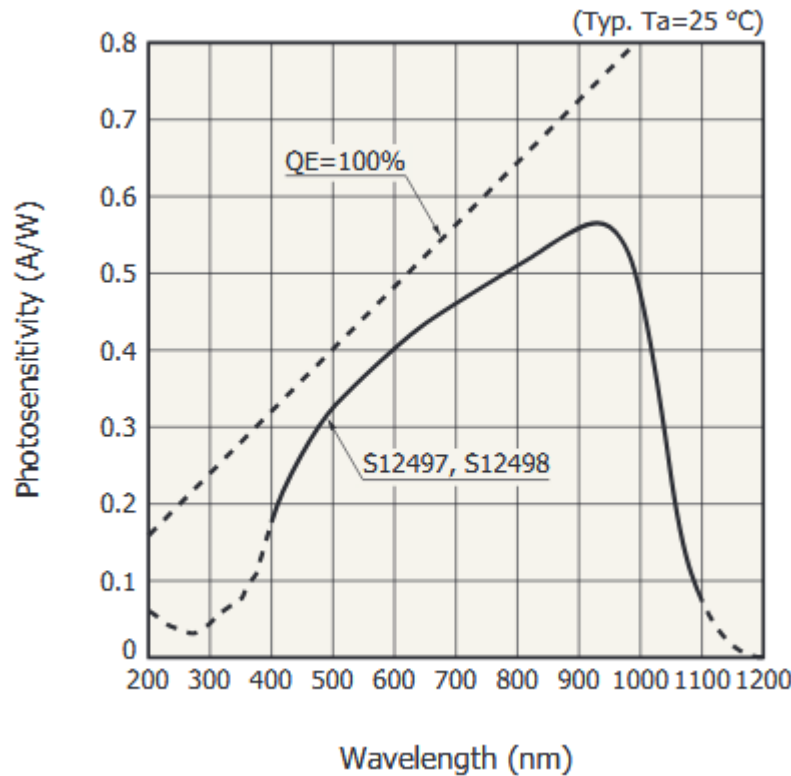
- Much higher operating voltage may be required.
- Avalanche photodiode produces a much higher level of noise than a PN photodiode
- Avalanche process means that the output is not linear

Si photodiodes

A commercial sensor example

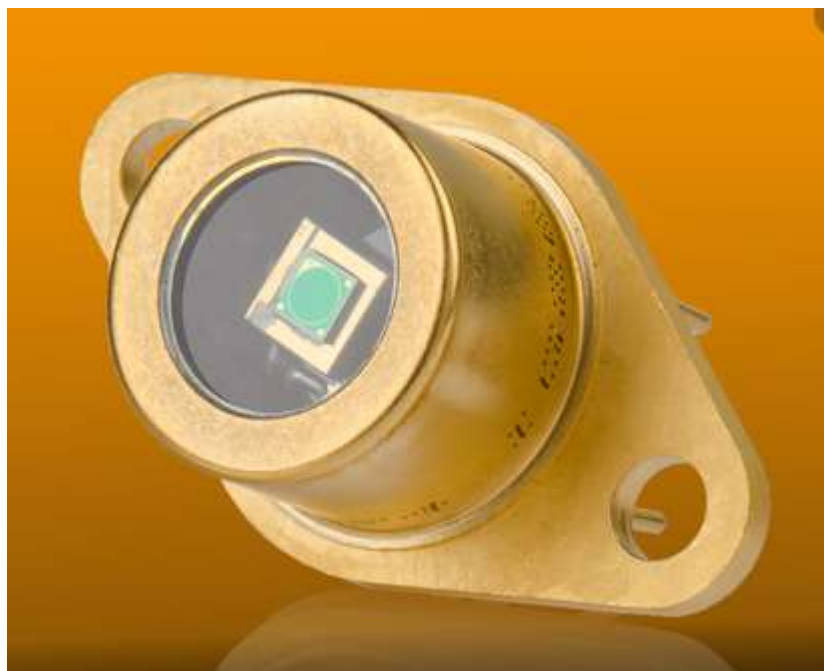
Spectral response range :
400 to 1100 nm

Photosensitive area
S12497: 9.5×9.5 mm,
S12498: 6.0×6.0 mm



► Electrical and optical characteristics (Ta=25 °C)

Parameter	Symbol	Condition	S12497			S12498			Unit
			Min.	Typ.	Max.	Min.	Typ.	Max.	
Spectral response	λ		400	-	1100	400	-	1100	nm
Peak sensitivity wavelength	λ_p		-	920	-	-	920	-	nm
Photosensitivity	S	$\lambda=540$ nm	0.32	0.36	-	0.32	0.36	-	A/W
		$\lambda=920$ nm	0.52	0.57	-	0.52	0.57	-	
Short circuit current	Isc	100 lx, 2856 K	60	75	-	15	30	-	µA
Dark current	Id	VR=10 mV	-	50	200	-	10	150	pA
Rise time	tr	VR=0 V, RL=1 kΩ 10 to 90%, $\lambda=658$ nm	-	15	-	-	15	-	µs
Terminal capacitance	Ct	VR=0 V, f=10 kHz	750	950	1150	330	380	430	pF



Si Photodiode



PHOTORESISTORS

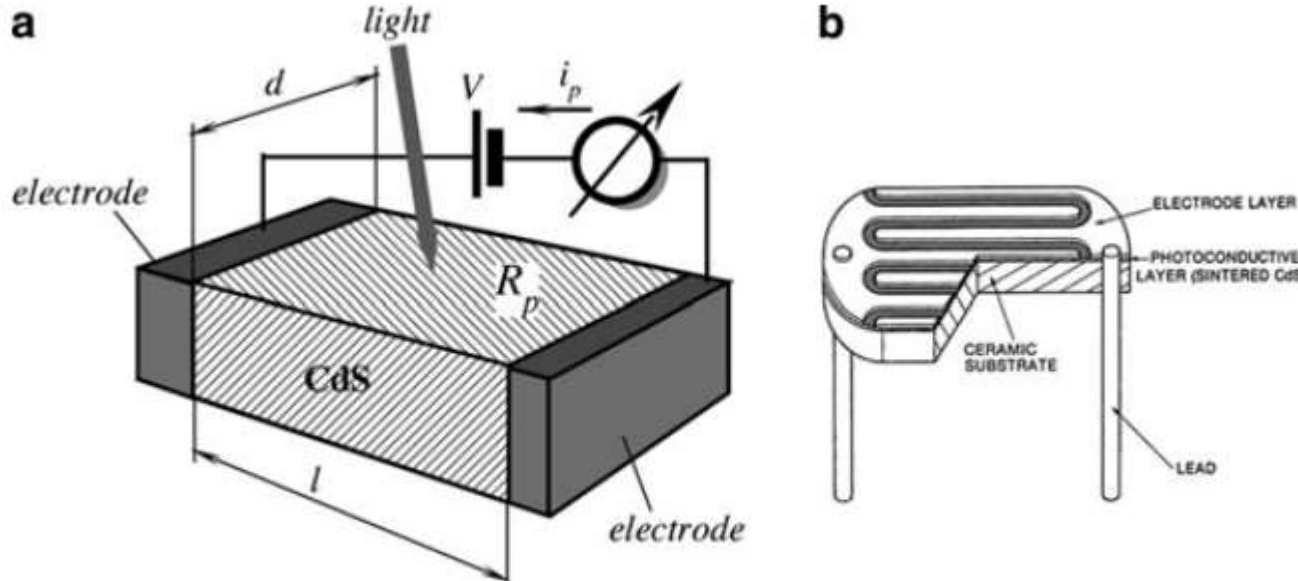


Fig. 14.11 Structure of a photoresistor (a) and a plastic-coated photoresistor having a serpentine shape (b)

As a photodiode, a photoresistor is a photoelectric device. It is a resistor whose resistance is called photoresistance R_p that changes as the function of incident light. The most common materials for its fabrication are cadmium sulfide (CdS) and cadmium selenide (CdSe), which are semiconductors whose resistances change upon light entering the surface. For its operation, a photoresistor requires a power source (excitation signal) because unlike a photodiode or phototransistor, it does not generate photocurrent – a photoeffect is manifested in change in the material's electrical resistance.

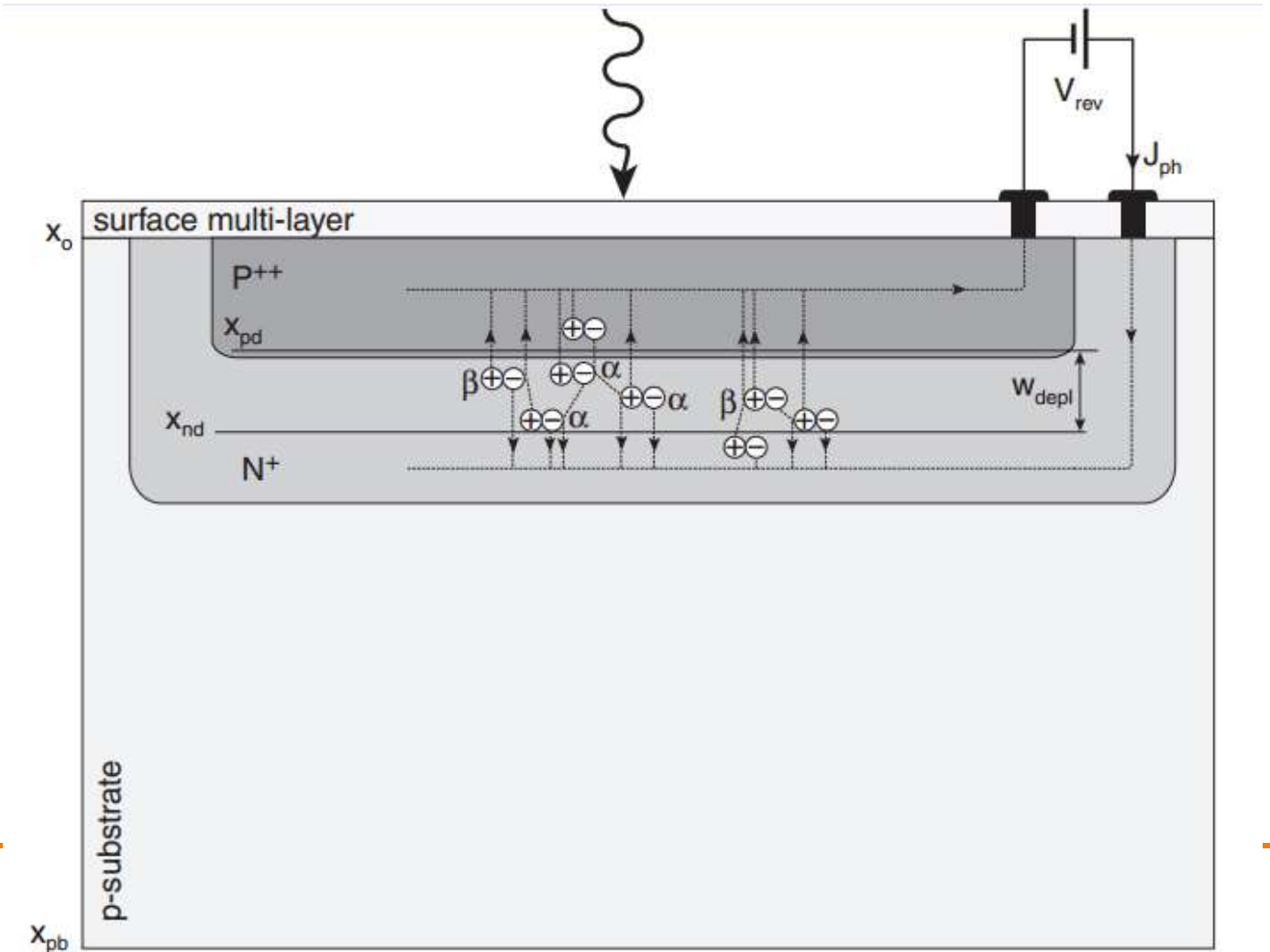
In darkness, the resistance of the material is high. Hence, the applied voltage V results in small dark current, which is attributed to temperature effect. When light is incident on the surface, current i_p flows.

When light illuminates the photoconductive crystal, photons are absorbed, which results in the added-up energy in the valence band electrons. This moves them into the conduction band, creating free holes in the valence band, increasing the conductivity of the material. Since near the valence band is a separate acceptor level that can capture free electrons not as easily as free holes, the recombination probability of the electrons and holes is reduced and the number of free electrons in the conduction band is high.

CdS has a band gap of 2.41 eV, the absorption edge wave length is 515 nm, which is in the visible spectral range. Hence, the CdS detects light shorter than 515 nm wavelengths. Other photoconductors have different absorption edge wavelengths. For instance, CdS is the most sensitive at shorter wavelengths range, while Si and Ge are the most efficient in the near infrared.

Avalanche photodiode

The avalanche photodiode is similar to the conventional pn junction, apart from the fact that the doping levels are relatively high. The operation of the avalanche photodiode is based on impact ionization within the depletion layer. The basic device structure is shown in Figure



The doping concentration of the p⁺⁺ layer exceeds 10^{19} cm^{-3} and n⁺ is in the order of $2 \times 10^{18} \text{ cm}^{-3}$ (this is generally referred to as the single-sided abrupt junction). Under these conditions and $V_{\text{rev}} \gg 10 \text{ V}$,

$$w_{\text{depl}} \approx \sqrt{\frac{2\epsilon}{qN_D} V_{\text{rev}}} \approx 0.1 \mu\text{m}$$

$$E_{\text{max}} = E(x_j) \approx \sqrt{\frac{2qN_D}{\epsilon} V_{\text{rev}}} \approx 10^7 \text{ V/m}$$

The avalanche photodiodes are named so because if a reverse bias is applied to the p-n junction and a high-intensity field is formed with the depletion layer, photon carriers will be accelerated by the field and collide with the atoms, producing the secondary carriers. In turn, the new carriers are accelerated again, resulting in the extremely fast avalanche-type increase in current. There-fore, these diodes work as amplifiers, making them useful for detecting extremely low levels of light.

The device is operated fully depleted and has two field regions: i) a light absorption region followed by the π region which is about (30–150) μm wide with a relatively low field ($\sim 2 \times 10^4 \text{ V cm}^{-1}$) wherein charge carriers are drifting; ii) a narrow (a few micrometers) high field region ($\sim 10^5 \text{ V cm}^{-1}$) wherein the multiplication takes place.

The principle of operation of an APD is based on the conversion of the energy of incoming photons into electron–holes pairs in silicon as in PIN and their further multiplication through an avalanche process in the depleted region by application of a very high reverse bias voltage to a p – n junction. The charge carriers created in the depleted region of the junction by the incident radiation, will drift in the π region towards the corresponding electrodes under the electric field applied across the junction: the holes will drift toward the p + side in a low electric field, while the electrons will drift toward the narrow n + side in a high electric field where an avalanche process will eventually take place, i.e., the electrons will be accelerated and acquire a kinetic energy large enough so that they can create additional electron-hole pairs via ionization through their collisions with atoms in the crystal lattice. At sufficiently high voltage, i.e., high electric field values, holes can also produce electron-hole pairs and therefore produce additional electrons. This electron multiplication generates avalanche breakdown that occurs at the so-called breakdown voltage which is the maximum reverse bias voltage which can be applied to an APD (when an APD operates close to avalanche breakdown, its gain is a very rapidly increasing function of the applied reverse bias voltage). The value of the breakdown voltage varies with the type of APD. Then, the operating voltage of an APD has to be kept lower than this breakdown voltage. In practice, this avalanche multiplication process - referred to as avalanche multiplication of photocurrent - occurs beyond a value of the applied voltage corresponding to an internal electric field

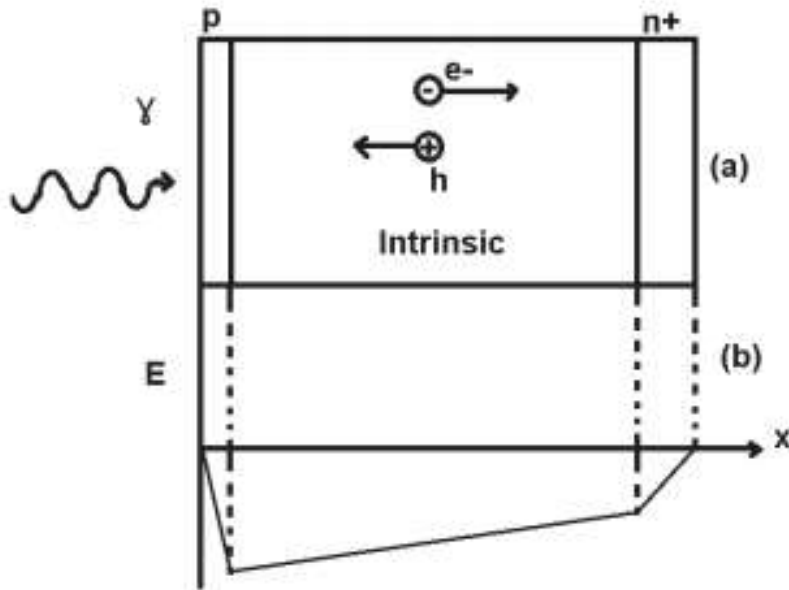


Fig. 6.1 a) Standard schematic representation of a photodiode; b) the electric field E generated by the application of a bias voltage.

depends on the voltage applied to the junction and gain of about 102 can be normally achieved for a bias voltage of (100–200) volts in silicon. The shape of the avalanche gain is an exponential (plus a constant) function of the applied bias voltage.

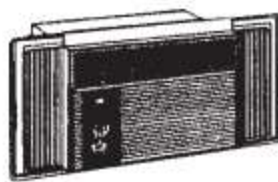
Heat transfer, thermal structures



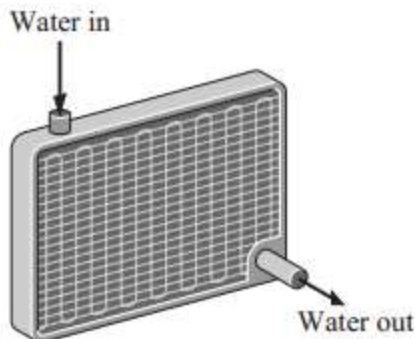
Application Areas of Heat Transfer



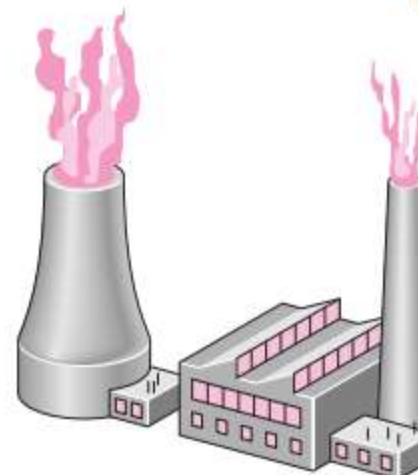
The human body



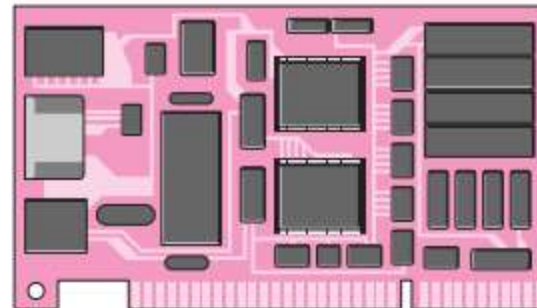
Air-conditioning systems



Car radiators



Power plants



Circuit boards



Refrigeration systems

Heat transfer equipment such as heat exchangers, boilers, condensers, radiators, heaters, furnaces, refrigerators, and solar collectors are designed primarily on the basis of heat transfer analysis.

The heat transfer problems encountered in practice can be considered in two groups: (1) rating and (2)sizing problems.

The rating problems deal with the determination of the heat transfer rate for an existing system at a specified temperature difference.

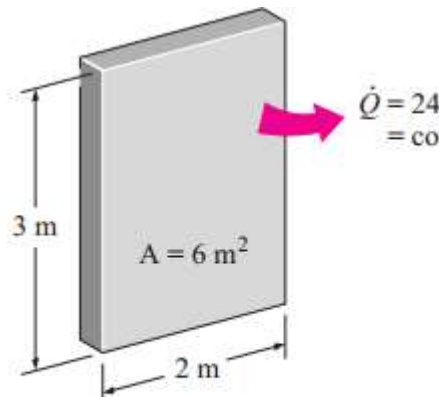
The sizing problems deal with the determination of the size of a system in order to transfer heat at a specified rate for a specified temperature difference.

Keeping in line with current practice, we will refer to the thermal energy as *heat* and the transfer of thermal energy as *heat transfer*. The amount of heat transferred during the process is denoted by Q . The amount of heat transferred per unit time is called **heat transfer rate**, and is denoted by \dot{Q} . The overdot stands for the time derivative, or “per unit time.” The heat transfer rate \dot{Q} has the unit J/s, which is equivalent to W.

The rate of heat transfer per unit area normal to the direction of heat transfer is called **heat flux**, and the average heat flux is expressed as (Fig. 1–11)

$$q = \frac{\dot{Q}}{A} \quad (\text{W/m}^2) \quad (1-8)$$

where A is the heat transfer area. The unit of heat flux in English units is Btu/h · ft². Note that heat flux may vary with time as well as position on a surface.



Heat flux is heat transfer *per unit time* and *per unit area*, and is equal to $q = \dot{Q}/A$ when \dot{Q} is uniform over the area A .

$$\dot{q} = \frac{\dot{Q}}{A} = \frac{24 \text{ W}}{6 \text{ m}^2} = 4 \text{ W/m}^2$$

The transfer of energy as heat is always from the higher-temperature medium to the lower-temperature one, and heat transfer stops when the two mediums reach the same temperature.

Thermodynamics describes the fundamental behavior of heat and temperature and includes the three laws of thermodynamics. Heat transfer goes further and describes the mechanisms of heat exchange and the rate at which heat flows, giving us a way to calculate heat flow within, to and from objects or the environment. **There are three modes of heat transfer: conduction, convection and radiation.**



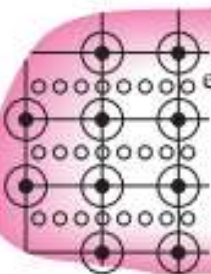
GAS

- * Molecular collisions
- * Molecular diffusion



LIQUID

- * Molecular collisions
- * Molecular diffusion



SOLID

- * Lattice vibrations
- * Flow of free electrons

The mechanisms of heat conduction in different phases of a substance.

Conduction is the transfer of energy from the more energetic particles of a substance to the adjacent less energetic ones as a result of interactions between the particles. Conduction can take place in solids, liquids, or gases.

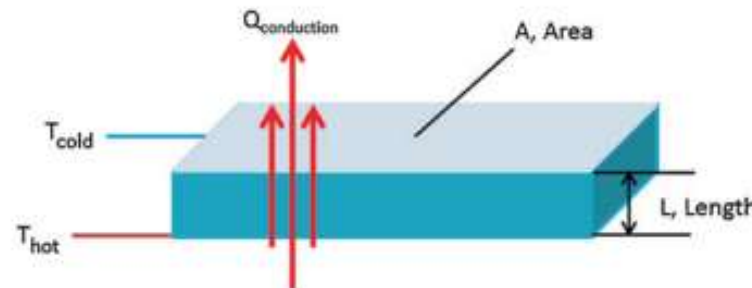
In gases and liquids, conduction is due to the collisions and diffusion of the molecules during their random motion. In solids, it is due to the combination of vibrations of the molecules in a lattice and the energy transport by free electrons.

Conduction is the heat transfer through solids. It can also occur with stagnant fluids. The one-dimensional rate of conductive heat transfer is determined by Eq. below:

Consider steady heat conduction through a large plane wall of thickness $\Delta x = L$ and area A , as shown in Fig. 1–21. The temperature difference across the wall is $\Delta T = T_2 - T_1$. Experiments have shown that the rate of heat transfer \dot{Q} through the wall is *doubled* when the temperature difference ΔT across the wall or the area A normal to the direction of heat transfer is doubled, but is *halved* when the wall thickness L is doubled. Thus we conclude that *the rate of heat conduction through a plane layer is proportional to the temperature difference across the layer and the heat transfer area, but is inversely proportional to the thickness of the layer*. That is,

$$\text{Rate of heat conduction} \propto \frac{(\text{Area})(\text{Temperature difference})}{\text{Thickness}}$$

$$Q_{\text{conduction}} = \frac{kA(T_{\text{hot}} - T_{\text{cold}})}{L}$$



1.3 Heat transfer through an object by conduction

where Q conduction is heat flow, k is the thermal conductivity of the material, A is the cross-sectional area of heat flow, T_{hot} is the temperature of the hot surface, T_{cold} is the temperature of the cold surface and L is the length of the material through which heat is conducting. Figure depicts the heat transfer through a solid material by conduction. The different variables of the conduction heat transfer are shown. The conduction resistance is defined by Eq.:

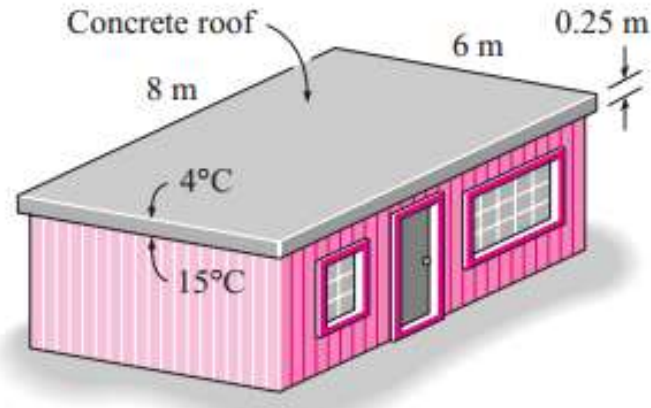
$$R_{\text{conduction}} = \frac{L}{kA}$$

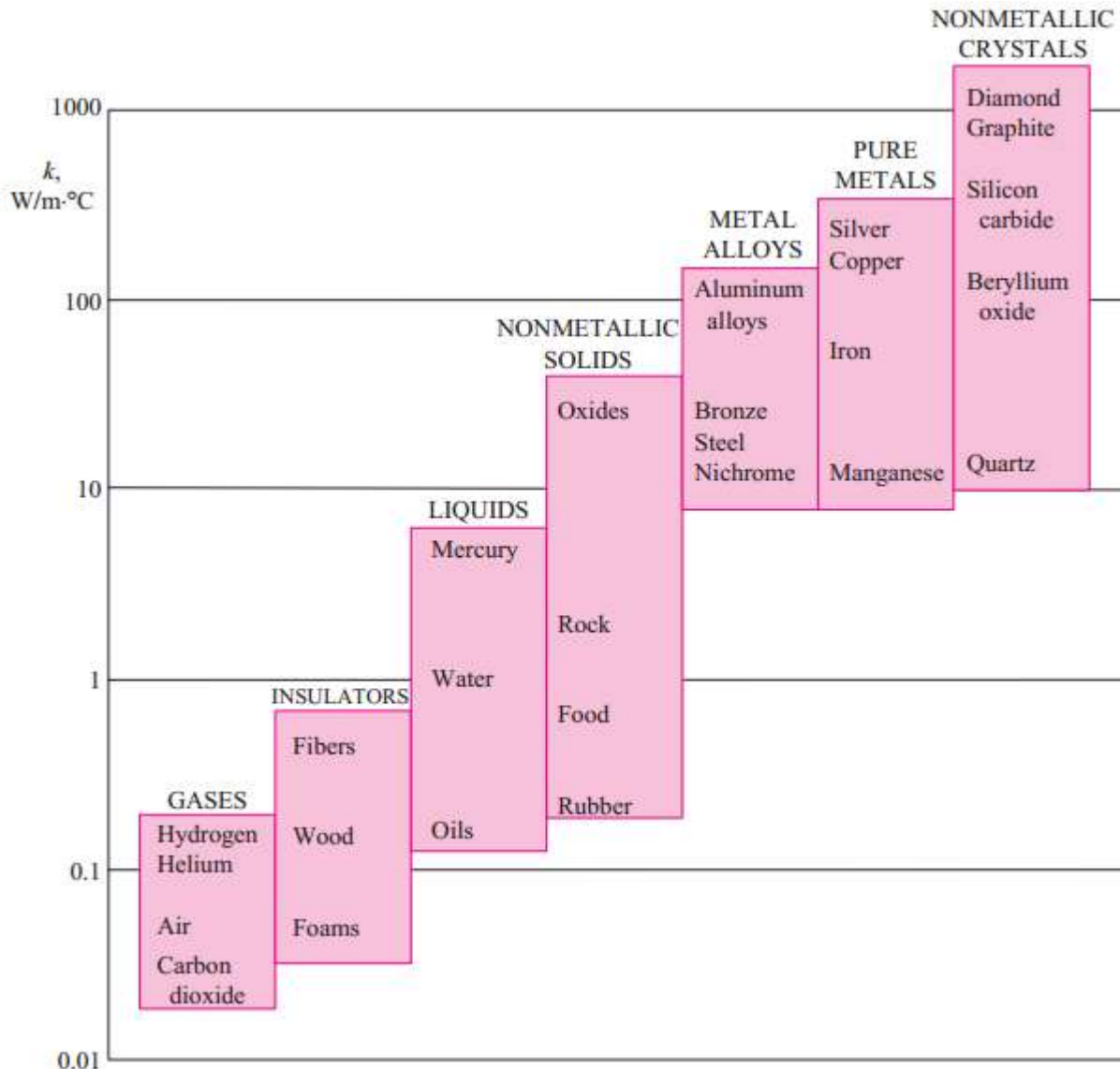
As shown in, in order to minimize the conduction resistance, conductivity of the material and cross-sectional area of material is maximized while the through-path (length) of the material is minimized.

The roof of an electrically heated home is 6 m long, 8 m wide, and 0.25 m thick, and is made of a flat layer of concrete whose thermal conductivity is $k = 0.8 \text{ W/m} \cdot ^\circ\text{C}$. The temperatures of the inner and the outer surfaces of the roof one night are measured to be 15°C and 4°C , respectively, for a period of 10 hours. Determine the rate of heat loss through the roof that night

Assume Steady operating conditions exist during the entire night since the surface temperatures of the roof remain constant at the specified values.

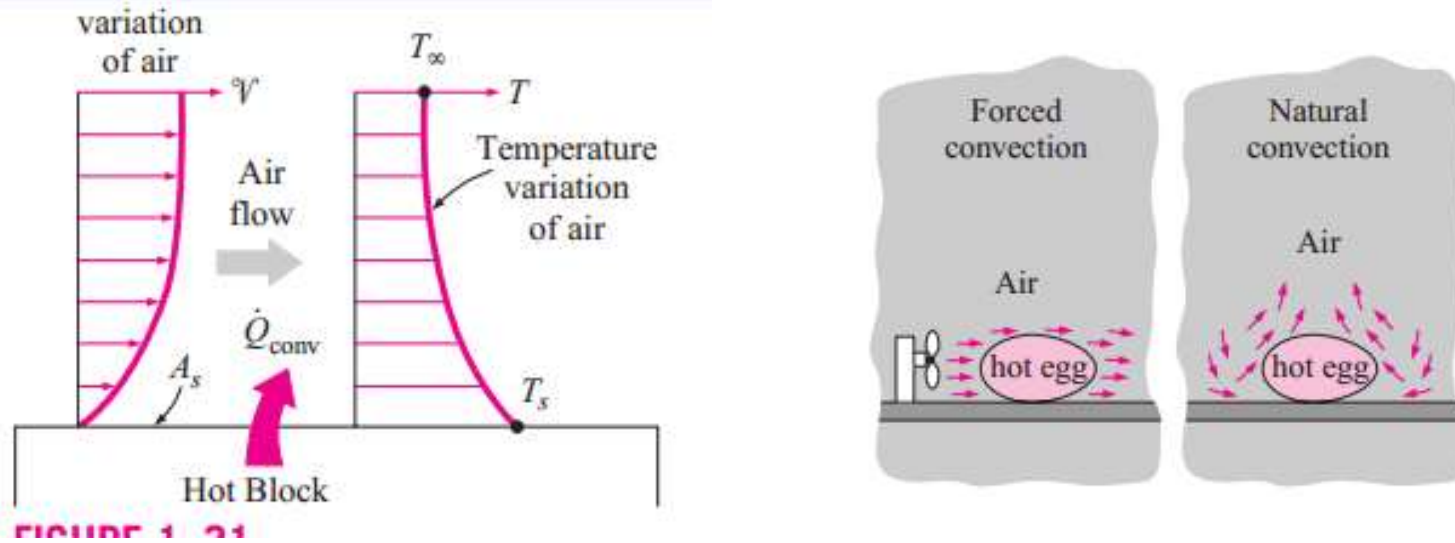
Constant properties can be used for the roof





The range of thermal conductivity of various materials at room temperature.

Convection is the mode of energy transfer between a solid surface and the adjacent liquid or gas that is in motion, and it involves the combined effects of *conduction* and *fluid motion*. The faster the fluid motion, the greater the convection heat transfer. In the absence of any bulk fluid motion, heat transfer between a solid surface and the adjacent fluid is by pure conduction. The presence of bulk motion of the fluid enhances the heat transfer between the solid surface and the fluid, but it also complicates the determination of heat transfer rates.

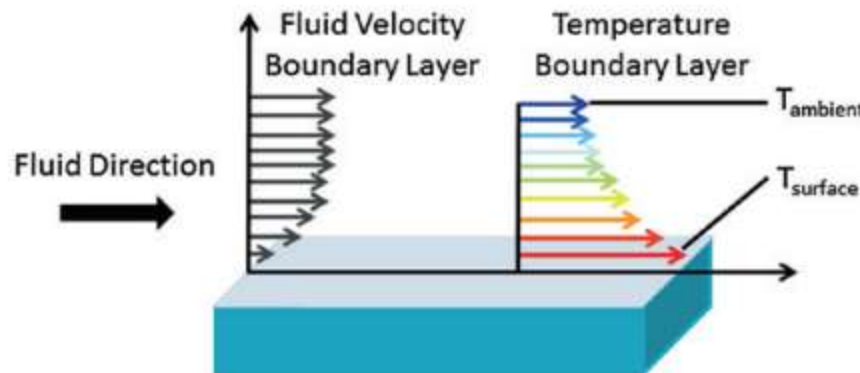


Convection: Convection is the heat transfer from a surface to a fluid. Some common fluids include air and water. Other fluids such as alcohol and oil can also be mentioned in cooling electronics. The rate of convection heat transfer is determined by Eq. 2.3 below

$$Q_{convection} = h_c A (T_{ambient} - T_{surface}) \quad (2.3)$$

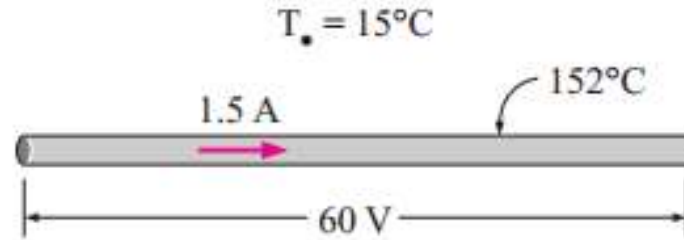
where Q convection is heat flow, h_c is the convection heat transfer coefficient, A is the surface area, T ambient is the ambient temperature of the fluid, and $T_{surface}$ is the temperature of the surface of the material. Figure 2.5 depicts the airflow profile and temperature profile you would expect through convection from the surface of the rectangular object. T surface is warmer than T ambient, which corresponds to the lower airflow velocity at the surface. The convection resistance is described by Eq. 2.4:

$$R_{convection} = \frac{1}{h_c A} \quad (2.4)$$



A 2-m-long, 0.3-cm-diameter electrical wire extends across a room at 15°C. Heat is generated in the wire as a result of resistance heating, and the surface temperature of the wire is measured to be 152°C in steady operation. Also, the voltage drop and electric current through the wire are measured to be 60 V and 1.5 A, respectively.

Disregarding any heat transfer by radiation, determine the convection heat transfer coefficient for heat transfer between the outer surface of the wire and the air in the room.



Radiation is the energy emitted by matter in the form of electromagnetic waves (or photons) as a result of the changes in the electronic configurations of the atoms or molecules. Unlike conduction and convection, the transfer of energy by radiation does not require the presence of an intervening medium.

In fact, energy transfer by radiation is fastest (at the speed of light) and it suffers no attenuation in a vacuum. This is how the energy of the sun reaches the earth.

In heat transfer studies we are interested in thermal radiation, which is the form of radiation emitted by bodies because of their temperature. It differs from other forms of electromagnetic radiation such as x-rays, gamma rays, microwaves, radio waves, and television waves that are not related to temperature.

All bodies at a temperature above absolute zero emit thermal radiation. Radiation is a volumetric phenomenon, and all solids, liquids, and gases emit, absorb, or transmit radiation to varying degrees.

However, radiation is usually considered to be a surface phenomenon for solids that are opaque to thermal radiation such as metals, wood, and rocks since the radiation emitted by the interior regions of such material can never reach the surface, and the radiation incident on such bodies is usually absorbed within a few microns from the surface.

The maximum rate of radiation that can be emitted from a surface at an absolute temperature T_s (in K or R) is given by the **Stefan–Boltzmann law** as

$$\dot{Q}_{\text{emit, max}} = \sigma A_s T_s^4 \quad (\text{W}) \quad (1-25)$$

where $\sigma = 5.67 \times 10^{-8} \text{ W/m}^2 \cdot \text{K}^4$ or $0.1714 \times 10^{-8} \text{ Btu/h} \cdot \text{ft}^2 \cdot \text{R}^4$ is the *Stefan–Boltzmann constant*. The idealized surface that emits radiation at this maximum rate is called a **blackbody**, and the radiation emitted by a blackbody is called **blackbody radiation** (Fig. 1–34). The radiation emitted by all real surfaces is less than the radiation emitted by a blackbody at the same temperature, and is expressed as

$$\dot{Q}_{\text{emit}} = \varepsilon \sigma A_s T_s^4 \quad (\text{W}) \quad (1-26)$$

where ε is the **emissivity** of the surface. The property emissivity, whose value is in the range $0 \leq \varepsilon \leq 1$, is a measure of how closely a surface approximates a blackbody for which $\varepsilon = 1$. The emissivities of some surfaces are given in Table 1–6.

Emissivities of some materials at 300 K

Material	Emissivity
Aluminum foil	0.07
Anodized aluminum	0.82
Polished copper	0.03
Polished gold	0.03
Polished silver	0.02
Polished stainless steel	0.17
Black paint	0.98
White paint	0.90
White paper	0.92–0.97
Asphalt pavement	0.85–0.93
Red brick	0.93–0.96
Human skin	0.95
Wood	0.82–0.92
Soil	0.93–0.96
Water	0.96
Vegetation	0.92–0.96

When a surface of emissivity ε and surface area A_s at an *absolute temperature* T_s is *completely enclosed* by a much larger (or black) surface at absolute temperature T_{surr} separated by a gas (such as air) that does not intervene with radiation, the net rate of radiation heat transfer between these two surfaces is given by (Fig. 1–36)

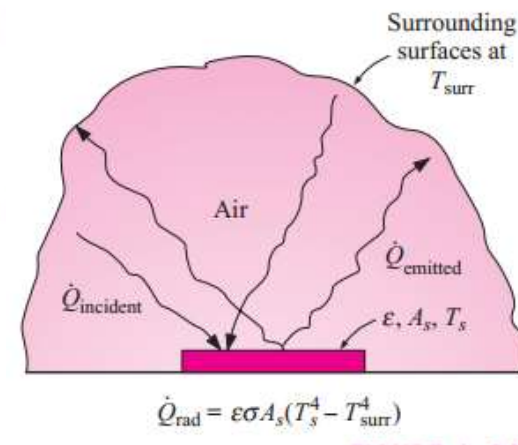
$$\dot{Q}_{\text{rad}} = \varepsilon \sigma A_s (T_s^4 - T_{\text{surr}}^4) \quad (\text{W}) \quad (1-28)$$

In this special case, the emissivity and the surface area of the surrounding surface do not have any effect on the net radiation heat transfer.

Radiation heat transfer to or from a surface surrounded by a gas such as air occurs *parallel* to conduction (or convection, if there is bulk gas motion) between the surface and the gas. Thus the total heat transfer is determined by *adding* the contributions of both heat transfer mechanisms. For simplicity and convenience, this is often done by defining a **combined heat transfer coefficient** h_{combined} that includes the effects of both convection and radiation. Then the *total* heat transfer rate to or from a surface by convection and radiation is expressed as

$$\dot{Q}_{\text{total}} = h_{\text{combined}} A_s (T_s - T_{\infty}) \quad (\text{W}) \quad (1-29)$$

Note that the combined heat transfer coefficient is essentially a convection heat transfer coefficient modified to include the effects of radiation.



1. Consider a person standing in a room maintained at 22°C at all times. The inner surfaces of the walls, floors, and the ceiling of the house are observed to be at an average temperature of 10°C in winter and 25°C in summer.

Determine the rate of radiation heat transfer between this person and the surrounding surfaces if the exposed surface area and the average outer surface temperature of the person are 1.4 m² and 30°C, respectively

Assumptions 1 Steady operating conditions exist.

2 Heat transfer by convection
is not considered.

3 The person is completely surrounded by the interior surfaces of the room.
4 The surrounding surfaces are at a uniform temperature.

The emissivity of a person is 0.95, $\sigma (5.67 \times 10^{-8} \text{ W m}^{-2} \text{ K}^{-4})$ is the Stefan-Boltzmann constant

2. A rectangular block has an area of 400 mm²

. An engineer would like to use it to cool his heat source that is producing a total of 50 W with a specification of 90 °C. The heat source is placed in a chamber with an air temperature of 65 °C. If the through-length is 10 mm, what is the minimum conductivity of the material in order to cool the heat source to specification using the block alone?

Thermal-sensing elements



What Is a Thermal Sensor?

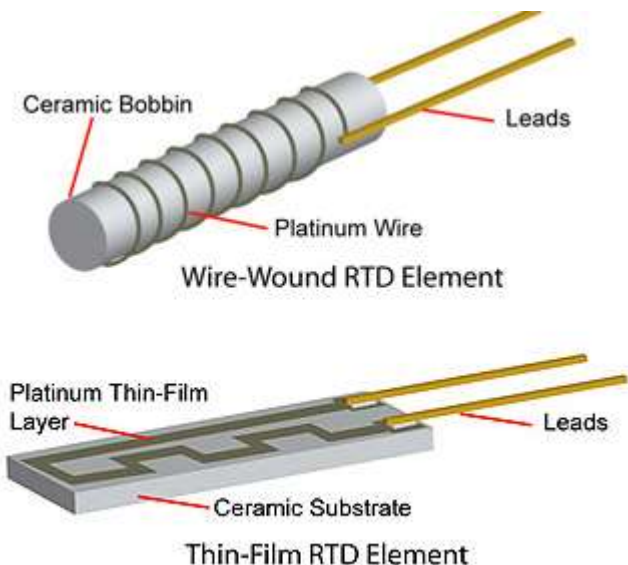
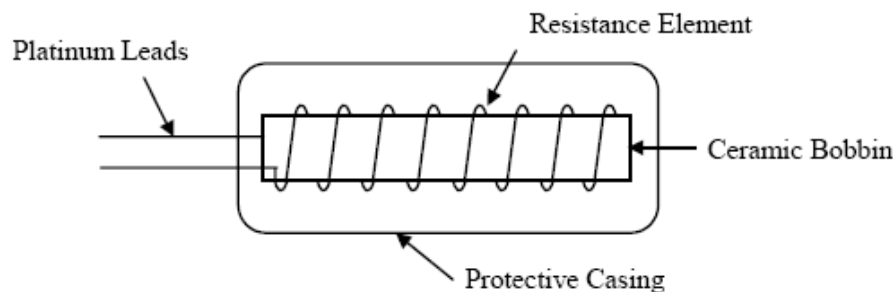
- Temperature is the measure of the average kinetic energy of the molecules of a gas, liquid, or solid.
- A thermal sensor is a device that is specifically used to measure temperature.

The most popular sensor in terms of market surveys and sales is the temperature sensor.

This sensor is used in a wide range of applications critical to the medical, agricultural, industrial, and automotive communities, to name just a few.

Resistance Thermometers

Resistance thermometers are also known as **resistance temperature detectors, or RTDs**. They are typically made of a single pure metal . Each metal has a material property of electrical resistance that is a function of temperature. The most accurate resistance thermometers are ones that use metals that have a very linear relationship with temperature, **such as platinum**. By using the relationship curves between electrical resistance and temperature, when the resistance of the metal is measured, a temperature can be calculated . Figure depicts the construction of one type of resistance thermometer



Type

Temperature Range

(K)

Resistance Ω

Medium

Platinum: Ceramic encased

250–350

100 (0°C)

Still air

Platinum (SPRT): Long stem

250–350

25.5 (0°C)

Still air

Thermistor: Glass enclosed

220–550

104 (25°C)

Still air

Thermistor: Glass enclosed

220–550

104 (25°C)

Still water

Germanium: Copper encased

10–30

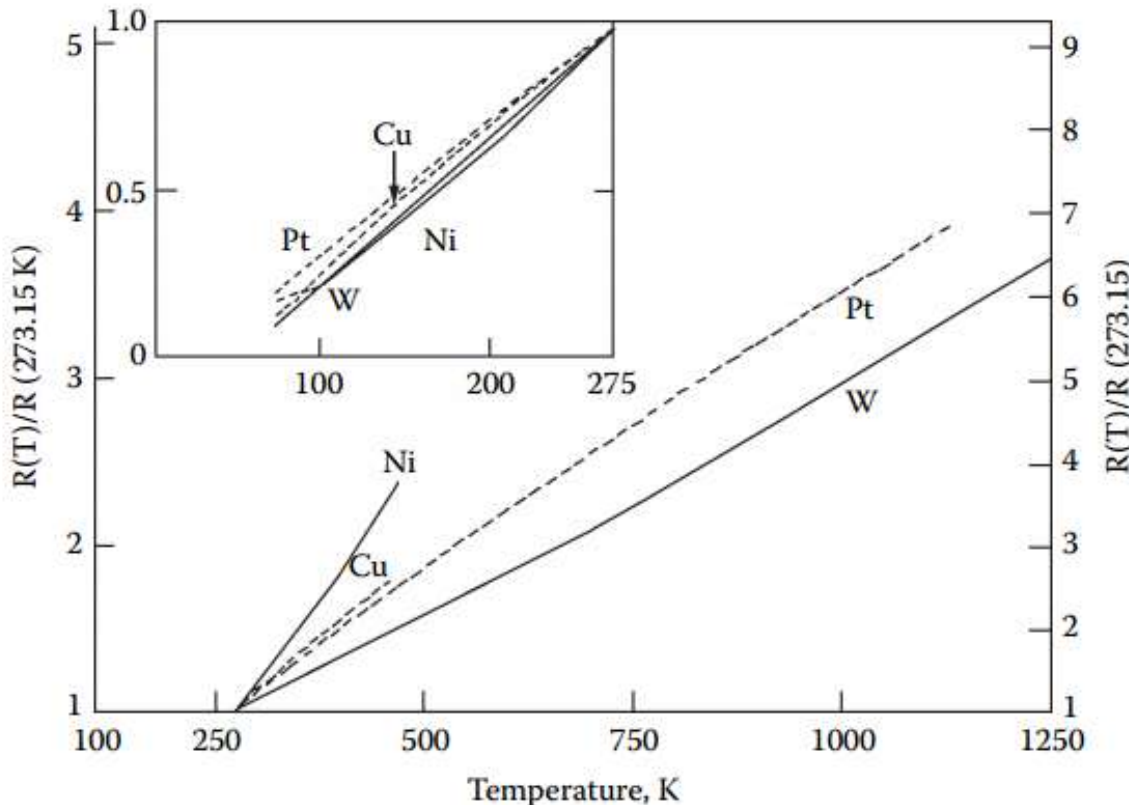
Metal block

Germanium: Copper encased

<2

Metal block

Experimental measurements clearly show that the resistance thermometers that use metals display an increase in resistance as temperature increases.



Basically the metal consists of ion cores immersed in a sea of electrons. The number of free electrons in the metal does not vary with temperature and is a constant. The only parameters that can vary with temperature are the motion of the electrons and the vibrations of the ion cores. As temperature increases, the electron motion increases and the electrons collide with themselves and the vibrating ion cores. Since the electrons are much smaller than the ion cores, one can neglect electron-electron collisions. The major contribution is therefore due to the electrons colliding with the vibrating ion cores.

Electrical conductivity of a metal sample may be expressed as follows:

$$\sigma = ne\mu$$

where n = electron density, e = electronic charge, and μ = electron mobility.

The electron mobility is defined as follows:

$$\mu = \frac{e\tau}{m} \quad (5.3)$$

where τ = average time between collisions, and m = electron mass.

Noting that the resistivity, ρ , of a metal is the inverse of the conductivity, one obtains, using Equations 5.2 and 5.3, the following relation:

$$\rho = \frac{1}{\sigma} = \frac{m}{ne^2} \left(\frac{1}{\tau} \right) \quad (5.4)$$

The most common material used in metal thermometers is platinum. PRTs typically have a resistance range between .1 Ω and 1 KΩ.

Other, less popular metal resistance thermometers use copper (Cu), iridium (Ir), or combinations of rhodium and cobalt (Rh-Co) or platinum and cobalt (Pt-Co). The Cu thermometer is the most linear, but it has a limited temperature range (0 to 100°C). The Ir thermometer provides an excellent match to aluminum substrates and is normally used as a thin film in surface temperature measurements. Rh-Co and Pt-Co are used primarily for low-temperature (.5 to 30 K) applications.

Thermometers that use semiconductors as the sensing element differ from metal-based thermometers in that the resistance decreases with increasing temperature.

Also, in contrast to metals, the free electron density in semiconductors is not constant but increases with temperature

The conductivity is given by the following equation

$$\sigma = e(n\mu_n + p\mu_p)$$

where μ_n and μ_p are the mobilities of the electrons and holes, respectively.

$$\sigma = e^2 \left(\frac{n\tau_n}{m_n} + \frac{p\tau_p}{m_p} \right)$$

where τ_n and τ_p are the average time between collisions for electrons and holes, respectively. In an intrinsic semiconductor the number of electrons is equal to the number of holes, and hence

$$n = p = n_i \quad (5.10)$$

where n_i = intrinsic carrier density.

Thermometers that use semiconductors are thermally sensitive resistors, or what is commonly called thermistors.

The semiconductors used in thermistors are not the common semiconductors such as silicon or gallium arsenide.

Typically thermistors use metal oxides or combinations of metal oxides.

Examples of metal oxides that are used in thermistors are the oxides of tungsten manganese, nickel, cobalt, iron, copper, lithium, magnesium, and chromium. The most stable mixed metal oxides are Mn-Ni and Mn-Ni-Co.

•

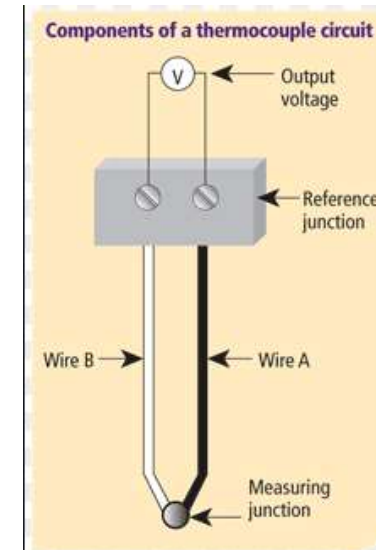
Thermistors typically have resistance between $10\ \Omega$ and $100\ M\Omega$. Due to the large resistance range, thermistors provide excellent sensitivity and are also very stable, particularly between 100 and 300°C . Thermistors can also be manufactured very cheaply

For applications greater than $1,000^{\circ}\text{C}$ thermistors made with zirconium oxide are the most popular. Zirconium is unique in its ability to withstand high temperatures.

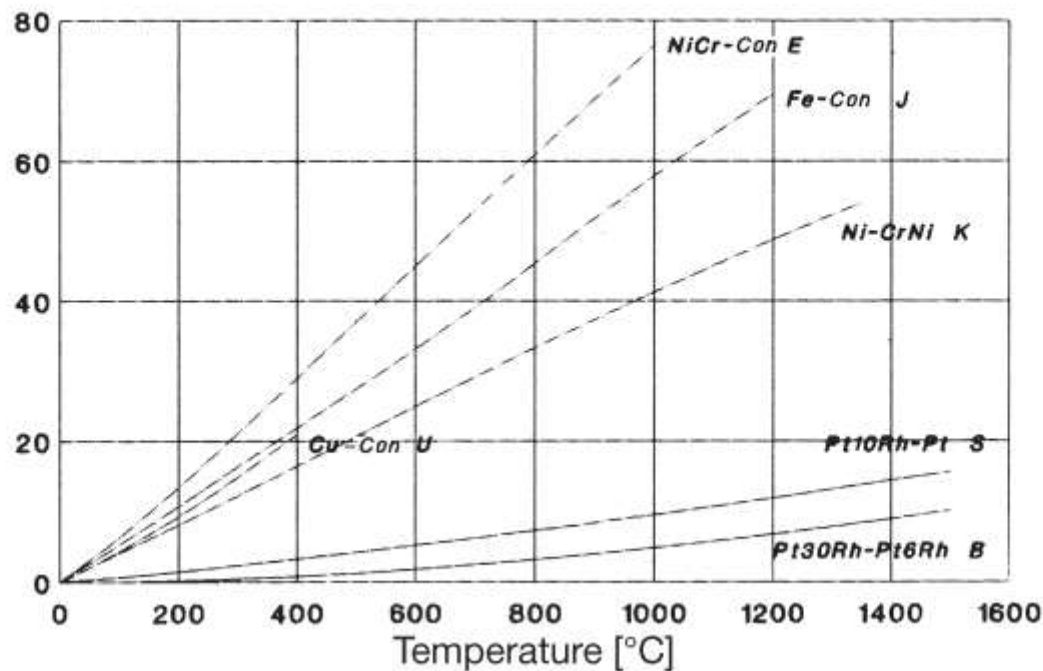
Temperature-Difference Sensing Elements

Thermocouples

Thermocouples are sensors composed of two different metals at their sensing end. A voltage is created when there is a temperature gradient between the hot sensor element and the cold reference junction. The change in voltage can be reported as a temperature through the Seebeck effect . **The Seebeck effect says that the change in voltage is linearly proportional to the change in temperature and the two variables are related to each other through a coefficient that is determined by the materials used in the thermocouple .** Figure depicts the construction of a thermocouple.



Voltage/mV

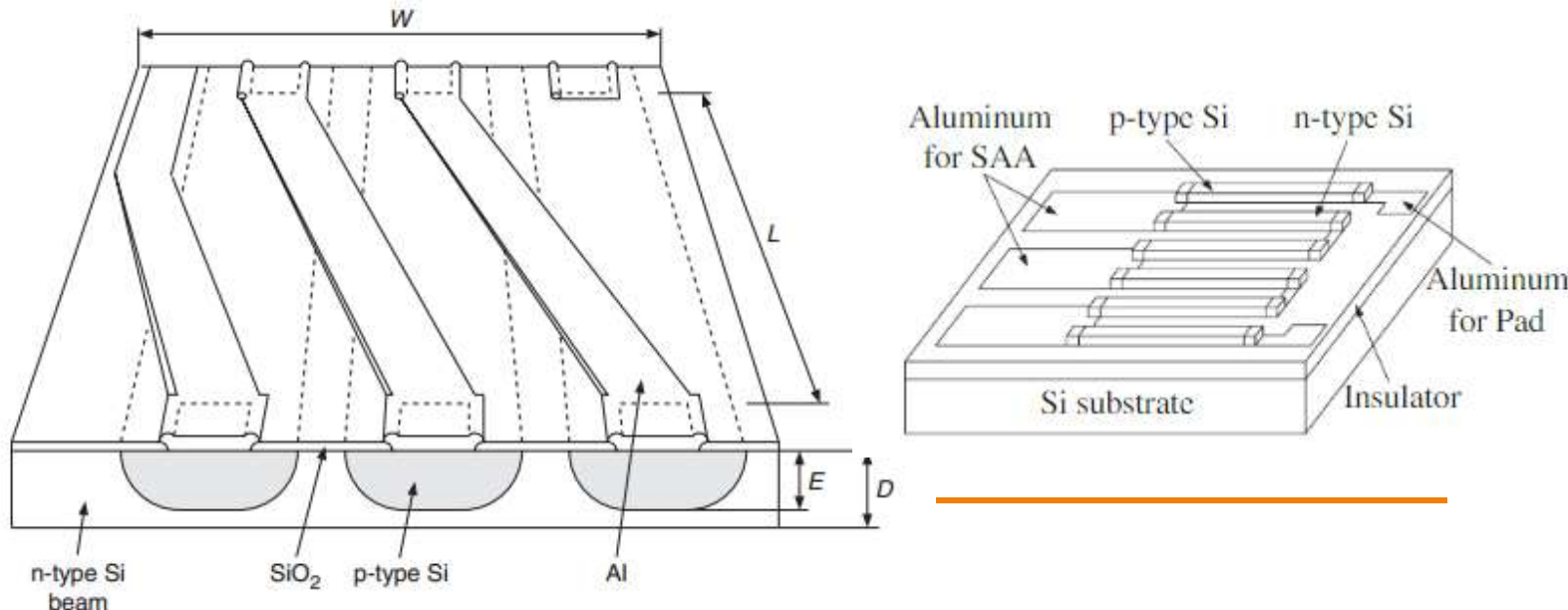


Characteristics of thermocouples

Thermocouples are two-lead elements that measure the temperature difference between the ends of the wires. The operating principle is based on the thermoelectric Seebeck effect, which says that a temperature difference ΔT in a (semi)conductor also creates an electrical voltage ΔV :

$$\Delta V = \alpha_s \Delta T \quad (6.29)$$

where α_s is the Seebeck coefficient expressed in V/K. The Seebeck coefficient α_s is a material constant. By taking two wires of materials with different α_s , we get different electrical voltages across the wires, even when the wires experience the same temperature gradients. With a junction of the wires at the hot point, the voltages are subtracted, and an effective Seebeck coefficient will remain. Thermocouples or thermopiles (several thermocouples in series) in thermal sensors are made of thin-film metals or polysilicon, or monocrystalline silicon



In practice, the Seebeck coefficient α_{mono} for monocrystalline silicon is related to the electrical resistivity ρ . At room temperature, this relation can be expressed as:

$$\alpha_{\text{mono}} = \frac{mk}{q} \ln \frac{\rho}{\rho_0} \quad (6.30)$$

with $\rho_0 \approx 5 \times 10^{-6} \Omega \text{ m}$ and $m \approx 2^{1/2}$ as constants [5] and k the Boltzmann constant, $k/q \approx 86.3 \mu\text{V/K}$. For practical doping concentrations, the Seebeck coefficients are of the order of 0.3 mV/K to 0.6 mV/K, where the sheet resistance depends on the layer depth.

For polycrystalline silicon, a similar expression is given by Von Arx [6] as a function of electrical resistivity:

$$\alpha_{\text{poly}} = \frac{m_{\text{poly}}k}{q} \ln \frac{\rho}{\rho_0} \quad (6.31)$$

with $\rho_0 \approx 1.4 \times 10^{-6} \Omega \text{ m}$ and $m_{\text{poly}} \approx 0.7$ as constants, and k the Boltzmann constant. In practice, the Seebeck coefficients are of the order of 0.1 mV/K to 0.2 mV/K, for instance at sheet resistances of $50 \Omega/\square$ to $100 \Omega/\square$ and a poly thickness of 300 nm.

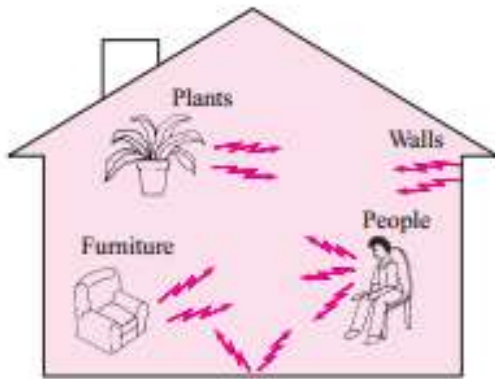
Seebeck coefficients for metals are much smaller than those for silicon and that the influence of aluminum interconnections on chips is negligible compared to the Seebeck coefficient for silicon. The electrical resistance and also the thermal conductivity play a part in determining how efficiently a thermopile functions in a thermal sensor. These parameters are much more favorable for bismuth telluride compounds or silicon–germanium compounds than for mono- or polysilicon [8]. However, the advantage of these compounds largely lies in their low thermal conductivity, compared with that of silicon, and in many microsensors the thermal resistance of the sensors is determined more by conduction through air or membranes than through the thermopile. In these, a silicon thermopile will lead to almost the same performance as thermopiles made of other compounds but has the big advantage that it can be produced in standard IC technology.

Table 6.3 Seebeck coefficients ($\mu\text{V/K}$) of some selected materials and standard thermocouples

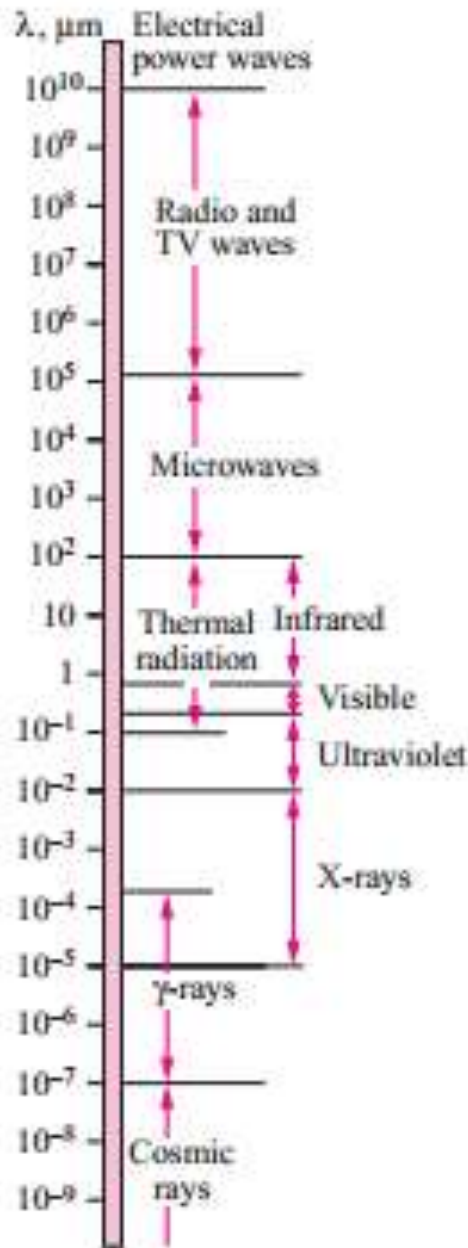
Material	273 K ($\mu\text{V/K}$)	300 K ($\mu\text{V/K}$)
Antimony (Sb)		43 ^a
Chromium (Cr)	18.8	17
Gold (Au)	1.79	1.94
Copper (Cu)	1.70	1.83
Silver (Ag)	1.38	1.51
Rhodium (Rh)	0.48	0.40
Lead (Pb)	-0.995	-1.047
Aluminum (Al)		-1.7
Platinum (Pt)	-4.45	-5.28
Nickel (Ni)	-18.0	
Bismuth (Bi)		-79 ^a
J-type thermocouple Fe–CuNi	50	51
T-type thermocouple Cu–CuNi	39	41
E-type thermocouple NiCr–CuNi	59	
K-type thermocouple NiCr–NiAl	39	41
S-type thermocouple Pt–Pt/10%Rh	5	7
T-type thermocouple Pt–Pt/13%Rh	5	6
Monocrystalline silicon (typical)	500	500
Polycrystalline silicon (typical)	150	150

^aAveraged over 0 °C to 100 °C.

The electromagnetic wave spectrum



Everything around us constantly emits thermal radiation



Thermal radiation is also defined as the portion of the electro-magnetic spectrum that extends from about 0.1 to 100 μm , since the radiation emitted by bodies due to their temperature falls almost entirely into this wave-length range. Thus, **thermal radiation includes the entire visible and infrared (IR) radiation as well as a portion of the ultraviolet (UV) radiation**

What we call light is simply the visible portion of the electromagnetic spec-trum that lies between 0.40 and 0.76 μm . Light is characteristically no different than other electromagnetic radiation, except that it happens to trigger the sensation of seeing in the human eye.
Light, or the visible spectrum, consists of narrow bands of color from violet (0.40–0.44 μm) to red (0.63–0.76 μm)

Radiation Thermometers

All substances and objects emit thermal radiation when it is at a temperature higher than absolute zero (0 K or -273.15°C). There is a **relationship between temperature and radiation energy emitted that can be used to calculate the temperature of the object surface**. Unlike other sensors discussed above, radiation thermometers are primarily used at a distance from the object of interest and can be used for hard-to-reach objects. An **example of a radiation thermometer is an infrared camera**, which measures infrared wavelengths that emit from an object.



Infrared Sensor

From the transduction point of view, the infrared sensor is fairly simple. The transduction from radiation to heat is carried out by a black absorber, which can have an efficiency up to 99 %. The first transduction step from incident radiation density P_{inc}'' (in W/m^2) to thermal power P is

$$P = Q P_{\text{inc}}$$

$$Q = \alpha A_D \tau_{\text{filter}}$$

where A_D is the sensitive area of the sensor (usually the area that is coated black), α is the absorptivity of the black coating of the sensitive area, and τ_{filter} is the transmittance of an infrared filter, which can be applied to select specific radiation wavelengths or simply for mechanical protection. The absorptivity α is between 0 and 1 and denotes the fraction of infrared radiation power which is absorbed by the black coating. Various types of black coatings are used for silicon infrared sensors.

Infrared sensors have many applications. Burglary alarms use infrared sensors of the pyroelectric type, which respond to changes in the infrared image. This is particularly useful in security applications, where an image without any movements is the proper one and a sudden movement indicates an intruder. For gas analysis, such as CO and CO₂, infrared sensors

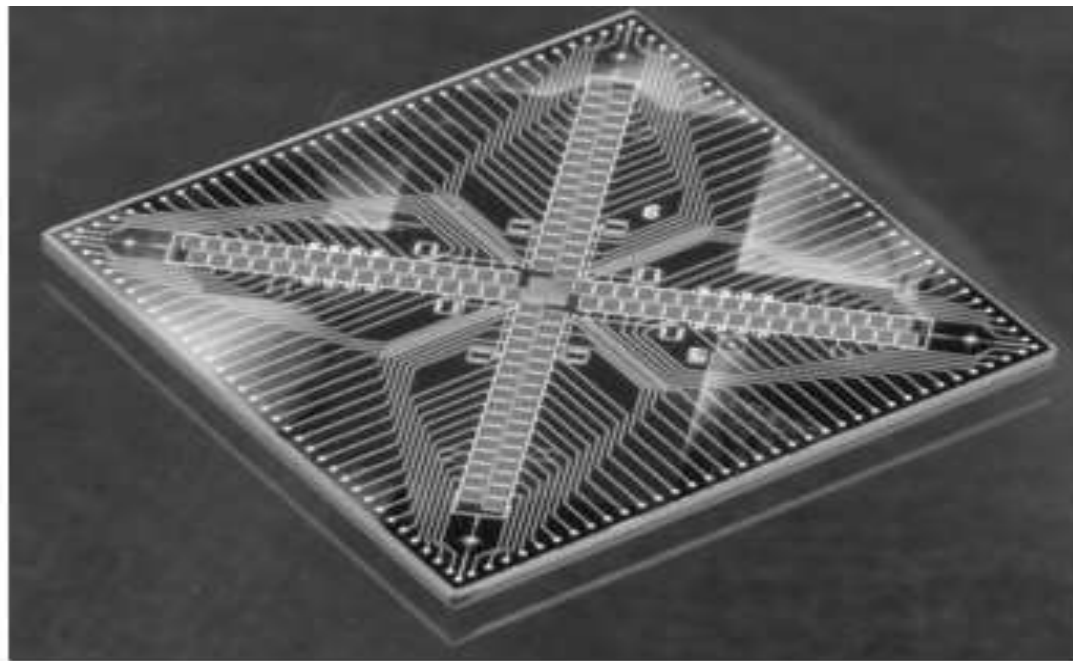


Figure 6.11 Focal plane array of 4×32 infrared detectors for satellite attitude control instrument, chip size $20.5 \text{ mm} \times 20.5 \text{ mm}$ (Xensor Integration)

based on thermopiles and thin membranes are used. Other applications include temperature measurement, where, for instance, the toasting of bread can be monitored using an infrared sensor. For space applications, EADS Sodern developed a focal plane array (FPA) of infrared detectors for a so-called Earth sensor, where the image of the Earth is projected onto the FPA chip using a germanium lens. The Earth sensor uses the image in the (14 to 16) μm band, emitted by the CO₂ of the atmosphere. This image of Earth is nicely round and is dependent neither on day or night nor on the seasons. In this way, the attitude of the satellite with respect to the Earth can be measured, and if necessary, corrected; as a result, for instance, a weather satellite will monitor the weather in the required region, instead of that of the North Pole or space. The FPA chip contains 132 infrared pixels (each with its own thermopile and black area) and measures $20.5 \text{ mm} \times 20.5 \text{ mm}$ (Figure 6.11) [17].

Interaction of gaseous species at semiconductor Surfaces-Catalysis



4.3.4.1 Adsorption/Desorption Mechanism

During the gas molecule–solid-state surface interaction, the gas species initially gets physisorbed and chemisorbed at the semiconductor surface. There is no charge transfer in case of physisorption. A molecule is considered to be chemisorbed when there is an electronic transfer between the gas and the solid, and the conductivity of the material gets affected.

As an illustrative example, the different oxygen species formed as the oxygen molecules interact with a solid-state surface are shown in Figure 4.12 (Kohl 1989, Liu et al. 2007). Oxygen can be adsorbed in the form of O_2^- , O^- , or O^{2-} . Due to energy considerations, near room temperature, the O^{2-} specie dominates the surface coverage, whereas at higher temperatures, O^- is the dominating specie. The adsorption of these species on the surface extracts electrons from the donor levels of the material. The extraction of electrons creates an electron-depleted or positive space charge region near the surface (Figure 4.12). This results in an increase in the resistance of an n-type material.

The adsorbed oxygen ions are present in large concentrations at any semiconductor surface. The gas-sensing mechanism depends on the decrease or increase in the concentration of the adsorbed oxygen ion at the semiconductor surface. It is clear that on interaction with a reducing gas, the number of adsorbed oxygen species will be reduced and a number of electrons will be released back to the semiconductor surface (conduction band of the semiconductor). The O_2^- and O^- species preferentially interact with the C–C bond of the incoming reducing gas. Increase in the concentration of electrons in the conduction band results in an increase in the conductivity of the n-type semiconductor. The large increase in the conductivity of the oxide semiconductor in the presence of a reducing gas is because of a decrease in the adsorbed oxygen species at the oxide surface. It is clear that the effect of an oxidizing gas will be reverse (increase in absorbed oxygen sites and decrease in the conductivity of the semiconductor).

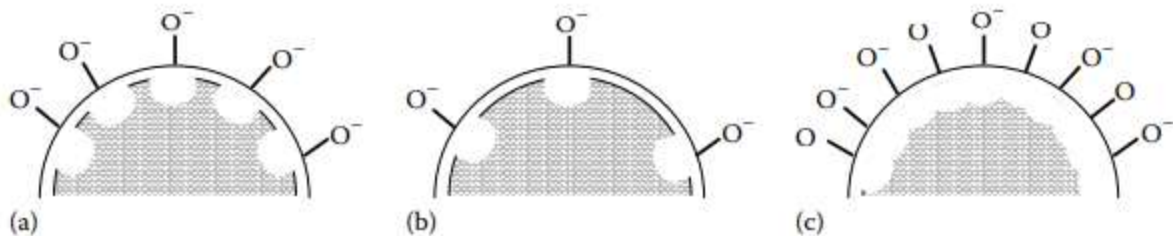
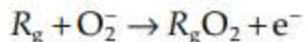
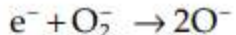
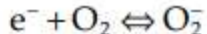


FIGURE 4.13

Effect of (a) air, (b) reducing gas, and (c) oxidizing gas on an n-type semiconductor material. Depletion region is shown as white region, and shadowed region shows the conducting regions of the oxide nanoparticles.

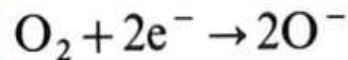
The reaction steps (Kohl 1989) are given below:



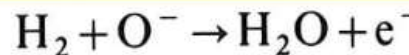
Here R_g represents the reducing gas.

If a p-type semiconductor is used in place of an n-type semiconductor, the reducing gas will decrease the adsorbed oxygen sites, take away electrons from the semiconductor surface, and create more holes in the semiconductor. This is also illustrated in Figure 4.13. The conductivity of the p-type semiconductor due to increase in the concentration of holes will thus increase.

- Typical operation principle “one explanation”
 - Resistive sensor, resistance decrease when a layer of powdered SnO_2 is exposed to combustible gas in present of ambient air.
 - Oxygen in air adsorbs at semiconductor surface, oxygen dissociates to form O^- . The electron is picked up from the semiconductor, which increases its resistance.



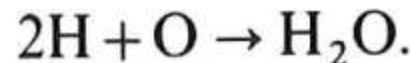
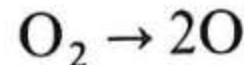
- O^- is highly reactive and easily react with combustible gases which contain hydrogen.



- Hydrogen react and form water, as a result an electron is released which lowers the resistance in the semiconductor.
- To increase the reaction rate a catalyst is often included.

Catalysis, the acceleration of chemical reactions

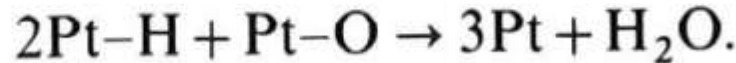
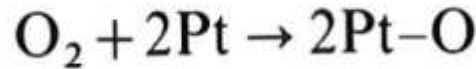
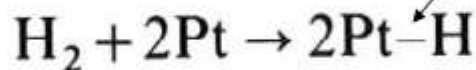
- Catalyst is needed to increase the sensitivity and accelerate the reaction in metal-oxide gas sensor
- A catalyst is not consumed and lower the activation energy for the reactions
- Without the catalyst, the reaction have a high activation energy:



chemical reactions

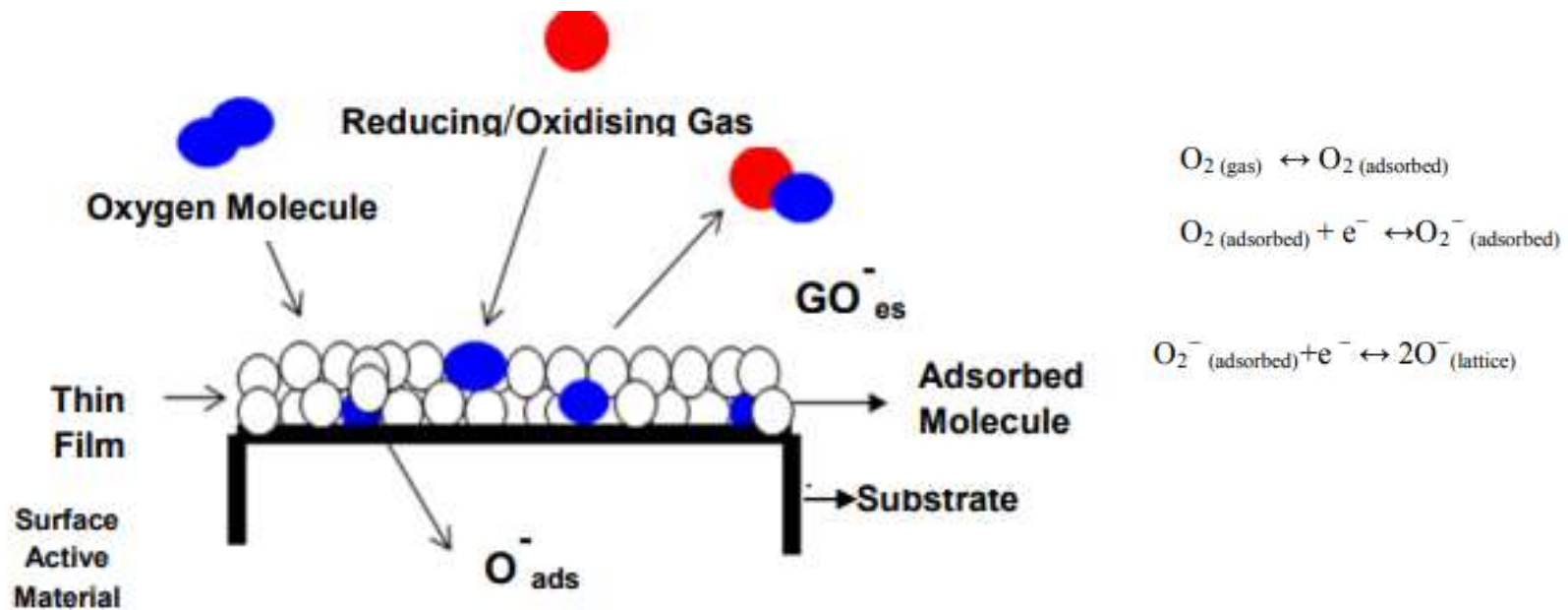
With Platinum as a catalyst

Hydrogen is adsorbed on a platinum surface ("group of")



The activation energy is drastic reduced

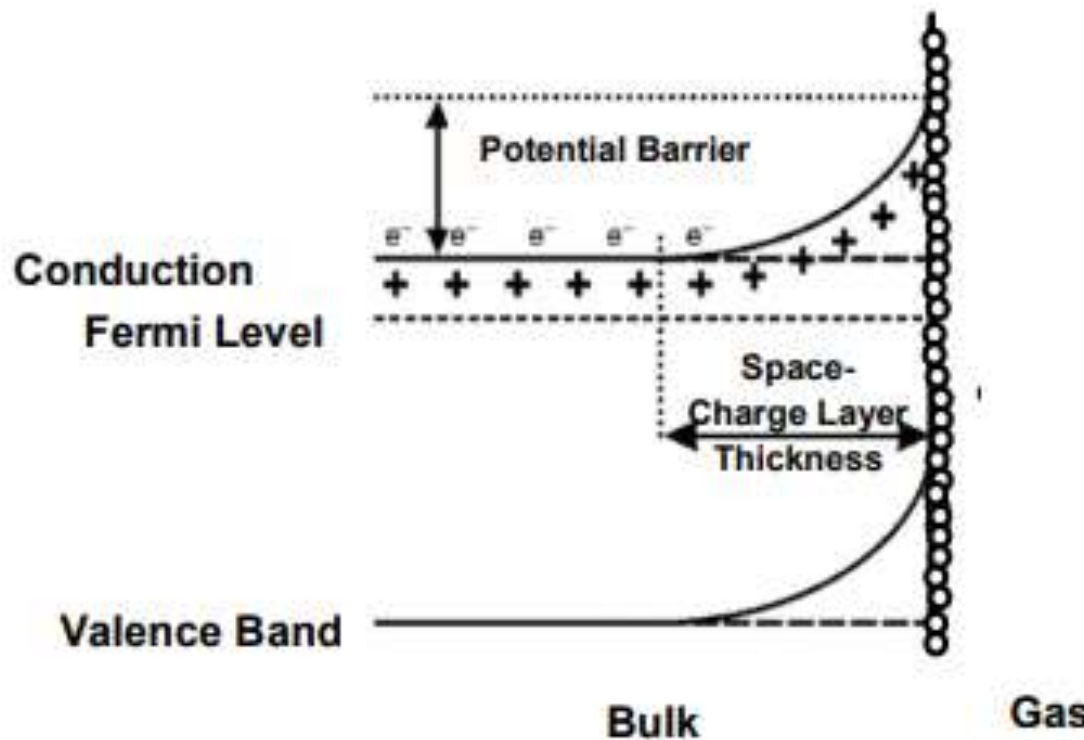
At elevated temperatures, reactive oxygen species such as O_2^- , O^{2-} and O^- are adsorbed on the surface of metal oxide semiconductor.



Schematic representation of metal oxide semiconductor as gas sensors

The sensing element of chemiresistive type sensors normally comprises of a semiconducting material with high surface-to-volume ratio on a ceramic (glass) substrate with ohmic contacts to measure the change in resistance/conductance. When, gas/volatile organic compounds (VOC) samples interact on the surface of metal oxide semiconductor, due to the combustion reaction that occurs with the oxygen species on the surface of metal oxide particles leads to change in resistance and forms the basic principle of detection.

As shown in Fig. when O₂ molecules are adsorbed on the surface of metal oxides, they would extract electrons from the conduction band Ec. This will lead to band bending and an electron depleted region (space charge region). The thickness of this space charge region is equivalent to the length of band bending region



Schematic representation of band bending after chemisorption of charged species

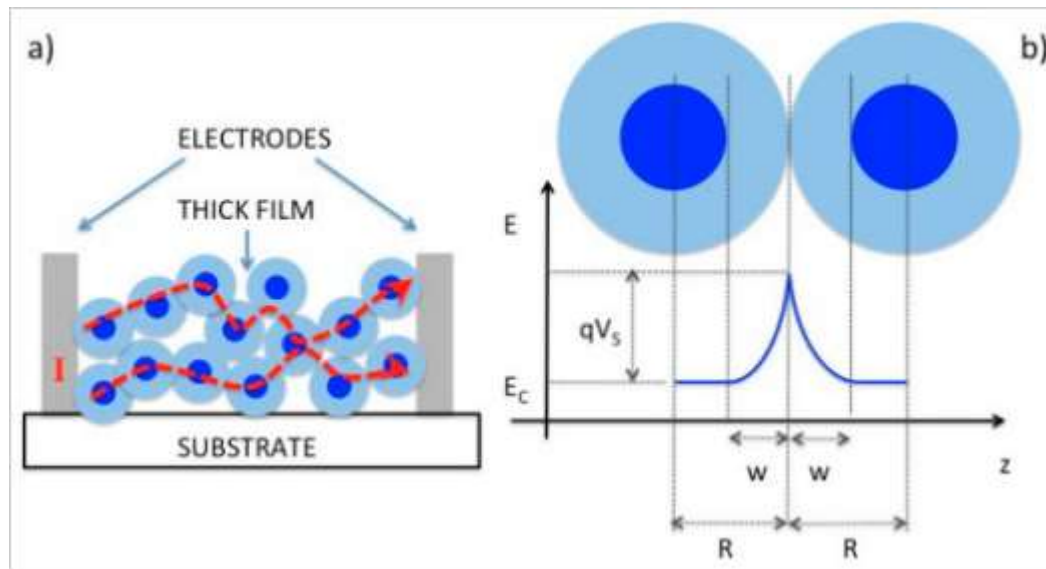
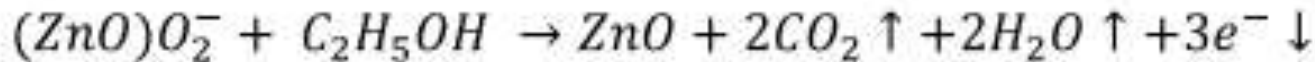
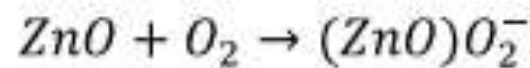
Table 1: Classification according to the changes in the response of sensing element

Classification	Oxidising Gases	Reducing Gases
n-type	Resistance increase	Resistance decrease
p-type	Resistance decrease	Resistance increase

Table 2: Classification of metal oxides based on the conductivity type

Type of Conductivity	Metal oxides
n – type	ZnO, MgO, CaO, TiO ₂ , WO ₃ , SnO ₂ , In ₂ O ₃ , Al ₂ O ₃ , Ga ₂ O ₃ , V ₂ O ₅ , Nb ₂ O ₅ , ZrO ₂
p – type	Y ₂ O ₃ , La ₂ O ₃ , CeO ₂ , Mn ₂ O ₃ , NiO, PdO, Ag ₂ O, Bi ₂ O ₃ , Sb ₂ O ₃ , TeO ₂

When the reducing gas like ethanol interacts with n-type semiconductor, then the surface conductivity increases based on the following reaction:



$$\therefore \frac{R_{\text{Gas}}}{R_{\text{Air}}} = \exp \frac{eV_{\text{Air}} - eV_{\text{Gas}}}{k_B T}$$

Thin-film sensors, FET devices for gas and ion sensing



Conducting polymer composites, intrinsically conducting polymers and metal oxides are three of the most commonly utilised classes of sensing materials in conductivity sensors. These materials work on the principle that a change in some property of the material resulting from interaction with a gas/odour leads to a change in resistance in the sensor.

The mechanisms that lead to these resistance changes are different for each material type; however, the structure and layout of conductivity sensors prepared using these materials are essentially the same.

A schematic of a typical conductivity sensor design is shown in Figure. 1. The sensing material is deposited over interdigitated or two parallel electrodes, which form the electrical connections through which the relative resistance change is measured. The heater is required when metal oxides are used as the sensing material because very high temperatures are required for effective operation of metal oxide sensors.

Typical structure of a conductivity sensor

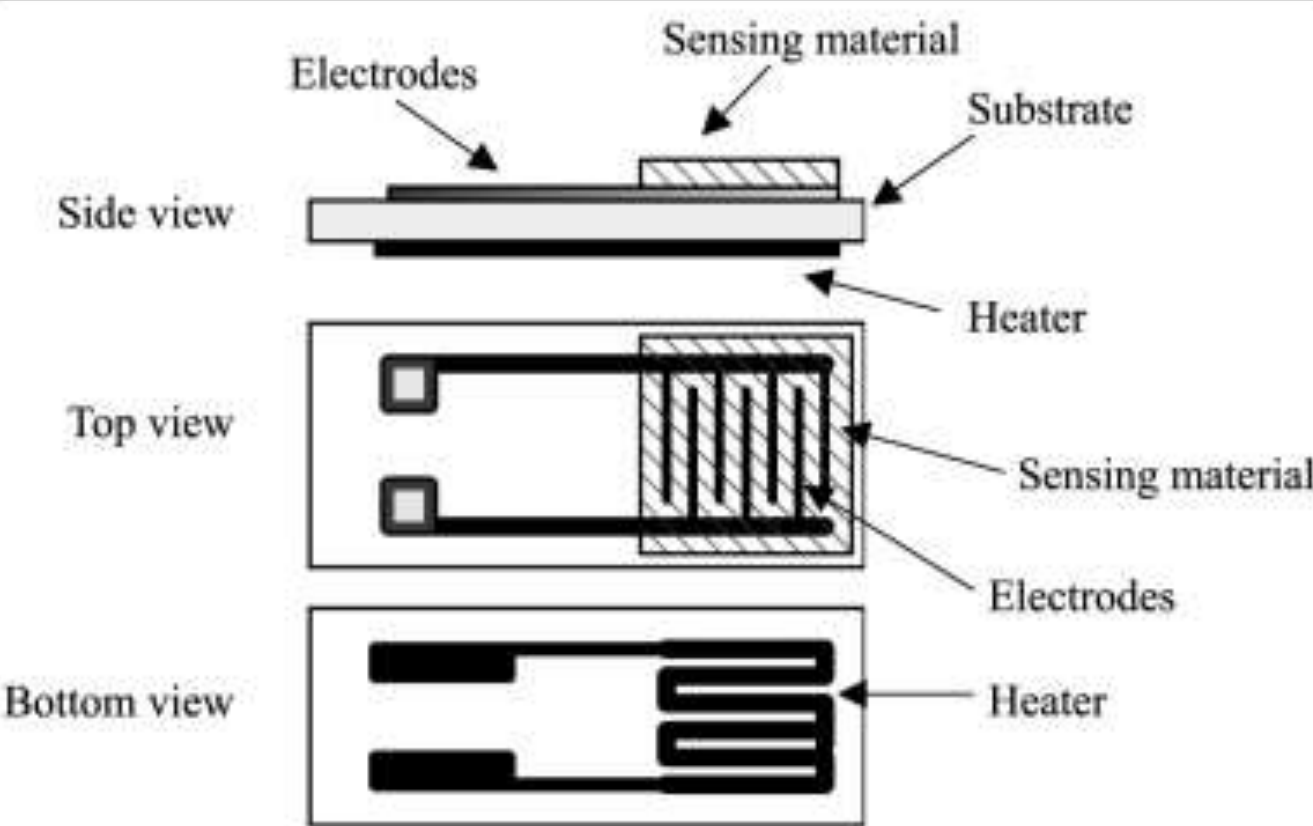
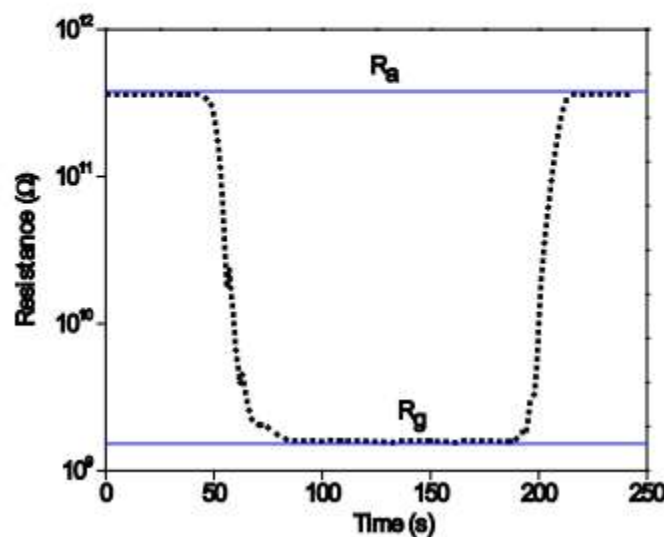


Figure. 1

Sensitivity It is the response of a gas sensor per unit change in the gas concentration. Since, metal oxide gas sensors are based on the principle of chemiresistivity; it is generally defined in terms of conductance or resistance. For n-type material in the presence of reducing gas and p-type material in the presence of oxidizing gas, sensitivity can be defined as,

$S = (R_a - R_g)/R_g$, where, R_a , R_g are the stable values of the resistance of the material before and after exposure to gas.

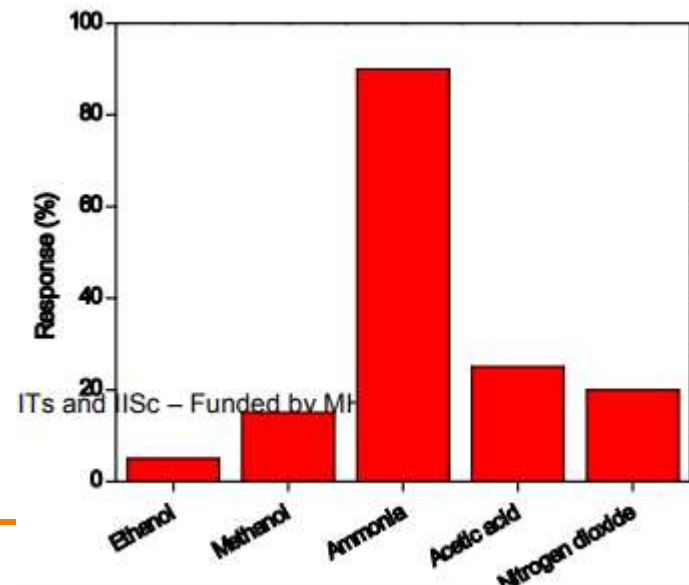


Selectivity

A sensor should respond to only a particular molecule in a mixture of environment. The selectivity of a gas sensor towards a particular molecule is the ratio of its response towards it and that of another dominant interfering molecule in the atmosphere.

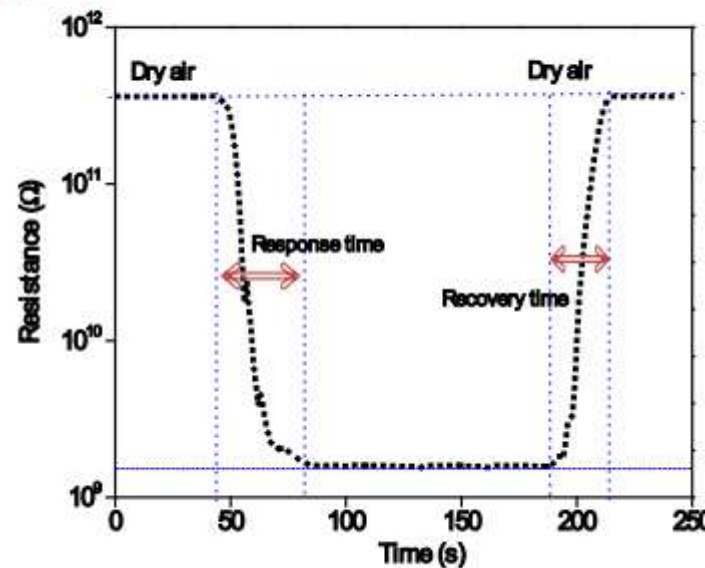
$$\text{Selectivity of an gas sensor} = \frac{\text{sensitivity of a particular molecule}}{\text{sensitivity towards an interferent}}$$

Selectivity of a gas sensor should be always greater than one.



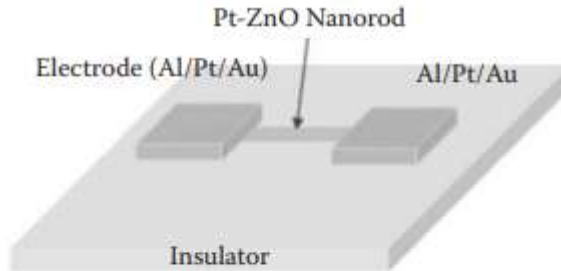
Speed of response

The time required for a sensor to reach 90% of total response of the signal such as resistance upon exposure to the target gas

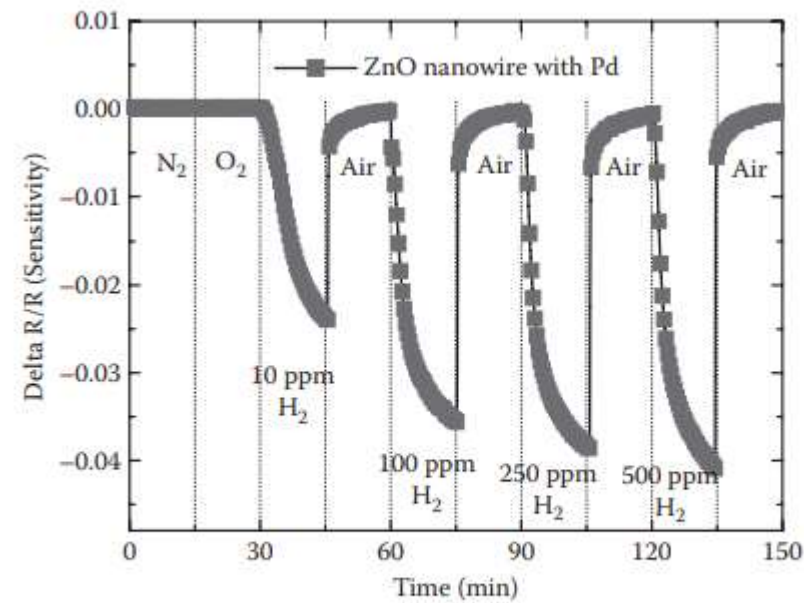
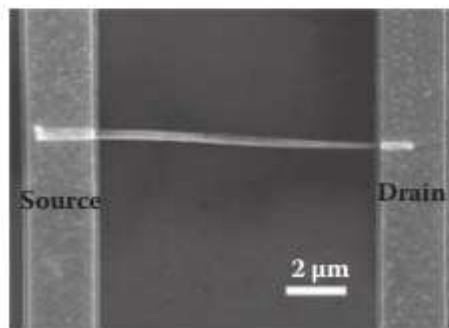


Recovery time

The time required for a sensor to return to 90% of original baseline signal upon removal of target gas



ZnO nanowire sensor (top), SEM of completed device



Change in resistance as a function of time when switching to H₂-containing ambient.

Gas-sensitive FETs and field-effect devices combined with catalytic metal gates



Gas-sensitive FETs and field-effect devices combined with catalytic metal gates

Catalytic-gate FETs are one of types of gas-sensitive FETs. In 1975, Lundström et al. first reported a Pd-gate FET sensitive to hydrogen. Pioneering research on catalytic-gate FETs opened up the field of FET-based gas sensors and other gas-sensitive field-effect devices such as capacitor-based and Schottky diode-based sensors . Catalytic-gate filed-effect devices feature a nanoscale layer of catalytic metals, such as palladium and platinum, as a gate electrode on insulating layers in a metal-insulator-semiconductor (MIS) structure . Figure 1 shows reported schematic illustrations of this structure and the threshold voltage shift of a Pd-gate FET that is sensitive to hydrogen . In initial reports of catalyticgate FETs, Pd as a catalytic-gate electrode was deposited onto the insulating layer of the MIS structure of the FET .

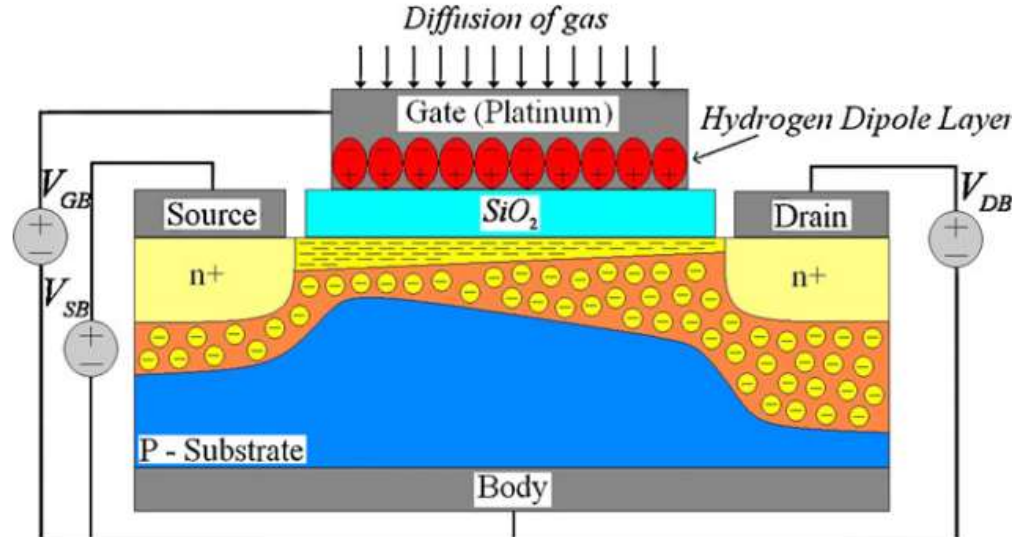
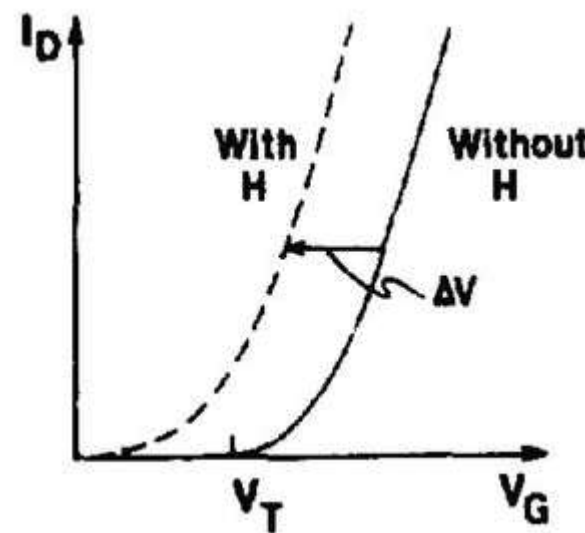


Fig. 1. Structure of a MOSFET gas sensor submitted to hydrogen gas.

Exposing the sensor to hydrogen gas causing formation of the dipole layer hydrogen molecules adsorb at the surface of the platinum and the attractive forces between the platinum and the hydrogen atoms weaken the H–H bond therefore the hydrogen molecules dissociate into the hydrogen atoms.

Some of the atoms landed on the platinum surface diffuse rapidly through the metal and adsorb at the Pt– SiO_2 junction where they become polarized under influence of the electric field and create the dipole layer shown Due to the dipole layer and causes shift in the metal work function:



MOSFET “Linear” Region

$$I_{DS} = \frac{W}{L} \mu_n C_{ox} (V_{GS} - V_{Th}) V_{DS} \quad V_{GS} > V_{Th} \quad V_{DS} \approx 100\text{mV}$$

$$V_{T0} = \phi_\infty - 2\phi_F - \frac{Q_{d0}}{C_{ox}} - \frac{Q_i}{C_{ox}}$$

$$\Delta W_M = W'_M - W_M$$

$$\Delta V_T = \frac{\Delta W_M}{q}$$

Suspended-gate FETs

In 1983, Janata et al. reported an SGFET sensitive to dipolar molecules such as methanol and methylene chloride. In the SGFET shown in Fig.

Figure 12. Scheme of a suspended gate GasFET. The gate electrode is suspended and covered with a gas sensitive layer. The electrical potential generated by gas adsorption acts as an additional gate voltage and changes the source-drain current. Reprinted from [150] with permission from Elsevier.

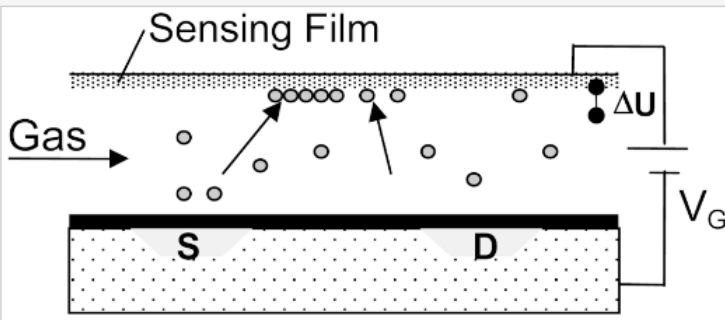
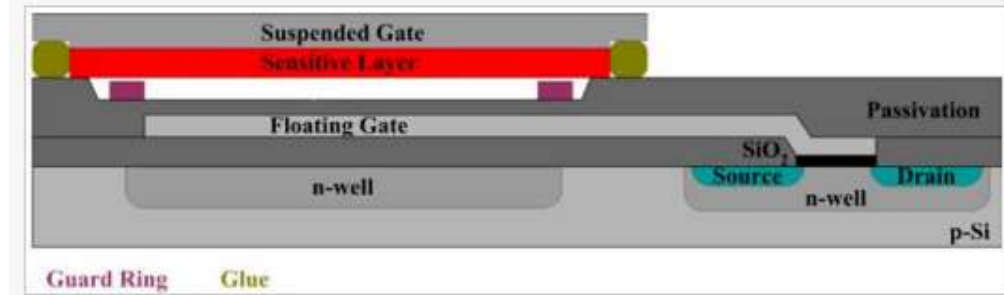


Figure 13. Schematic cross section of a floating gate (FGFET) type transducer that improves the coupling of the work function voltage to the FET. The capacitance well electrode can be additionally used to set the optimal working point in the transistor characteristics.

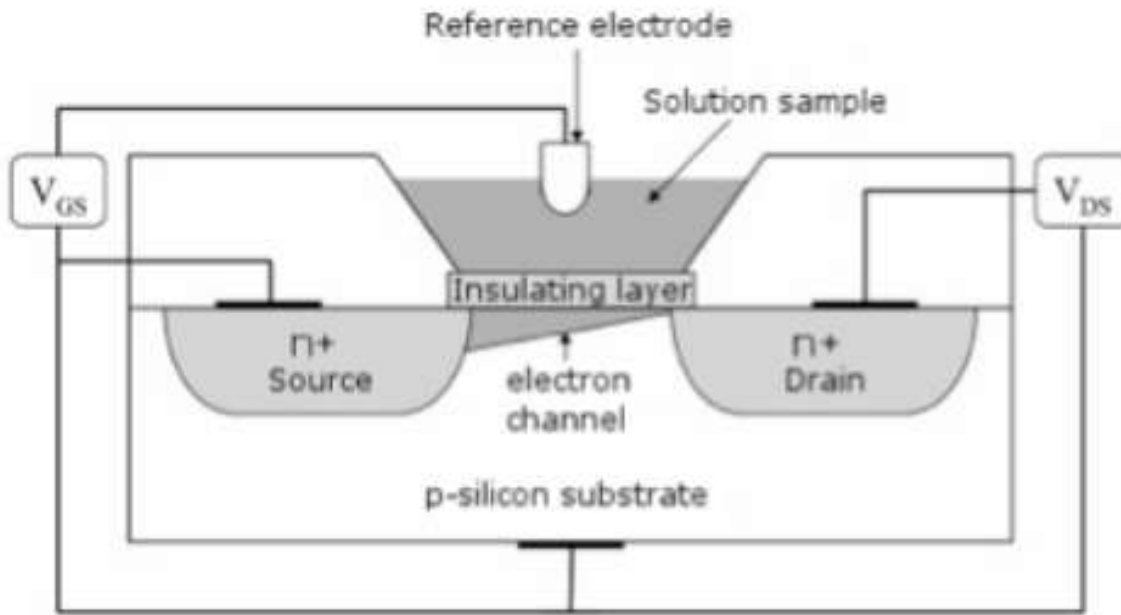


One significant improvement consists of the formation of a larger area capacitor build from the suspended gate and a floating gate. The floating gate then transmits the potential coming from the gas sensitive layer to a small FET-device with a short channel . This basically minimizes the loss of sensing signal due to weak coupling via the air gap

An appropriate sensing material is deposited on a flat carrier substrate forming what eventually becomes the gate-electrode. The preparation conditions are not limited by any Si-electronics related constraints.

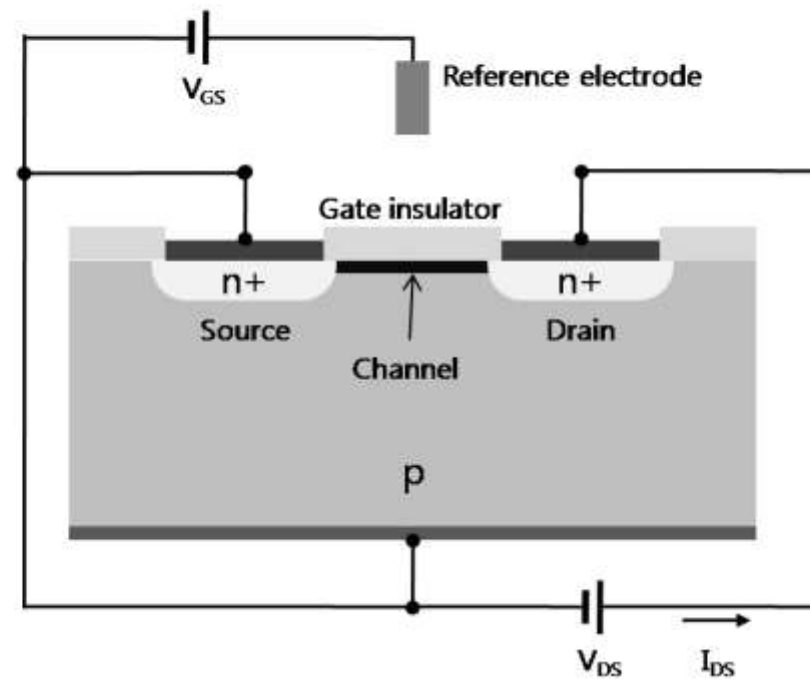
The Si FET-chip is separately prepared in standard CMOS. Electronics for driving the sensor may be integrated in the Si-Chip Finally both parts are bonded together so that a defined air gap is formed. These sensors are characterized by an unprecedented freedom in the choice of sensing materials. The gas receptor does not need to be an oxide. Organic molecules, polymers, metals, or salts may be used in the sensing platform. Since the sensors can be operated at room temperature, heating is not required. Multiple readout channels allowing for tiny sensing arrays can be realized on one single chip. The base potential of this sensing technology arises from the fact that the measurand comes from the direct measurement of surface effects. One consequence is that sensing materials in these devices do not need to be a semiconductor: metallic conductors or insulating materials can be used as well. One promising field for applications of such sensors is air monitoring in buildings. Due to their small dimensions and moderate costs, they can be used for distributed sensing networks allowing local sensing of air properties. Due to their low power consumption at ambient temperature operation, battery-operated sensing nodes that communicate wireless can be established. Since there are no high labor costs for wiring, an additional and decisive cost advantage for the sensor user occurs. An important application of such distributed sensors will be the control of the indoor air quality to allow for an on demand ventilation of different locations in a building. Good examples are meeting rooms. Usually, when the room is unused the ventilation is too high, and is much too low, when a meeting takes place. Similar situations occur at work places due to the changing occupancy and due to the varying loading of the air with contaminants

Ion Selective Field Effect Transistor



FET devices for ion sensing

Figure 1. Structure of ISFET. It consists of source, drain, gate insulator, and reference electrode.



In general, a field-effect transistor (FET) consists of three terminals; the source, drain, and gate. The voltage between the source and drain of the FET regulates the current flow in the gate voltage. Specifically, the current-control mechanism is based on an electric field generated by the voltage applied to the gate. The current is also conducted by only one type of carrier (electrons or holes) depending on the type of FET (n-channel or p-channel). A positive voltage applied to the gate causes positive charges (free holes) to be repelled from the region of the substrate under the gate. These positive charges are pushed downward into the substrate, leaving behind a carrier-depletion region. The depletion region is populated by the bound negative charge associated with the acceptor atoms. These charges are “uncovered” because the neutralizing holes have been pushed downward into the substrate [5]. The positive gate voltage also pulls negative charges (electrons) from the substrate regions into the channel region. When sufficient electrons are induced under the gate, an induced thin n-channel is in effect created, electrically bridging the source and drain regions. The channel is formed by inverting the substrate surface from p-type to n-type (inversion layer). When a voltage is applied between the drain and source with the created channel, a current flows through this n-channel via the mobile electrons (n-type FET). In the case of a p-type semiconductor, applying a positive gate voltage depletes carriers and reduces the conductance, whereas applying a negative gate voltage leads to an

accumulation of carriers and an increase in conductance (the opposite effect occurs in n-type semiconductors). The applied gate voltage generates an electric field which develops in the vertical direction. This field controls the amount of charge in the channel, and thus it determines the conductivity of the channel. The gate voltage applied to accumulate a sufficient number of electrons in the channel for a conducting channel is called the threshold voltage (V_{TH}). Note that V_{TH} for an n-channel (p-channel) FET is positive (negative).

With these properties, the FET can be configured as a biosensor by modifying the gate terminal with molecular receptors or ion-selective membranes for the analyte of interest. The binding of a charged biomolecule results in depletion or accumulation of carriers caused by change of electric charges on the gate terminal. The dependence of the channel conductance on gate voltage makes FETs good candidates for electrical biosensors because the electric field generating from the binding of a charged biomolecule to the gate is analogous to applying a voltage to a gate.

Generally, there are two types of planar FET-based biosensors, according to their structure; insulated-gate field-effect transistors (IGFET) and ISFET. In the case of IGFET, particularly MOSFET (metal-oxide-semiconductor field-effect transistor), the gate terminal is electrically isolated from the source and drain terminals. ISFET is similar to IGFET, but in the ISFET, the metal gate is replaced by an ion-selective membrane, electrolyte and a reference electrode (Figure 1). In the case of an ISFET biosensor, the amount of the current flow will be not only determined by the charges of biomolecules interacting on the gate dielectric, but also sensitive to pH, different ions, products of enzyme reactions, etc. An attractive feature of such FETs is that it is possible to detect biomolecular interactions in a label-free manner through a direct change in conductance or a related electrical property.